UNIVERSITY OF PISA

Research Doctorate School in

BIOLOGICAL AND MOLECULAR SCIENCES

Course in

MOLECULAR AND EXPERIMENTAL ONCOLOGY

SSD: MED/06

XXVI CYCLE (2011-2013)

THESIS TITLE:

The role of different molecular markers in thyroid epithelium transformation: functional studies and possible clinical implications.

Supervisor: Prof. Bevilacqua G. **Candidate:** Federica Panebianco

Tutor: Dr.ssa Chiara Mazzanti

INDEX

"Take up one idea. Make that one idea your life –think of it, dream of it, live on that idea. Let the brain, muscles, nerves, every part of your body, be full of that idea, and just leave every other idea alone. This is the way to success."

Swami Vivekananda

To Daria, my sister

ABSTRACT

Background. Papillary thyroid cancer (PTC) is the most common (~90%) endocrine malignancy. The first manifestation of the thyroid cancer is through thyroid nodules and the most sensitive and specific diagnostic tool to detect malignancy in patients with thyroid nodules is fine-needle aspiration biopsy (FNAB). Nevertheless, sometimes it is not efficient enough to give a specific diagnosis leading to the so called diagnoses of indeterminate or suspicious lesions for PTC which ranges from 20 to 30% of cases. BRAF mutational analysis is commonly used to assess the malignancy of thyroid nodules but unfortunately it still leaves indeterminate diagnoses. Recent studies conducted in our laboratories have shown a significant highly decrease rather than increase in transcript of c-KIT in malignant thyroid lesions compared to the benign ones, and it was demonstrated to be effective as a new biomarker in the preoperative diagnosis of thyroid tumors.

Aim: The aim of the present study is mainly to investigate thoroughly the role of the c-KIT gene in thyroid cancerogenesis, and to characterize in details the c-KIT signaling pathway and the cause of its down-regulation in thyroid cancer. Another aim of this present study is to identify other molecular markers in order to improve the cytological diagnosis and to better understand the mechanisms underlying thyroid epithelium transformation.

Methods: We have collected 169 pre-operative thyroid Fine Needle Aspirate (FNA) sample. All 169 FNA samples analyzed in this study were molecularly characterized for the presence of the V600E BRAF mutation in exon 15. SNP analysis, methylation analysis and various gene expression analyses were conducted in order to clarify c-Kit role in thyroid neoplastic trasformation. Gene expression computational models (Neural Network Bayesian Classifier, Discrimination Analysis) were built, together with ROC curves and PCA (Principal Component Analysis) to distinguish a malignant/benign status and BRAF status. Finally a panel of 84 Human Tyrosine Kinases gene array was amplified on 8 benign samples and 12 malignant samples.

Results: 64/103 malignant samples carried the V600E mutation while all 66 benign samples were wild type for BRAF exon15. The results of the analysis related to c-KIT function support our hypothesis that this receptor controls a differentiation pathway in thyrocytes. Methylation biochemal process and 146b/222 miRNA expression account for part of the c-KIT dowregulation.

The Bayesian Artificial Neural Network and Discriminant Analysis, made of 4 gene (KIT, TC1, miRNA222, miRNA146b) showed a very strong predictive value (94.12% and 92.16%

respectively) in discriminating malignant from benign patients and it is interesting to notice that Discriminant Analysis showed a correct classification of 100.00 % of the samples in the malignant group, and 95.00 % by BNN. This same model defines two clearly different genetic background related to BRAF mutational status. In the panel of 84 Human Tyrosine Kinases gene array we found in three (malignant vs benign; V600E vs benign; WT malignant vs benign) of the four conducted comparisons, four genes (ALK, CSK, HCK e MSTR1) in common that had a significantly altered expression.

Conclusion: The results of this research support the idea that c-KIT is driving a thyroid cell differentiation pathway, which results altered in thyroid neoplasm transformation. In the same study a 4 gene model was build able to discriminate with high probability between benign and malignant FNAs. The model is proposed to be added to the routinely BRAF diagnostic test in order to improve FNA diagnostic accuracy solving the problems of the nodules that otherwise would remain suspicious. Moreover the present study shows clearly how the presence of the BRAF V600E mutation is accompanied by a unique genetic scenario in which sets of genes specifically discriminate the mutational and wild-type status. Several tyrosine kinase genes showed statistically significant differential expression between malignant and benign thyroid nodules.

1 INTRODUCTION

1.1 Anatomy and histology of the thyroid

The thyroid gland, which is the largest endocrine organ in humans, regulates systemic metabolism through thyroid hormones. The thyroid gland is a highly vascularized organ located anteriorly in the neck, deep to the platysma, sternothyroid and sternohyoid muscles, and extending from the 5th cervical (C5) to the 1st thoracic (T1) vertebrae. The gland consists of two lobes (left and right) connected by a thin, median isthmus overlying the 2nd to 4th tracheal rings, typically forming an "H" or "U" shape. Occasionally the isthmus is absent and the thyroid exists as two distinct lobes (Figure 1.1)

The thyroid is divided into lobules, each composed of about 20 to 40 evenly dispersed follicles. Thyroid follicles are surrounded by a single layer of thyroid epithelial cells surrounding a gel-like pinkish material called colloid (Figure 1.2 A). Follicular cells (or "thyroid epithelial cells") are the most numerous cells present in the simple epithelial layer and are responsible for iodine uptake and thyroid hormone synthesis as well as thyroglobulin, a glycoprotein. Thyroid hormones are stored extracellularly as part of the thyroglobulin which is the main component of the colloid. The size of follicles and the height of follicular cells vary even within one section of the gland. Squamous principal cells indicate a relatively inactive gland whereas cuboidal to columnar cells indicate more activity in removing the hormone from the stored form. In addition to follicular cells there is another type of functional cell in the thyroid gland, the *parafollicular cell*, which may be found as single cells in the epithelial lining of the follicle or in groups in the connective tissue between follicles (Figure 1.2 B). They usually appear as large, clear cells since they do not stain well with hematoxylin and eosin; sometimes, these cells are called parafollicular cells, because of their location, or clear cells (C cells), for their appearance of their cytoplasm. Parafollicular cells are dedicated to the production of the hormone calcitonin, which lowers the level of calcium in the blood [1,2].

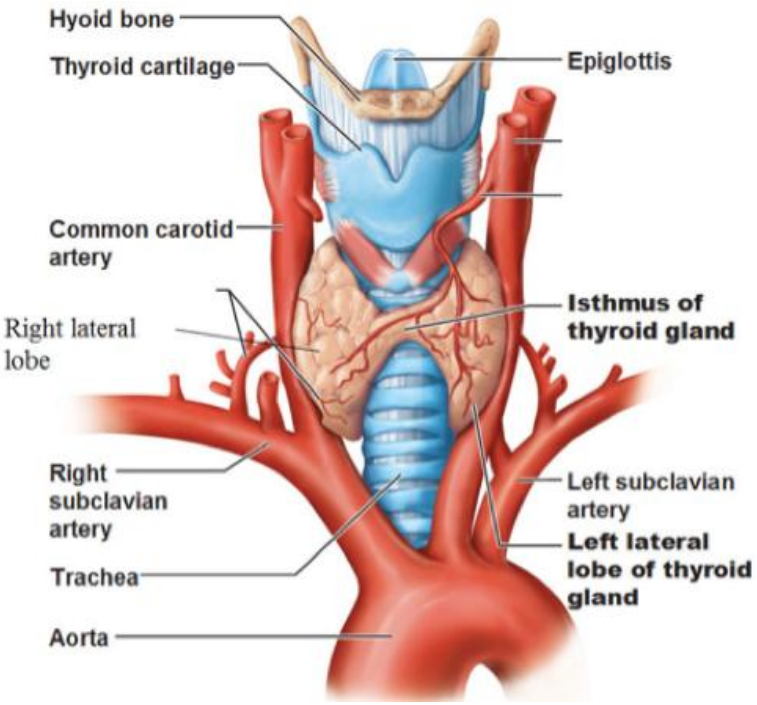

Figure 1.1: Gross anatomy of the thyroid gland

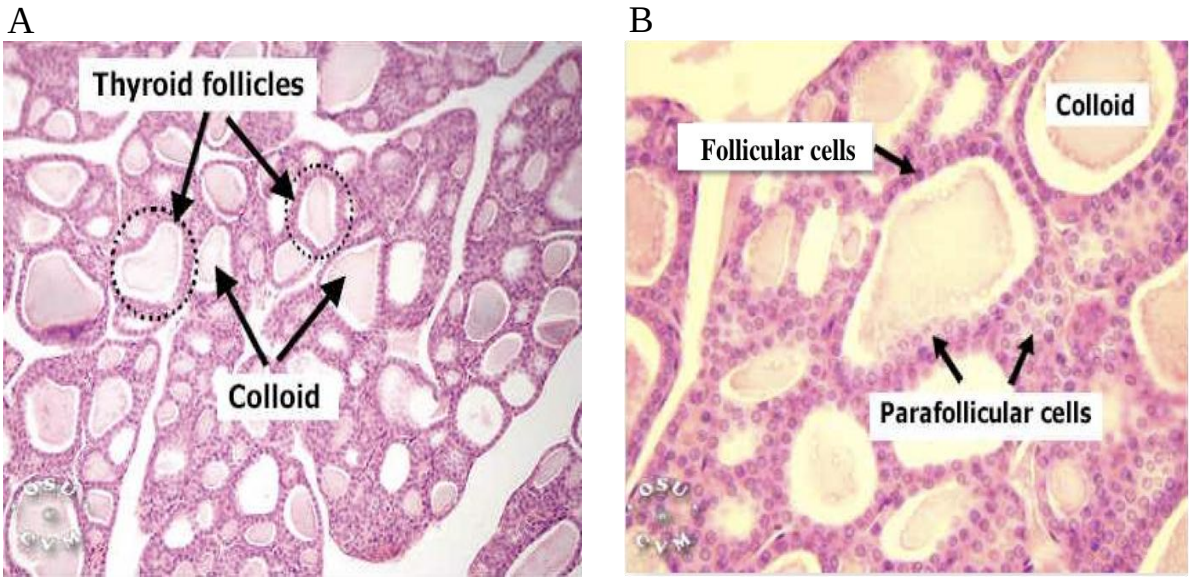

Figure 1.2: A thyroid follicles; B follicular and parafollicular cells

1.2 Thyroid neoplasm

The thyroid gland gives rise to a variety of neoplasms, ranging from circumscribed, benign adenomas to highly aggressive, anaplastic carcinomas [3]. Thyroid cancer is the most common malignant tumor of the endocrine system and accounts for approximately 1% of all newly diagnosed cancer cases. Its incidence has increased significantly in the USA and other countries over the last several decades [4,5]. Age- adjusted global incidence rates vary from 0.5 to 10 cases per 100,000 population, occurring in most of the cases between 20 and 50 years of age.

From a clinical standpoint, the possibility of neoplastic disease is of major concern in individuals who present thyroid nodules. The overwhelming majority of solitary nodules are benign lesions. Carcinomas of the thyroid, in contrast, are uncommon, accounting for much less than 1% of solitary thyroid nodules. Adenomas are benign neoplasms derived from follicular epithelium. The malignant tumours of the thyroid can originate from each of the cell types that populate the gland such as the follicle cells, the C cells that produce calcitonin, lymphocytes, and cells originating from the vascular and stromal elements; moreover malignant tumors may be due to metastasis from other organs [3].

The most frequent type of thyroid malignancy is papillary carcinoma, which constitutes approximately 80% of all cases, and this tumor type is primarily responsible for the overall increase in incidence of thyroid cancer (Figure 1.4 A) [6].

The second most common tumor type is follicular carcinoma, which accounts for approximately 15% of all thyroid malignancies and may be of conventional or oncocytic (Hurthle cell) type [7]. It is likely that follicular carcinomas can develop either from pre-existing benign follicular adenomas or directly, by passing the stage of adenoma. These follicular cell-derived tumors are well differentiated, in contrast to poorly differentiated and anaplastic thyroid carcinomas, which can arise de novo or from pre-existing well-differentiated papillary or follicular carcinomas (Figure 1.4 B).

Anaplastic and poorly differentiated carcinomas are rare (~2% of all thyroid cancer cases) and represent the most aggressive types of thyroid cancer (Figure 1.4 C).

Thyroid medullary carcinoma originates from parafollicular C cells and accounts for approximately 3% of thyroid cancer (Fifure 1.4 D) (Fifure 1.5) [7].

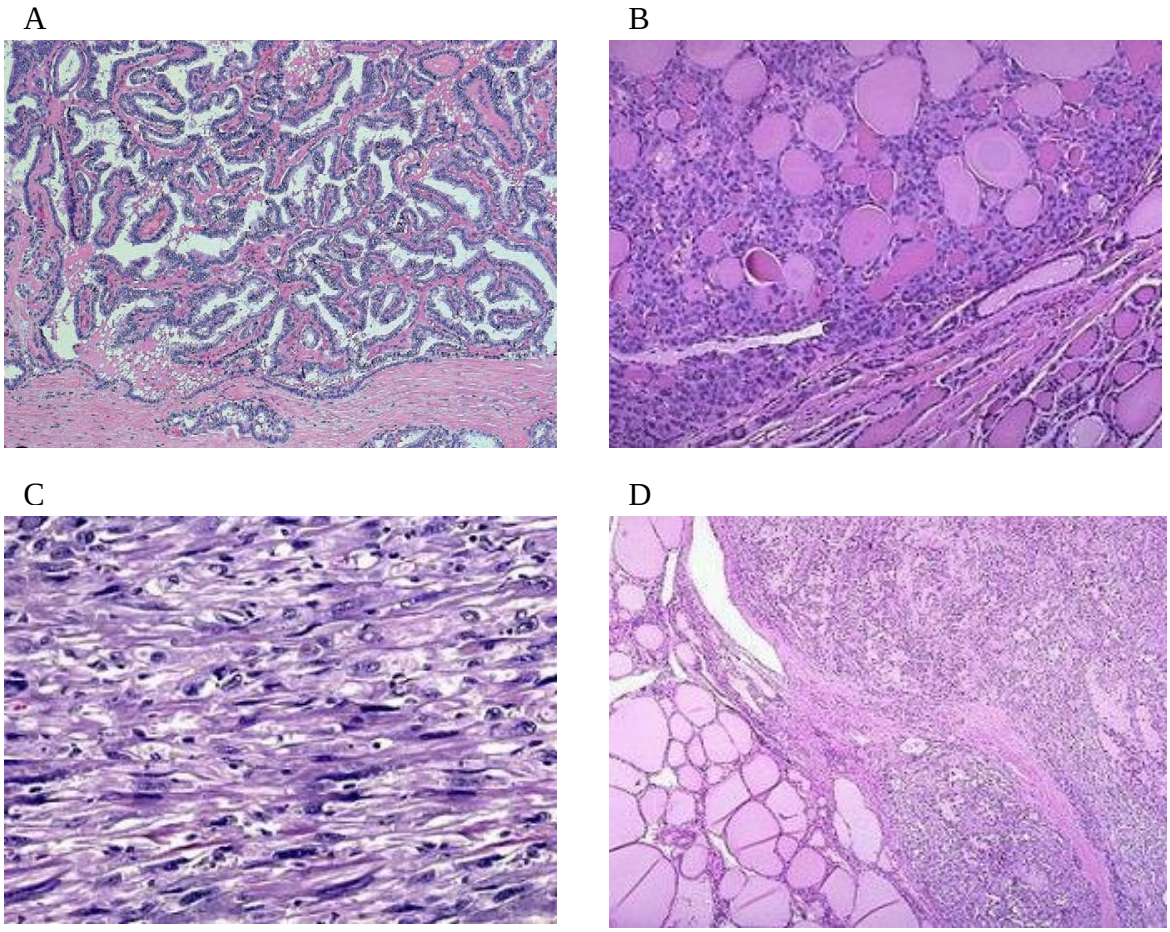

Figure 1.4: A) Classic papillary thyroid carcinoma is formed of papillae with fibrovascular cores; B) Follicular carcinoma; C) Anaplastic carcinoma; D) Medullary carcinoma

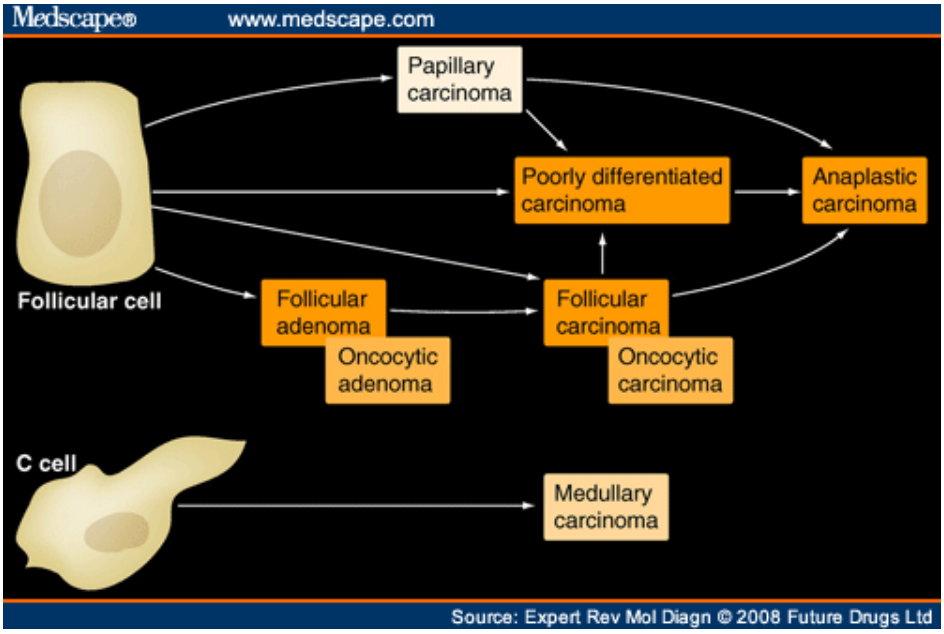

Figure 1.8: Schematic representation of thyroid cancer origin and its putative progression. Oncocytic adenoma and carcinoma are currently considered to be variants of follicular adenoma and carcinoma. Papillary carcinoma may be of the classical type or manifests as one of its variants, including oncocytic variant of papillary carcinoma. (Pathology and Genetics of Tumours of Endocrine Organs. IARC Press, Lyon, France, 2004) [7].

1.3 Common alterations in thyroid cancer

Similar to other cancer types, thyroid cancer initiation and progression occur through gradual accumulation of various genetic and epigenetic alterations, including activating and inactivating somatic mutations, alterations in gene expression patterns, microRNA (miRNA) deregulation and aberrant gene methylation. Among these alterations, most of the data that have accumulated relate to somatic mutations, many of which occur early in the transformation process and are essential for cancer development. Point mutation and chromosomal rearrangements are very frequent in thyroid cancer progression. The former is a result of single nucleotide change within the DNA chain, whereas the latter represents a large-scale genetic abnormality with breakage and fusion of parts of the same or different chromosomes. Importantly, a growing body of evidence suggests that these two distinct mutational mechanisms are associated with specific etiologic factors involved in thyroid carcinogenesis.

1.4 Altered signalling pathways in thyroid cancer

Recent years have been marked by significant expansion in the understanding of the molecular basis of thyroid carcinogenesis. Most mutations in thyroid cancer involve the effectors of the MAPK pathway and the PI3K-AKT pathway (Figure 1.6).

It has become apparent that thyroid tumors, especially those of the papillary type, frequently have genetic alterations leading to activation of the MAPK signaling pathway. These include RET/PTC rearrangement and point mutations of the BRAF, a RAS genes and, in some cases, by the recently discovered ALK mutations[43]. In thyroid follicular carcinomas, in addition to RAS mutations and PAX8-PPARγ rearrangement, alterations involving the PI3K/AKT signaling pathway are likely to play a role, particularly in later stages of tumor progression. Many of these mutations are associated with distinct phenotypical features of tumors, and some of them serve as markers of more aggressive tumor behavior. Current molecular techniques allow the detection of these genetic alterations in thyroid fine-needle aspiration (FNA) samples and surgically removed samples, offering useful information for diagnosis and management of patients with thyroid cancer. Many of these mutations, particularly those leading to the activation of the MAPK pathway, are being actively explored for targeted therapy of thyroid cancer. These tumors frequently have mutations in genes coding for proteins that signal

along the MAPK signaling pathway. This ubiquitous intracellular cascade regulates cell growth, differentiation and survival in response to growth factors, hormones and cytokines that interact with cell surface receptor tyrosine kinases [8]. Activating mutations of the BRAF, RET or RAS genes are found in approximately 70% of papillary carcinomas, and they rarely overlap in the same tumor, suggesting that activation MAPK signaling is essential for tumor initiation and that alteration of a single effector of the pathway is sufficient for cell transformation [9–11]. Despite their common ability to activate the MAPK pathway, each of these mutations is likely to have additional and unique effects on cell transformation, as they are associated with unique gene expression signatures and distinct phenotypical and biological properties of papillary carcinomas (Figure 1.7) [12,13].

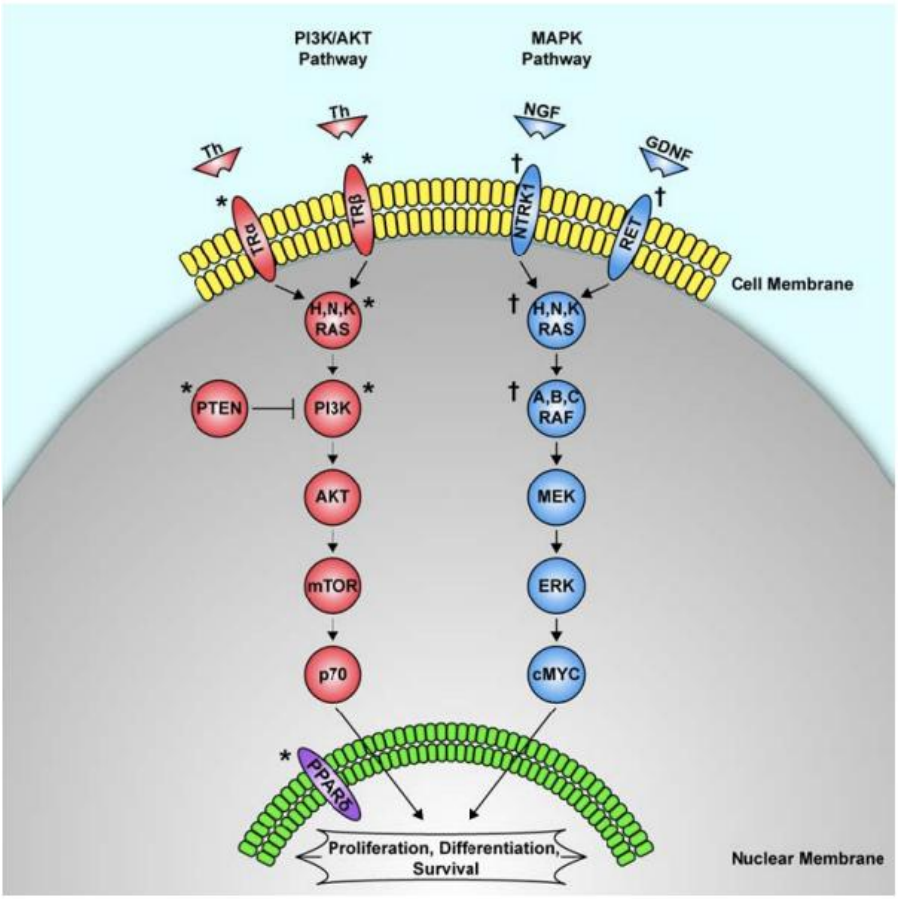

Figure 1.6: Mutations of the MAPK pathway (in blue) are associated with papillary thyroid cancer. * Denotes known genetic mutations associated with sporadic follicular thyroid cancer. Sporadic mutations of the PI3K/AKT pathway have been associated with follicular thyroid cancer. In the third pathway, mutations of the nuclear receptor PPARgamma have been associated with follicular thyroid cancer. Th = thyroid hormone, TR = thyroid hormone receptor, NGF = nerve growth factor, GDNF = glial cell line-derived neurotrophic factor. (The Evolution of Biomarkers in Thyroid Cancer—From Mass Screening to a Personalized Biosignature: Raymon H. Grogan , Elliot J. Mitmaker †and Orlo H. Clark)

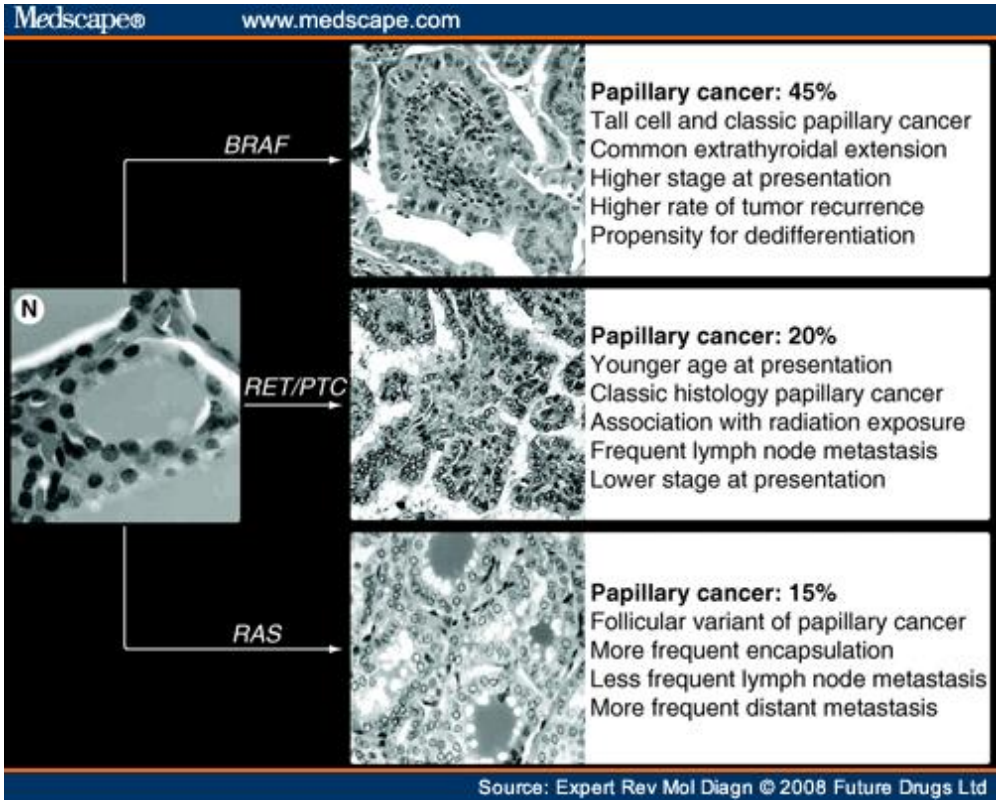

Figure 1.7: Molecular pathways in thyroid papillary cancer and typical microscopic presentation and clinical-pathological features of tumors associated with specific mutations. N: Normal thyroid. (Nikiforov, Y.E. & Nikiforova, M. N., Nature Reviews, 2011)

The PI3K/Akt signaling pathway, also plays an important role in the regulation of cell growth, proliferation and survival. This pathway can be activated by the upstream stimulatory molecules (i.e., RAS, RET/PTC), through the loss of function of PTEN protein that normally inhibits PI3K signaling or as a result of activating mutations or amplification of genes coding for the effectors of this pathway. The PIK3CA gene, coding for a catalytic subunit of PI3Ks, has been shown to harbor mutations in thyroid tumors, although at low frequency. Specifically, it has been found in 6–13% of follicular carcinomas and in 0–6% of follicular adenomas [14,15]. Mutations typically involve various nucleotides in exons 20 and 9 of the PIK3CA gene. Mutations of the PTEN gene have been reported in a small proportion of follicular carcinomas (~7%), but not in follicular adenomas [15,16].

1.5 Gene mutations

1.5.1 BRAF

BRAF is a serine-threonine kinase that belongs to the family of RAF proteins, which are intracellular effectors of the MAPK signaling cascade. Upon activation triggered by RAS binding and protein recruitment to the cell membrane, these kinases phosphorylate and activate MEK, which in turn activates ERK and consequent effectors of the MAPK cascade. Point mutations of the BRAF gene are found in about 45% of thyroid papillary carcinomas (9, 17). Virtually all point mutations involve nucleotide 1799 (generally T>A, Figure 1.8) and result in a valine-to-glutamate substitution at residue 600 (V600E) (19, 20).

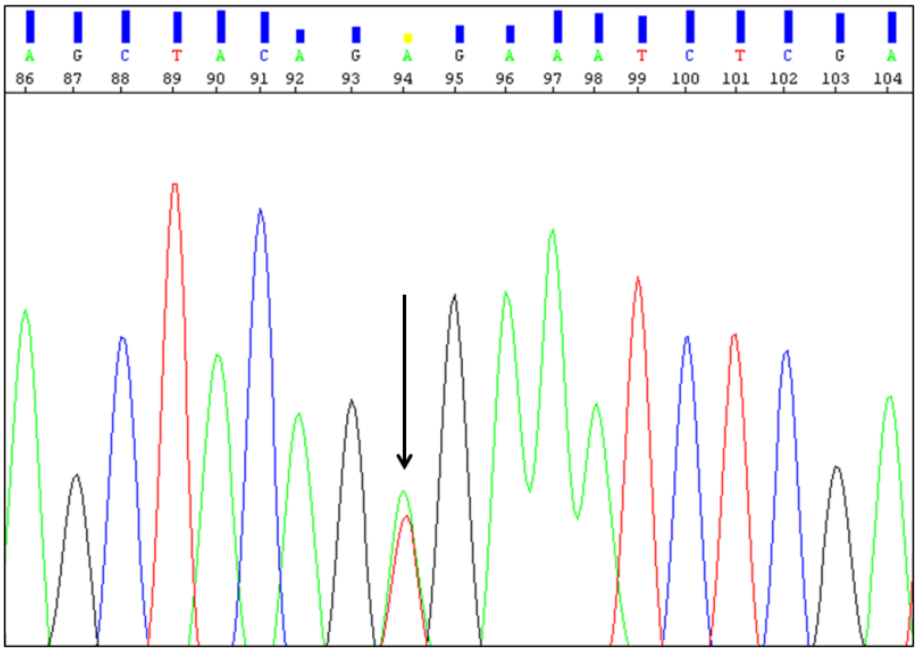

Figure 1.8: BRAF 1799T>A point mutation.

BRAF V600E mutation leads to constitutive activation of BRAF kinase and the mechanisms of activation have been recently elucidated. In the dephosphorylated, wild type BRAF protein the hydrophobic interactions between the activation loop and the ATP binding site maintains the protein in an inactive conformation. The V600E substitution disrupts these interactions and allows the formation of new interactions that keep the protein in a catalytically competent conformation, resulting in continuous phosphorylation of MEK. BRAF mutations are highly prevalent in papillary carcinomas with classical

histology and in the tall cell variant, but are rare in the follicular variant [20, 18]. In many studies, the presence of BRAF mutation has been found to correlate with aggressive tumor characteristics such as extra thyroidal extension, advanced tumor stage at presentation, tumor recurrence, and lymph node or distant metastases [22-23]. Importantly, BRAF V600E mutation has been found to be an independent predictor of tumor recurrence even in patients with stage I-II of the disease [23, 24]. BRAF mutations have also been associated with the decreased ability of tumors to trap radioiodine and treatment failure of the recurrent disease, which may be due to the deregulation of function of the sodium iodide symporter (NIS) and other genes metabolizing iodide in thyroid follicular cells [23, 25].

Other and rare mechanisms of BRAF activation in papillary thyroid cancer include K601E point mutation, small in-frame insertions or deletion surrounding codon 600 [26-28]. In addition to papillary carcinomas, BRAF is found mutated in thyroid anaplastic and poorly differentiated carcinomas, typically in those tumors that also contain areas of well-differentiated papillary carcinoma [22, 29, 30]. In those tumors, BRAF mutation is detectable in both well-differentiated and poorly differentiated or anaplastic tumor areas, providing evidence that it occurs early in tumorigenesis. Therefore, the detection of V600E *BRAF* mutation in thyroid FNA samples or in surgically removed samples is virtually diagnostic for papillary carcinoma [22,23].

1.5.2 RAS

The RAS genes (HRAS, KRAS and NRAS) encode highly related G-proteins that are located at the inner surface of the cell membrane and play a central role in the intracellular transduction of signals arising from cell membrane receptors tyrosine kinase and G-protein-coupled receptors. In its inactive state, RAS protein is bound to guanosine diphosphate (GDP). Upon activation, it releases GDP and binds guanosine triphospate (GTP), activating the MAPK and other signaling pathway, such as PI3K/AKT. Normally, the activated RAS-GTP protein becomes quickly inactive due to its intrinsic guanosine triphosphatase (GTPase) activity and the action of cytoplasmic GTPase-activating proteins, which catalyze the conversion of the active GTP form to the inactive GDP-bound form. In many human neoplasms, point mutations occur in the discrete domain of the RAS gene, which result in either an increased affinity for GTP (mutations in codons 12 and 13) or inactivation of the autocatalytic GTPase function (mutations in codon 61). As a result, the mutant protein becomes permanently switched in the active position and constitutively activates its downstream signaling pathways.

Point mutations of RAS occur with variable frequency in all types of papillary thyroid follicular cell-derived tumors. In papillary carcinomas, RAS mutations are relatively infrequent, as they occur in about 10% of tumors [31, 32]. Papillary carcinomas with RAS mutations almost always have the follicular variant histology; this mutation also correlates with significantly less prominent nuclear features of papillary carcinoma, more frequent encapsulation, and low rate of lymph node metastases [33]. Some studies have reported the association between RAS mutations and more aggressive behavior of papillary carcinoma and with higher frequency of distant metastases [34]. In follicular thyroid carcinomas, RAS mutations are found in 40-50% of tumors and may also correlate with tumor dedifferentiation and less favorable prognosis [35-38]. RAS mutations may predispose to tumor dedifferentiation, as they are found with high prevalence in anaplastic (undifferentiated) thyroid carcinomas. This may be due to the effect of mutant RAS to promote chromosomal instability, which has been documented in the *in vitro* settings. Mutations of the *RAS* gene are not restricted to papillary carcinoma and also found in other benign and malignant thyroid neoplasms, as well as in tumors from other tissues [39].

The diagnostic use of RAS mutation detection is controversial. On the one hand, it is not specific for malignancy since RAS mutations also occur with significant prevalence in benign follicular adenomas. On the other hand, RAS mutations frequently occur in follicular carcinomas and the follicular variant papillary carcinomas, both of which are difficult to diagnose cytologically in thyroid FNA samples. Moreover, since mutant RAS is likely to predispose to progression from follicular adenoma to carcinoma and to further tumor dedifferentiation, it may be justifiable to surgically remove the RAS- positive adenomas to prevent such a progression. In a prospective study aimed to assess the role of detection of different mutations in improving the preoperative FNA diagnosis of thyroid nodules, the detection of RAS mutations was found to improve the diagnostic accuracy and allowed to diagnose malignant tumors in several samples with negative or insufficient cytology [40].

1.6 Gene translocations

1.6.1 RET/PTC

The RET proto-oncogene codes for a cell membrane receptor tyrosine kinase. In the thyroid gland, RET is highly expressed in parafollicular C-cells but not in follicular cells, where it can be activated by chromosomal rearrangement known as RET/PTC rearrangement [42]. RET/PTC rearrangement is another genetic alteration that is frequently found in papillary carcinomas, [29] and is a result of the fusion between the 3′-portion of the RET receptor tyrosine kinase gene and the 5′-portion of various genes.

At least 11 types of RET/PTC have been reported to date, all formed by the RET fusion to different partners [43, 44]. All fusions leave the tyrosine kinase domain of the RET receptor intact and enable the RET/PTC oncoprotein to bind SHC and activate the RAS-RAF-MAPK cascade [48]. The two most common rearrangement types, RET/PTC1 and RET/PTC3 account for the vast majority of all rearrangements found in papillary carcinomas. Several studies suggest that the oncogenic effects of RET/PTC require signaling along the MAPK pathway and the presence of the functional BRAF kinase [45-47]. Indeed, BRAF silencing in cultured thyroid cells reverses the RET/PTC-induced effects such as ERK phosphorylation, inhibition of thyroid specific gene expression, and increased cell proliferation [46, 47]. RET/PTC is found on average in about 20% of adult sporadic papillary carcinomas, although its prevalence is highly variable between different observations [43, 44]. In general RET/PTC incidence is higher in tumors from patients with a history of radiation exposure and in pediatric populations. The distribution of RET/PTC rearrangement within each tumor may vary from involving almost all neoplastic cells (clonal RET/PTC) to being detected only in a small fraction of tumor cells (non-clonal RET/PTC) [31, 48]. The heterogeneity may be of potential problem for the RET receptor-targeted therapy, since tumors with non-clonal RET/PTC frequently have other genetic alterations and may not respond to RET inhibitors in the same way as tumors harboring the clonal

1.6.2 PAX8/PPARγ

PAX8/PPARγ rearrangement results from the translocation t(2;3)(q13;p25) that leads to the fusion between the PAX8 gene, which encodes a paired domain transcription factor, and the peroxisome proliferator-ativated receptor (PPARγ) gene [50]. PAX8-PPARγ occurs in about 35% of conventional follicular carcinomas, and with lower prevalence in oncocytic (Hurtle cell) carcinomas [50-52]. Tumors harboring PAX8-PPARγ rearrangement tend to present at

a younger age, be smaller in size, and more frequently have vascular invasion. The rearrangement causes the over expression of the PPARγ protein which can be detected by immunohistochemistry [49, 53].

The mechanisms of cell transformation induced by PAX8-PPARγ are not fully understood. Some evidence has been presented for inhibition of normal PPARγ function via a dominant-negative effect of the PAX8-PPARγ protein on wild type PPARγ [49, 45]. Other studies have found the activation of known PPARγ target genes in tumors harboring PAX8-PPARγ, arguing against the dominant-negative effect. Other possible mechanisms include deregulation of PAX8 function, known to be critical for thyroid cell differentiation, and activation of a set of genes related to neither wild type PPARγ nor wild type PAX8 pathways [55, 56].

PAX8-PPARγ rearrangements and RAS point mutations rarely overlap in the same tumor, suggesting that follicular carcinomas may develop via at least two distinct molecular pathways, initiated by either PAX8-PPARγ or RAS mutation [51].

1.7 Other molecular events

Distinct alterations in gene expression have been observed in papillary carcinomas and other types of thyroid cancers [12, 1, 57, 58]. These alterations include down regulation of genes responsible for specialized thyroid function (such as thyroid hormone synthesis), up regulation of many genes involved in cell adhesion, motility and cell-cell interaction, and different patterns of deregulation of the expression of genes that encode cytokines and other proteins involved in inflammation and immune response.

Among papillary carcinomas, different mRNA expression profiles have been observed in the classic papillary, follicular and tall-cell variants [57-60]. Moreover significant correlations have been observed between BRAF, RAS, RET/PTC and TRK (tyrosine receptor kinases) mutations and specific patterns of gene expression. This information has shed light on the molecular basis for the distinct phenotypic and biological features associated with each mutation type [12]. Acquisition of more invasive tumor characteristics and dedifferentiation of BRAF- mutated cancers seems to coincide with profound deregulation of the expression of genes that encode proteins involved in cell adhesion and the inter-cellular junction, which provides evidence for induction of an epithelial-mesenchimal transition along with increased cell motility and invasiveness [61, 62].

Moreover, several miRNAs have been found to be deregulated in thyroid cancer [63-66]. Generally miRNA expression profiles of papillary carcinoma are different from those of follicular carcinoma and other thyroid tumors [67]. Several specific miRNAs, such as miR-146b, miR-221 and miR-222, are highly up regulated in papillary carcinomas and many have a pathogenic role in the development of these tumors [64, 66, 67]. Alterations in gene expression owing to aberrant methylation of gene promoter regions or histone modification also occur in thyroid cancer. These epigenetic events can alter the function of tumor suppressor genes and thus contribute to activation of important signaling pathways, such as PI3K-AKT and MAPK cascade. Changes in epigenetic regulation might also result in down regulation of thyroid specific genes during tumor progression and dedifferentiation [68-69]. Hypermethylation of the metalloproteinase inhibitor gene TIMP3 and other tumor suppressor genes is frequently observed in thyroid cancers with the BRAF V600E substitution, which may contribute to the aggressive biological behavior of tumors carrying this mutation [71].

1.8 Fine-needle aspiration cytology to management of a patient with a thyroid nodule: limitations and clinical utility of molecular markers

The best available test in the evaluation of a patient with a thyroid nodule is fine needle aspiration biopsy (FNA) followed by cytologic examination, which together reliably establish the diagnosis in 70% to 80% of cases. FNA of thyroid nodules has greatly reduced the need for thyroid surgery and has increased the percentage of malignant tumors among excised nodules [72]. In addition, the diagnosis of malignant thyroid tumors, combined with effective therapy, has led to a marked decrease in morbidity due to thyroid cancer. Although FNA biopsy of thyroid nodule is very sensitive in the detection of malignancy, unfortunately, many thyroid FNAs are not definitively benign or malignant, yielding an indeterminate or suspicious diagnosis in 20-30% of cases. In general, thyroid FNAs are indeterminate because of overlapping or undefined morphological criteria for benign *versus* malignant lesions or focal nuclear atypia within otherwise benign specimens. Therefore, when the diagnosis is unclear on FNA, these patients are classified as having a suspicious or indeterminate lesion only. The question then arises: should the surgeon perform a thyroid lobectomy, which is appropriate for benign lesions or a total thyroidectomy, which is appropriate for malignant lesions when the diagnosis is uncertain both preoperatively and intraoperatively? Thyroid lobectomy as the initial procedure for every patient with a

suspicious FNA could result in the patient with cancer having to undergo a second operation for completion thyroidectomy. Conversely, total thyroidectomy for all patients with suspicious FNA would result in a majority of patients undergoing an unnecessary surgical procedure, requiring lifelong thyroid hormone replacement and exposure to the inherent risks of surgery [73]. There is a compelling need to develop more accurate initial diagnostic tests for evaluating a thyroid nodule. New approaches to diagnosis of cancer in thyroid nodules are based on mutational and other molecular markers, which can be reliably detected in cells aspirated during the FNA procedure. These markers offer significant improvement in the diagnostic accuracy of FNA cytology and are poised to make a profound effect on the management of patients with thyroid nodules to distinguish benign from malignant thyroid nodules [72]. Diagnostic use of mutational markers for the analysis of thyroid FNA samples has been explored for single genes and for a panel of mutations. Among single genes, the majority of studies have focused on BRAF mutations, molecular testing of samples classified as malignant by cytology can identify BRAF-positive tumors. Recently, several studies have demonstrated that the BRAF gene V600E mutation represents a diagnostic and prognostic biomarker in PTC, with a prevalence of 40-66%, whereas it is never found in benign lesion. However, despite high specificity for cancer, testing for BRAF mutation alone misses many thyroid cancers that are negative for this mutation. The discovery of single genetic mutations remains important for understanding cancer formation, but single mutations are not practical clinical biomarkers for thyroid cancer. The performance of molecular testing can be improved by including other frequently occurring mutations in the analysis. Use of a panel of mutations including BRAF and RAS point mutations and RET/PTC and PAX8/PPARγ rearrangements, with the possible addition of the TRK rearrangement, for analysis of thyroid FNA samples has been explored [74-77]. Studies that evaluated the use of this panel in a setting of the clinical diagnostic laboratory demonstrated that finding any mutation was a strong predictor of malignancy in thyroid nodules irrespective of the cytological diagnosis (Figure 1.9).

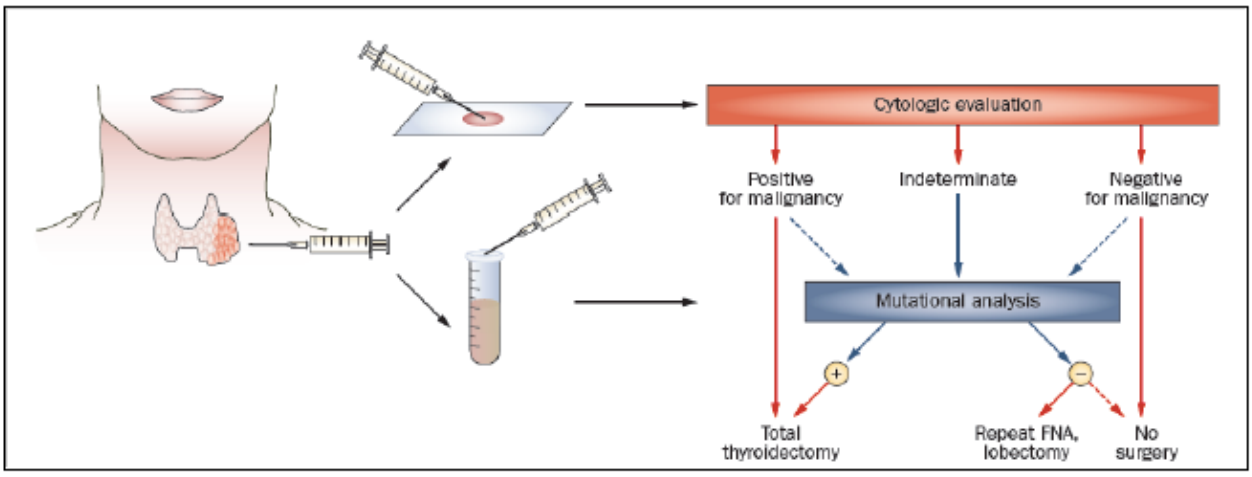

Figure 1.9: Potential clinical management of patients with thyroid nodules on the basis of a combination of cytological examination and molecular analysis. (Nikiforov,Y.E. & Nikiforova, M. N., Nature Reviews, 2011)

Up to 30% of thyroid cancers will have no currently known mutations, thus decreasing the utility of current DNA mutation panels [78].

Thus molecular testing can be particularly helpful for nodules with indeterminate cytology, but a certain percentage of malignant nodules still remains indeterminate, that's why some malignant tumors are negative for mutations and might require a repeated FNA and diagnostic lobectomy, urging the finding of other specific tumour markers.

1.9 C-kit

Based on studies (Tomei S. at al) conducted in our laboratory by real-time PCR the c-KIT gene, that codes for is a type III receptor thyrosine-kinase activated by SCF (Stem Cell Factor), is another tumor marker that was proven to be useful in the preoperative diagnosis of thyroid tumors being statistically downregulated in malignant versus benign thyroid lesions [79].

The proto-oncogene KIT is cellular homologue of the viral oncogene of the feline sarcoma retrovirus HZ4-FeSV. It plays various roles in haematopoiesis, melanogenesis and spermatogenesis, and in the development of the interstitial cells of Cajal. The role of KIT in human neoplasia is not fully cleared yet. A number of tumor types are associated with activation of KIT through its over expression or through activating mutations [80-82], while in highly metastatic melanomas, breast cancer and thyroid carcinoma the progression into a malignant phenotype correlates mostly with loss of KIT expression [83, 84]. Among the few papers studying KIT status in thyroid cancer, Natali *et al.* in 1995 [85] reported the loss of

the receptor during the transformation of normal thyroid epithelium to papillary carcinoma. Similarly, in 2004 Mazzanti *et al.* [65], by using microarray assay, were able to identify out of thousand of genes, KIT as one of the most significant down expressed gene in PTC compared to benign lesions. Other laboratories confirmed this result by using qPCR [86]. Moreover, multiple miRNAs, predicted to target KIT, have been reported to be up regulated in PTC [87]. These findings indicate that KIT receptor may be involved in the growth control of thyroid epithelium and that this function may be lost in malignant transformation. Based on recent studies conducted in our lab (Tomei S. at al) was found a highly preferential decrease rather than increase in transcript of c-KIT in malignant thyroid lesions compared to the benign ones. To explore the diagnostic utility of c-KIT expression in thyroid nodules, its expression values were divided in four arbitrarily defined classes, with class I characterized by the complete silencing of the gene. Class I and IV represented the two most informative groups, with 100% of the samples found malignant or benign respectively (Figure 1.10)

A

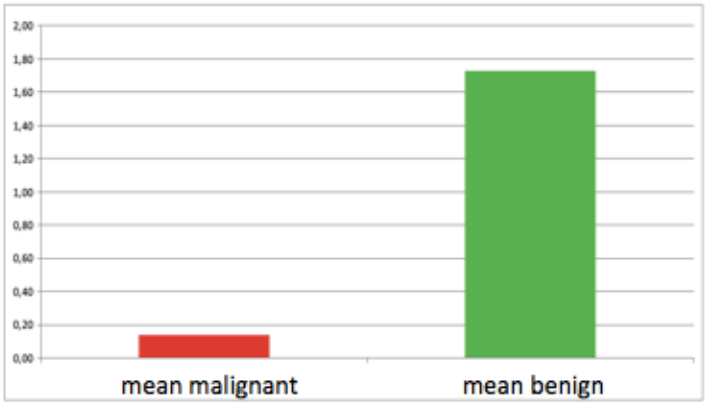

B

Class	KIT ev	PTC		BN		p value
		n	%	n	%	
I	0	19	100	0	0	< 0.0001
II	> 0 - ≤ 0.5	24	65	13	35	= 0.1400
III	> 0.5 - ≤ 3.0	3	14	18	86	< 0.0001
IV	> 3	0	0	5	100	= 0.0091
		46		36		

Figure 1.10: a) For each group (malignant and benign) the mean of all sample ratios between c-KIT expression value and B2M expression value was calculated. There is a highly significant statistical difference between the two groups with a p-value of < 0.0001. b) Classes of KIT expression value (KIT ev: KIT expression value. PTC: papillary thyroid carcinoma. BN: benign nodule).

2 AIM

The biological meaning of c-KIT down-regulation in thyroid epithelium trasformation is unknown. Based on our previous results it is suggested that c-KIT, being downregulated, is involved in the differiantion rather than in the proliferation during thyroid malignant transformation. (Figure 1.11)

The aim of the present study is mainly to investigate thoroughly the role of the c-KIT gene in thyroid cancerogenesis and to understand the cause of its down-regulation in malignant thyroid lesions. We intend also to use computational approaches and to identify new biomarkers, in order to improve the preoperative cytological diagnosis and to better understand the mechanisms underlying thyroid epithelium transformation.

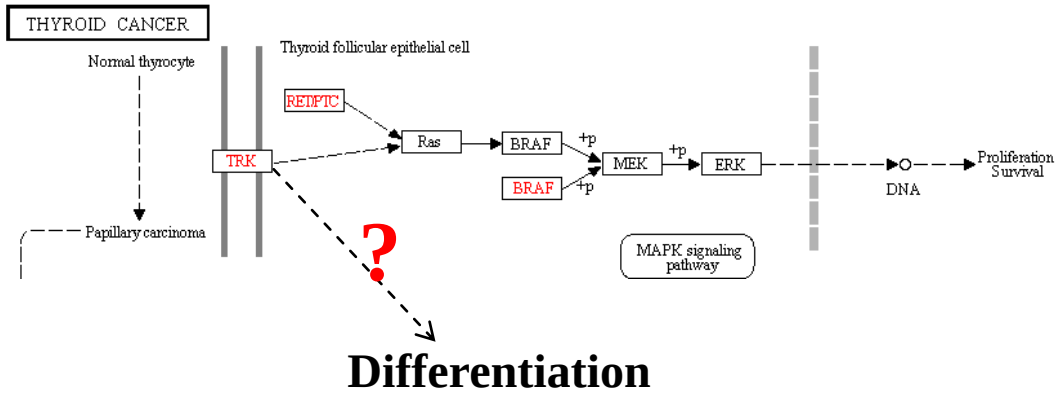

Figure 1.11: Molecular pathway of thyroid epithelium

2.1 The cause of c-kit down-regulation in malignant thyroid lesions:

2.1.1 Methylation status of c-KIT promoter

Since it's well known from the literature that aberrant gene methylation plays an important role in human tumorigenesis, including thyroid tumorigenesis, we have investigated if down-expression of c-KIT is due to the methylation of its promoter.

DNA methylation is an epigenetic regulatory mechanism involved in silencing gene expression that is particularly important in normal embryogenesis. It occurs by adding a methyl group to the cytosine residue of a CpG dinucleotide. Regions of DNA that contain multiple copies of CpG dinucleotides are termed CpG islands and are usually located at the 5' end of gene promoters. Gene silencing after methylation of a CpG island occurs by either blocking the binding of transcription factors to the promoter region or by recruitment of methyl-binding DNA transcription repressors to the promoter. Aberrant gene methylation, or hypermethylation, has been identified in many human tumors including thyroid tumors, leading to inappropriate silencing of genes. Such methylation in human cancers has been frequently found in tumor suppressor genes that are silenced and plays a fundamental role in human tumorigenesis. Many tumor suppressor genes are aberrantly methylated in thyroid cancer, and some even in benign thyroid tumors, suggesting a role of this epigenetic event in early thyroid tumorigenesis. Hypermethylation of multiple genes has been identified in association with the PIK3/AKT pathway in follicular thyroid cancers, and of the MAPK pathway in papillary thyroid cancers [88].

2.1.2 MicroRNAs and SNP

MicroRNAs (miRNAs) are endogenous noncoding RNAs that negatively regulate gene expression by binding the 3' noncoding region of the messenger RNA targets inducing their cleavage or blocking the protein translation (Figure 1.12) [89]. They play important roles in multiple biological and metabolic processes, including developmental timing, signal transduction, and cell maintenance and differentiation. Their deregulation can predispose to diseases and cancer; miRNA expression has been demonstrated to be deregulated in many types of human tumors, including thyroid cancers, and could be responsible for tumor initiation and progression. The overexpression of specific miRNAs could lead to the repression of tumor suppressor gene expression, and conversely the downregulation of specific miRNAs could result in an increase of oncogene expression; both these situations induce subsequent malignant effects on cell proliferation, differentiation, and apoptosis that lead to tumor growth and progress [90].

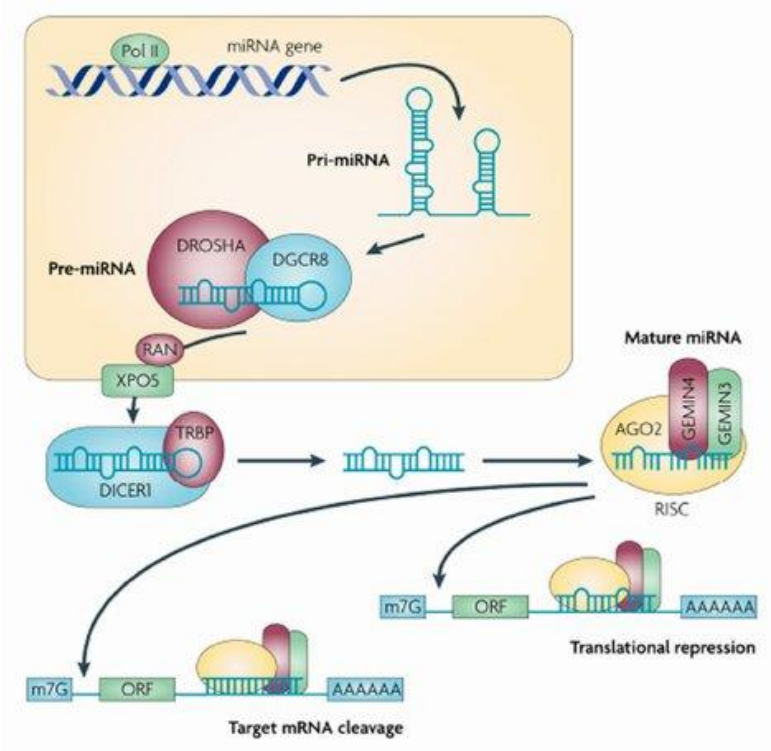

Figure 1.12: Illustrative overview of the miRNA network. RNA polymerase II (Pol II) produces a 500 3,000 nucleotide transcript, called the primary microRNA (miRNA), or pri- miRNA, that is then cropped to form a pre-miRNA hairpin by a multi-protein complex that includes DROSHA (~60 100 nucleotides) (a simplified view is shown here). This double- stranded hairpin structure is exported from the nucleus by RAN GTPase and exportin 5 (XPO5)112. Finally, the pre-miRNA is cleaved by DICER1 to produce two miRNA strands, a mature miRNA sequence, approximately 20 nucleotides in length, and its short-lived complementary sequence, which is denoted miR* and sometimes called the passenger strand or 3p strand 159. The thermodynamic stability of the miRNA duplex termini and the identity of the nucleotides in the 3 overhang determines which of the strands is incorporated into the RNA-inducing silencing complex (RISC)160. In some cases, in which both the lead and passenger strands have a similar thermodynamic stability, both strands will be loaded. The single stranded miRNA is incorporated into RISC, which then targets it to the target 3 untranslated region mRNA sequence to facilitate repression and cleavage. AA, poly A tail; m7G, 7-methylguanosine cap; ORF, open reading frame [89].

Computational predictions and experimental approaches support the idea that different miRNAs target the same mRNA. Multiple miRNAs have been predicted to target KIT, including those overexpressed in PTC [91]. Infact in PTC tissues in which miR-146b, miR-221, and miR-222 were strongly overexpressed there was a downregulation of KIT transcript and KIT protein, in conclusion the upregulation of miR-146b, miR-221, and miR-222, and the subsequent downregulation of KIT seem to be involved in PTC pathogenesis. The binding of microRNA to mRNA can be affected by single-nucleotide polymorphisms that can reside in the microRNA target site, which can either abolish existing binding sites or create illegitimate binding sites. The increase or decrease in microRNA binding caused by

the SNP variation would probably lead to a corresponding decrease or increase in protein translation. Single nucleotide polymorphisms may fall within coding sequences of genes, non coding regions of genes, or in the intergenic regions between genes. SNPs within a coding sequence will not necessarily change the aminoacid sequence of the protein that is produced, due to degeneracy of the genetic code. A SNP in which both forms lead to the same polypeptide sequence is termed synonymous (sometimes called a silent mutation) - if a different polypeptide sequence is produced they are non-synonymous. SNPs that are not in protein coding regions may still have consequences for gene splicing, transcription factor binding, or the sequence of non-coding RNA. Several studies indicate that some SNPs in both miRNA genes and miRNA target genes increase the risk of specific types of cancers. The synonymous G–C SNP rs3733542 in exon 18 of the KIT mRNA affects the binding of miR-146a and miR-146b by changing miRNA–mRNA duplex conformation and results in hybridization with a different region (Figure 1.13) [92]. We decided therefore to analyze the presence or absence of the SNP rs3733542 in our population of malignant and benign FNA samples and evaluate a possible correlation with c-KIT gene expression. Moreover, we evaluated the correlation of the expression levels of miR-146b and miR-222 with c-KIT expression in order to better understand the cause of the down-expression of c-KIT in PTC lesion.

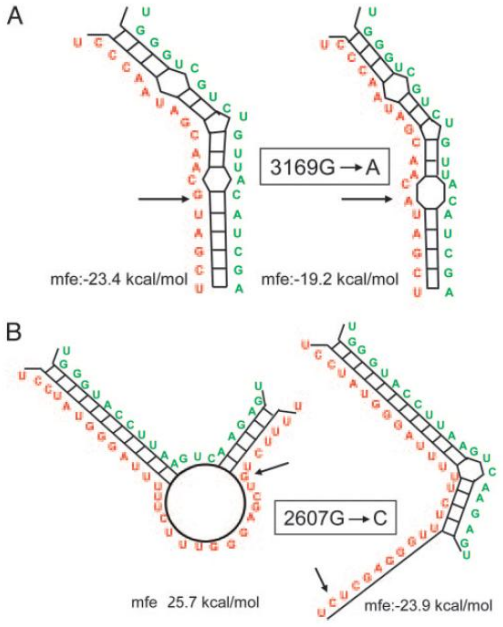

Figure 1.13: Computational modeling of the interaction of miR-221 and miR-146 with the *KIT* gene. (*A*) Hybridization of miR-221 (green color) and *KIT* mRNA(red color); arrows highlight a polymorphic site within the binding domain (SNP rs17084733). Mfe, minimum free energy. (*B*) Hybridization of miR-146b (green color) and *KIT* mRNA (red color); arrows highlight a polymorphic site within the binding domain (SNP rs3733542).

2.2 Investigating the role of the c-KIT gene in thyroid cancerogenesis:

In order to demonstrate an hypothetical role of c-KIT in the differentiation pathway of thyroid epithelium, we compared expression levels of c-KIT in thyroid malignant and benign samples with the expression levels of genes known to be thyroid-specific differentiation markers from the literature such as PAX8, TTF1 (tissue-specific transcription factors expressed in the thyroid follicular cells, contributing to the maintenance of the differentiated phenotype), which are possible downstream targets of the c-kit pathway.

In the thyroid gland, TTF-1 (also known as NKX2-1, T/EBP or TITF-1) is expressed in the follicular cells and, together with Pax8, controls the expression of Tg, thyroperoxydase (TPO), thyrotropin receptor (TSH), the sodium/iodide symporter (NIS) and calcitonin.

TTF-1 mRNA is detected in papillary carcinomas (PTC) but not in anaplastic carcinomas; therefore TTF-1 is considered as a marker to distinguish between these two types of thyroid neoplasms [93].

PAX8 is a paired-box gene important in embryogenesis of the thyroid and its expression has been previously described in Thyroid carcinomas.

Moreover, in order to evaluate a possible role of c-kit in thyroid neoplastic transformation, we have performed functional studies by over expressing this gene in thyroid cell lines that do not express the gene, expecting therefore to revert the malignant phenotype; and different functional studies were performed such as proliferation, migration, and survival assays.

2.3 New molecular markers to improve cytological diagnostic accuracy

We evaluated NIS, TC1, miRNA146b, miRNA222 expression as a new pre-operative diagnostic biomarker. Because of the lack of useful pre-operative diagnostic biomarkers, we sought to determine whether the expression profile of these genes on FNA cytological smears, could be performed on a routine basis so to improve the diagnostic sensitivity for malignancy in indeterminate or suspicious thyroid nodules without adding time and discomfort to the patient after a FNA procedure. Moreover in order to discover new molecular markers we performed receptor and non-receptor tyrosine kinase gene PCR Array analysis.

2.3.1 NIS and TC1 gene:

The Na+/I− symporter (NIS) is a key plasma membrane protein, located at the basolateral portion of the thyroid follicular cell, that mediates active iodide transport in the thyroid. Altered expression of the gene encoding the sodium iodine symporter (NIS) may be an important factor that leads to the reduced iodine accumulation characteristic of most benign and malignant thyroid nodules. Some studies have demonstrated a decrease or loss on NIS expression in thyroid cancer cells suggesting a possible role of this gene in the pathway of thyroid cell transformation [94], while either increased or decreased NIS expression in benign lesions has been reported [95].

Regarding TC1, the expression of the thyroid cancer-1 (TC1) gene resulted to be related to malignant transformation in thyroid, and the potential use of TC1 gene expression as a marker of malignancy in thyroid nodules is also shown in literature [96]; therefore the overexpression of TC-1 in papillary carcinoma suggests that it may have an important role in thyroid carcinogenesis.

2.3.2 miRNA as biomarker in Thyroid cancer:

Several independent studies have analyzed miRNA expression in numerous and different types of thyroid tumors, evidencing a miRNA deregulation in cancer tissues compared to their normal counterparts; in thyroid tumors 32% of all known human miRNAs resulted in being upregulated and 38% to be downregulated with more than a 2-fold change as compared to normal tissues [97]. Moreover, the miRNA expression profile presents a significant variability between different kinds of thyroid cancers, even if they originate from the same type of thyroid cells.

At the moment the exact biological roles of miRNAs in thyroid carcinogenesis remain to be fully elucidated but it seems reasonable that the distinctive pattern of miRNA expression in thyroid tumors compared to normal thyroid tissue may be useful in diagnosis and/or therapy of thyroid neoplasia and that different miRNA expression patterns in different types of thyroid tumors could be useful tools for their classification.

Comparing global miRNA expression in human PTCs versus unaffected thyroid tissue He et al. [98] individuated a set of five miRNAs (miR-146, miR-221, miR-222, miR-21, and miR-181a) that were significantly overexpressed in PTCs compared to the adjacent normal tissue. Particularly, three of them, miR-146, miR-221, and miR-222, showed 11- to 19-fold higher

level in tumor tissues. Deregulation of miR-146b, miR-221, and miR-222 in the thyroid may be a crucial component of PTC initiation and development. In my study, we analyzed the expression levels of miRNA146b and miRNA222 to better understand the relationships of their expression between malignant and benign FNA samples and the possibility to use them as biomarker in thyroid cancer.

2.3.3 Molecular computational model

Several biomarkers data were used to perform Discriminant Analysis and to build Bayesian Neural Networks (BNN) in order to obtain a molecular computational model able to preoperatively diagnose malignant and benign thyroid nodules.

2.3.3.1 Bayesian Neural Networks: clinical utility

Several attempts to use Bayesian Neural Networks in the clinical setting are described in literature [99-100], more specifically Liu and colleagues [101] have shown the clinical utility of a Bayesian network for differentiating benign from malignant thyroid nodules using sonographic and demographic features.

The procedure uses a Probabilistic Neural Network (PNN) to implement a nonparametric method for classifying cases into groups of data based on a set of *p* observed quantitative variables. Rather than making any assumption about the nature of the distribution of the variables within each group, it constructs a nonparametric estimate of each group's density function at a desired location based on neighboring observations from that group. Observations are assigned to groups based on the product of three factors: 1) the estimated density function in the neighborhood of the point; 2) the prior probabilities of belonging to each group; 3) the costs of misclassifying cases that belong to a given group.

The approach to classifying cases can be formulated as a *neural network*, whose basic setup consists of four layers: **input layer,** with *p* neurons, one for each of the input variables; **pattern layer,** with *n* neurons, one for each case that will be used to train the network; **summation layer**, with *g* neurons, one for each output class; **output layer**, also having one binary neuron for each output class that turns on or off depending on whether or not a case is assigned to the corresponding group. The input layer provides the information from the predictor variables by feeding their values (standardized by subtracting the mean and dividing by the standard deviation) to the neurons in the pattern layer. The pattern layer

passes the values through an “activation function”, which uses the input values to estimate (nonparametrically) the probability density function for each group at a given location. The density estimates are then passed to the summation layer, which combines the information from the training cases with prior probabilities and misclassification costs to derive a score for each group. The scores are then used to turn on the binary neuron in the output layer corresponding to the group with the largest score and turn off all other output neurons.

2.3.3.2 Discriminant analysis

Discriminant Analysis is a statistical classification method used to distinguish between two or more groups of data based on a set of *p* observed quantitative variables. It can help to describe observed cases mathematically in a manner that separates them into groups as well as possible, but also it can be used to classify new observations as belonging to one or another of the groups (*prediction*).

The classification is implemented by constructing “discriminant functions”, which are linear combinations of the *p* quantitative variables. Prior probabilities of belonging to each group may be defined according to some prior knowledge of the phenomenon, or directly derived from the observed data, by considering the proportions of the groups in the data. For an observation, the discriminant functions are used to assign a *score* to each group and, combining it with the prior probabilities, we will label the new observation as belonging to the group with the largest value of score*prior, i.e. the group which is the most likely to belong to. In particular, if the data are assumed to come from multivariate normal distributions, then the scores are related to the probabilities that an observation belongs to a particular group.

In order to estimate the discriminant functions, the *p* quantitative variables should be standardized by subtracting the sample means and dividing by the sample standard deviations. The discriminant functions are derived so as to maximize the separation of the groups. Sometimes, it could be useful to use a stepwise selection procedure (forward or backward) to select only those variables that are statistically significant discriminators amongst the groups.

2.3.4 Data analysis

The present study evaluates the expression of the analyzed markers (TC1, PAX8, NIS, TF1, miRNA 222, miRNA 146b, Tyrosine Kinases Array) in a molecular diagnostic approach to a

series of thyroid FNAC, together with the study of BRAF gene status.

First of all we stratified, through the Histological diagnosis, our casistic of FNA in malignant or benign lesions. Then, we stratified the samples by means of BRAF V600E mutational status.

Afterwards, we analyzed the expression levels of TC1, PAX8, NIS, TF1, miRNA 222, miRNA 146b, Tyrosine Kinases Array on FNA smears.

We conducted an association analysis between the expression level of each single marker with benign and malignant samples, and the expression level of single marker and BRAF status.

Based on the results we have conducted a molecular stratification of our population to evaluate the biological importance and diagnostic potential of the analyzed biomarkers.

2.5 Human Tyrosine Kinases RT Profiler PCR Array

RT² Profiler™ PCR Arrays are the most reliable and sensitive gene expression profiling technology for analyzing a panel of genes in signal transduction pathways, biological process or disease related gene networks.

In this present study we have used Human Tyrosine Kinase PCR Array**,** which profiles the expression of 84 receptor and non-receptor tyrosine kinase genes. The protein tyrosine kinase superfamily includes roughly 60 receptor tyrosine kinases (RTKs) and about 30 intracellular tyrosine kinases. Tyrosine kinases are involved in many basic biological processes, such as cell growth, proliferation and differentiation. These processes are commonly dysregulated during oncogenesis, often due to mutation of key tyrosine kinases or regulators. These oncogenic processes make the tyrosine kinase superfamily members attractive drug targets, and there are several chemotherapeutics targeting tyrosine kinases already on the market (e.g., imatinib mesylate). Since in our laboratory we have already conducted deep studies on the expression of a tyrosine kinase gene, c-kit, whose expression was found strictly associated with the biological behaviour of thyroid nodules, studying the arrays of other tyrosine kinases could be really interesting. In fact they could yield new insights into the expression of more tyrosine kinase in our FNA samples, in order to investigate their involvement in the carcinogenesis of the thyroid.

3. MATERIALS AND METHODS

3.1 Thyroid specimens

Pre-operative thyroid FNAs of 169 patients (Tab 1) were selected from archived materials in the Section of Cytopathology, Division of Surgical, Molecular and Ultrastructural Pathology. All patients had a thyroidectomy with histopathological examination based on clinical elements or of a cytological diagnosis of malignancy, suspected malignancy, or if indeterminate.

For ethical reasons, we used only cases with two or more slides per patient, and the molecular analysis was performed on only one of the available smears. In all cases FNA has been performed using ultrasonographic guidance.

Table 3.1 Cytology, sex, and BRAF status of 169 thyroid nodules

Histological Diagnosis	**SEX**	**BRAF**	
	56 **M**	**WT**	**V600E**
MN: 103 cases	47 **F**	39	64
	26 **M**	**WT**	**V600E**
BN: 66 cases	40 **F**	66	0

MN: malignant nodule, BN: benign nodule, M: male, F: female, WT: wild type.

3.2 Ethical Board

This study was approved by the Internal Review Board (IRB) of the University of Pisa. All patients gave their consent for the participation to the study.

3.3 FNA slides

The slides were obtained from FNA samples and fixed in ethyl alcohol for Papanicolaou staining. Smears were reviewed by a senior cytopathologist. All archival FNA slides were kept in xylene for 1 to 3 days, depending on the time of storage, to detach slide coverslips. Slides were then hydrated in a graded series of ethanol baths, followed by a wash in distilled H_2O for 1 minute and finally air-dried. The processing of the slides was performed in a range of few days to a maximum of 10 years after FNA procedure.

3.4 DNA extraction

DNA extraction was performed using a commercial kit (Nucleospin; Macherey-Nagel, Düren, Germany) mainly following manufacturer's instruction. A modification was added to the first step: 50% of the lysis solution with no Proteinase K was initially poured on the slides to scrape off the cytological stained sample using a single-edged razor blade. Any scraped tissue was then collected in a microcentrifuge tube containing the other half of the lysis solution with the Proteinase K. The extracted DNA was kept at -20 °C until used. The quantity/quality of extracted DNA was estimated with Nanodrop 1000 spectrophotometer by using 1 μl of undiluted DNA solution .

3.5 RNA extraction and cDNA synthesis

RNA extraction was performed by using a commercial kit (High Pure RNA Paraffin kit, Roche) mainly following the manufacturer's instructions and adding the same modification step as for DNA extraction. The lysis solution was poured on the slide to scrape off the cytological stained sample by using a single edged razor blade. Whole scraped material was then collected in a microcentrifuge tube and processed for RNA extraction. The quantity/quality of extracted RNA was estimated with Nanodrop 1000 spectrophotometer by using 1 μl of undiluted RNA solution. RNA was treated with DNase I recombinant, RNase-free (Roche). RNA was reverse transcribed in a final volume of 20 μl, containing 5X RT buffer, 10 mM dNTPs, 50 ng/μl Random Primers, 0.1M DTT, 40 U/μl RNaseOUT, 50 μM oligo(dT), DEPC- Treated Water, 15 U/μl Cloned AMV reverse transcriptase (Invitrogen, Carlsbad, CA).

3.6 BRAF V600E detection

BRAF exon 15 was analyzed by polymerase chain reaction (PCR) followed by direct sequencing. Primers were selected using Primer3 software (Tm 56^0C):

BRAF 15 F: 5’-TCATAATGCTTGCTCTGATAGGA-3’

BRAF 15 R: 5’-GGCCAAAAATTTAATCAGTGGA-3’

PCR reactions were run on agarose gel to check the presence of the specific amplification products. PCR bands were cut and purified using the Genelute Gel Extraction Kit (St. Louis, MO). Purified products were then sequenced on the ABI PRISM 3100 Genetic Analyzer (Applied Biosystem).

3.7 Primer Design

3.7.1 Designing and optimization of primers using Primer 3 software

Table 3.2

PRIMERS FOR EXPRESSION STUDY		
NAME	SEQUENCE (5’-3’)	Annealing temperature (C^0)
KIT F	GCACCTGCTGCTGAAATGTATGACATAAT	60
KIT R	TTTGCTAAGTTGGAGTAAATATGATTGG	60
PAX8 F	GTGGCAGATCCTCACTCACC	60
PAX8 R	ATGGGGAAAGGCATTGAAG	60
TFF1 F	GATGTCCTCGGAAAGTCAGC	60
TFF1 R	CTCCAGGGGACTCAAGATGT	60
TC1 F	AAATCTTCTGACTAATGCTAAAACG	60
TC1 R	TTATTGTTGCATGACATTTGC	60
NIS F	CCCTCATCCTGAACCAAGTG	60
NIS R	AACCCAGAAGCCACTTAGCA	60
B2M F	CATTCCTGAAGCTGACAGCATTC	60
B2M R	TGCTGGATGACGTGAGTAAACC	60

Table 3.3

PRIMERS USED DURING SUBCLONING AND SCRENING BY PCR OF THE COLONIES		
NAME	SEQUENCE (5'-3')	Annealing temperature (C^0)
C-KIT_B_LONG F	AGCTGGAACGTGGACCAGAG	58
C-KIT_B_LONG R	TGTGCTCAGAAAGACAGGATTG	58
C-KIT 1F	AGCTGGAACGTGGACCAGAG	59
C-KIT 1R	ACGTTGCCTGACGTTCATAA	59
C-KIT 2 F	AGGGAAGGGGAAGAATTCAC	59
C-KIT 2 R	AAGGAGTGAACAGGGTGTGG	59
C-KIT 3 F	AGTGCATTCAAGCACAATGG	59
C-KIT 3 R	AGTCTAGGGCCAACTCGTCA	59
C-KIT 4 F	GCCGACAAAAGGAGATCTGT	59
C-KIT 4 R	TGTGCTCAGAAAGACAGGATTG	59

Table 3.4

PRIMERS FOR REFLP ANALYSIS		
NAME	SEQUENCE (5'-3')	Annealing temperature (C^0)
C-KIT-EXON8 F (DNA)	TAGTATTTTTTGGTTTGGGAA	60
C-KIT-EXON8 R (DNA)	CTAACCCCTACTCTTTCAACAT	60
C-KIT-EXON8 F (cDNA)	TGACTTACGACAGGCTCGTG	60
C-KIT-EXON8 R (cDNA)	CTCTGCTCAGTTCCTGGACA	60

3.7.2 Designing and optimization of primers using MSP (methylation-specific PCR) tool

Table 3.5

PRIMERS METHYLATION STATUS OF C-KIT PROMOTOR		
NAME	SEQUENCE (5'-3')	Annealing temperature (C^0)
C-KIT_MSP _U F	TAGTATTTTTTGGTTTGGGAA	59
C-KIT_MSP_U R	CTAACCCCTACTCTTTCAACAT	59
C-KIT_MSP_M F	TATTTTTTTGGTTCGGGAAC	59
C-KIT_MSP_M R	ACCCCTACTCTTTCGACGTA	59

3.8 PCR protocol

PCR were performed in a 30 µl final volume, containing 150 ng of genomic DNA or 2 µl of cDNA, 0.05 mM dNTP (Invitrogen, Carlsbad, CA), 2.5ng/µl of each primer (Invitrogen), 1.5 mM MgCl2, 1x PCR Gold Buffer, and 0.75U AmpliTaq Gold (Applied Byosistems, Foster City, CA). PCRs were performed on a 9700 GenAmp PCR System (Applera Corporation, Foster City, CA) with the following cycling conditions at 94 °C for 7 minutes; 40 cycles at 94 °C for 45 seconds, 56/60/59 °C (the Tm for each pairs of primers are shown in the section "Designing and optimization of primers") for 45 seconds, and 72 °C for 1 minute; and final step at 72 °C for 10 minutes

3.8.1 Quantitative Real-Time PCR (qPCR)

The level of KIT, PAX8, NIS, TC1, TFF1, expression was analyzed by quantitative Real-Time PCR (qPCR) on the Rotor-Gene 6000 real time rotary analyzer (Corbett, Life Science, Australia) following the manufacturing instructions. Endogenous reference gene (B2M, beta 2 microglobulin) was used to normalize each gene expression level. PCR products were previously sequenced on an Applied Biosystems 3130xl Genetic Analyzer (Foster City, CA) to confirm gene sequence. PCR was performed in 25 µl final volume, containing 5 µl of cDNA, 12.5 µl of MESA GREEN qPCR MasterMix Plus (EUROGENTEC, San Diego, CA), 40 pmol of each primer (Invitrogen, Carlsbad, CA) *per* reaction with the following cycling conditions: initial denaturation

95°C for 5 min; 40 cycles at 95 °C for 15 sec and 60 °C for 40 sec and 72 °C for 40 sec; final step 25 °C for 1 min. Primers were selected using Primer3 software (primer sequences and Tm are shown in the Table 3.2). A first PCR run was performed on control sample expressing the markers and run on 2% agarose gel. The PCR product was excised from the gel, purified by using GenEluteTM PCR Clean-Up (Sigma-Aldrich) and measured spectrophotometrically at 260 and 280 nm. The purified product was diluted in a 10-fold series to create the standards for a ten-point standard curve that was run in triplicate. Standard curves were generated for each gene and B2M and showed a good linearity with consistent correlation coefficient (R2 = 0.999). Ct was determined by the Rotor-Gene 6000 software and exported for analysis after background subtraction. Threshold was set by standard curve and then imported in all the runs for data analysis. PCR efficiencies resulted similar for the marker genes and B2M in each experiment and ranged between 98-102%. The experiment was run in duplicate for each sample. For each cDNA sample the ratio between the gene of interest expression value and B2M expression value was calculated. The expression ratio mean values and standard deviations of malignant and benign groups were calculated. To verify primers specificities, melting curve analysis was performed. Fluorescent data were acquired during the extension phase. After 40 cycles a melting curve for each gene was generated by slowly increasing (0.1°C/s) the temperature from 60°C to 95°C, while the fluorescence was measured. For each experiment a no-template reaction was included as a negative control. The expression of all the markers was ultimately represented as the ratio of absolute quantification by standard curve of the expression of the markers and B2M expression.

3.9 Methylation status of c-KIT promoter after bisulfite treatment

Total DNA (500 ng) was modified with sodium bisulfite, which converts all unmethylated cytosines to uracil and the methylated cytosines remain unchanged using the EZ DNA Methylation™ Kit (Zymo Research) according to the manufacturer's protocol.

Namely, Dna was denatured by the addition of Zymo M-Dilution buffer and incubated for 15 min at 37^0 C. CT-conversion reagent (bisulfite-containing) was added to the denatured DNA and incubated for 16 h at 50^0 C. After bisulfite conversion, the DNA was bound to Zymo spin column and desulfonated on the column using M-desulfonation reagent per manufacturer's protocol. The bisulfite-converted DNA was eluted from the column in 10 μl of elution buffer.

PCR was conducted on bisulfite treated DNA with primers designed by means *MSP (methylation-specific PCR) primer design tool* (primer sequences and Tm are shown in the Table 3.5): particularly two pairs of primers were designed, one is specific for methylated DNA (M pair), and

the other for unmethylated DNA (U pair). For each sample to be studied, two PCRs were performed with each pair of primers to amplify methylated and unmethylated c-KIT promoter sequences and after the PCR products were run on 3% agarose gel. The Amplification with M pair indicates methylation of CpG site(s) within the primer sequences, U pair no methylation, and both pairs partial methylation.

To confirm c-KIT promoter sequence, PCR products were purified and sequenced by means an Applied Biosystems 3130*xl* Genetic Analyzer (Foster City, CA)

3.10 c-KIT SNP rs3733542 genotyping by restriction fragment length polimprphisms RFLP analysis

We genotyped 118 samples: in some case DNA was available and in some case only the cDNA was available therefore for each analysis we designed primers appropriate for cDNA and DNA. The PCR primers (C-KIT-EXON 8 F [DNA], C-KIT-EXON 8 R [DNA], C-KIT-EXON 8 F [cDNA], C-KIT-EXON 8 R [cDNA]),were designed upstream and downstream of the restriction site in exon 18 of C-KIT using Primer3 software (primer sequences and Tm are shown in the Table 3.4).

To verify the c-KIT sequence the PCR products were purified by ABI PRISM 3100 Genetic Analyzer (Applied Biosystems). The PCR products were subjected to restriction enzyme digest in 20 µl final volume, containing 0.2 μl of Restriction Enzyme SAC I (10 U/ μl), 0.2 μl BSA (10 mg/ ml), 2 μl NEBuffer (10X) (Promega Comporation), 5.1 μl water and 12.5 μl PCR product. The Restriction Enzyme SAC I recognizes the sequence " GAGCTC" and the digestion occurs between the thymine and cytosine nucleotide. After incubation at 37°C overnight DNA fragments were separated by electrophoresis on 3% agarose gel: one single fragment represents a non-digestion equal to a wild type, 2 different fragments represent the SNP in homozygosity, while 3 different fragments represent the SNP in heterozygosity.

3.11 miRNA extraction from FNA samples and miRNA expression assay by RT-PCR

Purification of miRNA was performed by using miRNeasy Mini Kit (Qiagen) according to the manufacturer's instructions. Quantitative reverse transcription (RT) was performed using miScript II RT Kit that is an integral component of the miScript PCR System for miRNA detection and quantification (Qiagen). cDNA generated with the miScript II RT Kit was used as a template

for real-time PCR with the miScript SYBR Green PCR Kit with miRNA specific primers for miR-146b and miR-222 (Qiagen).

These 2 miRNAs were chosen based on previous reports of miRNA expression in thyroid cancer specimens. Quantitative polymerase chain reaction was run on an Rotor-Gene 6000 (Corbett, Qiagen), the cycling conditions were: 1 cycle at 95 °C for 15 minutes, 40 cycle at 94 °C for 15 seconds, 55 °C for 30 seconds and 70 °C for 30. After 40 cycles a melting curve was generated by slowly increasing (0.1°C/s) the temperature from 55°C to 99°C, while the fluorescence was measured. Samples were detected in duplicate and relative expression levels were calculated using U61 small nuclear RNA (SNORD61, Qiagen) as the endogenous control.

3.12 Human Tyrosine Kinases RT² Profiler PCR Array

The clearance of genomic DNA contamination in RNA samples and cDNA Synthesis was conducted using the RT² First Strand Kit (Qiagen). The cDNA generated with RT² First Strand Kit was preamplified by RT² PreAMP Pathway Primer Mix and after was used as a template for Real-Time PCR Array in Rotor-Disc 100 format with RT² SYBER Green Mastermix. Real-Time PCR Array in Rotor-Disc 100 contains primer assays for 84 genes and 5 housekeeping genes, and in addition one well contain a genomic DNA control, 3 wells contain reverse-transcription controls, and 3 wells contain a positive PCR control (the list of the 84 Tyrosine analyzed are shown in Table 3.6). Cycling conditions for Rotor-Gene cyclers were:

1 cycle at 95 °C for 10 minutes, 40 cycle at 95 °C for 15 seconds, and 60 °C for 30 seconds. Melting curva was perfermed to verify the PCR specificity.

Afterwards the threshold cycle (C_t) was calculated manually by using the log view of the amplification plots, and the treshold value was chosen above the background signal.

All CT values was exported to a blank Excel spreadsheet for use with the PCR Array Data Analysis Template Excel on Qiagen website; in order to analyze the date was used the $2^{-\Delta\Delta CT}$.

Table 3.6 List of the 84 Human Tyrosine Kinases analyzed

Receptor Tyrosine Kinases
ALK Family: ALK, LTK.
AXL Family: AXL, MERTK, TYRO3.
DDR Family: DDR1, DDR2.
EGFR Family: EGFR, ERBB2 (HER2), ERBB3, ERBB4.
EPH Family: EPHA1, EPHA2, EPHA3, EPHA4, EPHA5, EPHA7, EPHA8, EPHB1, EPHB2, EPHB3, EPHB4, EPHB6.
FGFR Family: FGFR1, FGFR2, FGFR3, FGFR4
INSR Family: IGF1R, IGF2R, INSR, INSRR.
MET Family: MET, MST1R (RON).
PDGFR Family: CSF1R, FLT3, KIT (CD117), PDGFRA, PDGFRB.
ROR Family: ROR1, ROR2
TIE Family: TIE1, TEK (TIE2).
TRK Family: NTRK1, NTRK2, NTRK3
VEGF Family: FLT1 (VEGFR1), FLT4 (VEGFR2), KDR (VEGFR3).
Other Genes: MUSK, PTK7, RET, ROS1, RYK.

Non-Receptor Tyrosine Kinases
ABL Family: ABL1, ABL2 (ARG).
ACK Family: TNK1, TNK2 (ACK1).
AXL Family: AXL, MERTK, TYRO3.
CSK Family: CSK, MATK.
FAK Family: PTK2 (FAK), PTK2B (PYK2).
FES Family: FER, FES.
FRK Family: FRK, PTK6 (BRK), SRMS.
JAK Family: JAK1, JAK2, JAK3, TYK2.
SRC-A Family: FGR, FYN, SRC, YES1.
SRC-B Family: BLK, HCK, LCK, LYN.
TEC Family: BTK, ITK, TEC, TXK
SYK Family: SYK, ZAP70.

3.13 Functional studies

3.13.1 Cell culture, RNA isolation and RT-qPCR

K1 cells (Human papillary thyroid carcinoma cell line from SIGMA-ALDRICH, St Louis, MO, USA) were grown in DMEM:Ham′s F12 (2:1) medium supplemented with 10% FBS, 1% L-glutamine, 1% penicillin-streptomycin (Life Technologies). SKMEL-28 cells (Human Melanoma Cell Line) were grown in Dulbecco's Modified Eagle Medium supplemented with 10% FBS, 1% L-glutamine, 1% penicillin-streptomycin (Life Technologies). Cells were kept at 37°C in a 5% CO2/95% humidified air environment.

To extract the RNA, cells were spun for 5 min at 12000 rpm, the supernatant was removed and cells were resuspended in PBS 1X. Then, the resuspended pellet was spun at 12000 rpm for 5 min, the supernatant was removed and total cellular RNA was isolated using TRIZOL reagent (Gibco-BRL) according to the manufacturer's protocol and precipitated with isopropanol.

The RNA pellet was washed in 80% ethanol and resuspended in H_2O.

The RNA was retro-transcribed to cDNA and the level expression of c-kit was conducted in K1 and SKML-28 cell lines by Quantitative Real-Time PCR as described in previous section.

3.13.2 Immunocytochemistry

K1 and SKMEL cancer cell lines where grown in the appropriate media and after reaching confluency incubated with trypsin. The collected cells were used to prepare the slides by means of monolayer THIN PREP technique. Afterwards we followed the immunocytochemistry protocol: we fixed and permeabilized the slides in acetone for 10 min at -20 °C, we washed 2 times 5 min each with PBS 1X and dried on air; the slides were incubated with citrate buffer for antigen retrieval and washed 3 times with PBS 1X. Then we have incubated with blocking solution (PBS 1X, 0,1% Triton X100, 1% albumin) to eliminate background for 1h at room temperature. After we have incubated with primary anti-c-kit antibody (Ab81) (Santa Cruz Biotechnology) in blocking solution at 4°C over night. The day after we have conducted washes with PBS1X and Triton X100 for 3 times 5 min each, subsequently we have incubate with secondary antibody anti-human CD117 polyclonal rabbit (DAKO) in PBS1X 1 h at room temperature. Then we have washed with PBS 1X for 3 times 5 min each and we have conducted ABC (avidin-biotin complex) detection system for 30 minutes, washed with PBS1X for 3 times 5 min each, and we have treated the slides with DAB for 2 min and washed with water. We immersed the slides in hematoxylin 5-10 times and washed with water. Finally we dehydrated the slides

(95% ethanol 5 min, 100% ethanol 5 min, xylene 10 min) and were mounted with a drop of balm and viewed under a fluorescence microscope.

3.13.3 Subcloning

The purified Plasmid (pBluescriptR vector: IRATp970H0287D), containing the cDNA sequence of c-kit (2031 bp), was purchased form Source BioScience (GenomeCube); the c-kit sequence was amplified by PCR using primer (C-KIT_B_LONG F, C-KIT_B_LONG R) designed with Primer 3 software (primer sequences and Tm are shown in the Table 3). Then the PCR product was purified (QIAquick PCR Purification Kit, Qiagen) and validated by sequencing on ABI PRISM 3130XL Genetic Analyzer.

Afterwards the C-KIT cDNA was subcloned into the mammalian expression vector pTARGET™ (Promega) with ampicillin and neomycin resistance genes, according to the manufacturer's protocol. The competent E.coli DH5α cells were transformed, by heat-shock treatment, with the recombinant vector pTARGET™-C-KIT and selected on ampicillin agar plates.

Screening by PCR and validation by sequencing were conducted on colonies, with a percentage of correct recombinant clones greater than 80%. The primers were designed by Primer 3 software :

C-KIT 1F, C-KIT 1R, C-KIT 2 F, C-KIT 2 R, C-KIT 3 F, C-KIT 3 R, C-KIT 4 F, C-KIT 4 R (primers sequences and Tm are shown in the Table 3.3).

The sequencing was conducted with a first step of purification of the PRC products with one Multi Screen PCR Plates (Millipore) and the sequencing reactions were performed in 20 μl final volume using Big Dye Terminator kit v3.1 (Applied Biosystems) and 2.5 pmol/μl of each primer, and then purified with Multi Screen PCR Plates (Millipore). The sequence reactions were loaded on ABI PRISM 3100 Genetic Analyzer (Applied Biosystems) and analyzed using the Sequencing Analysis software 3.4 version.

3.14 Statistical analyses

Statistical analyses were carried out by specific computer programs.

Quantitative data were expressed as mean ± standard deviation. The expression levels of NIS, Pax8, TTF1 and TC1, miRNA 146b, miRNA 222, KIT among benign and malignant samples were statistically analyzed by Student's t-test and linear regression. The Kruskal-Wallys test was performed to study the association between c-KIT classes distribution and expression values of the afore mentioned genes. Data sets were also screened by one-way analysis of variance (ANOVA),

and a Tukey test was used for post hoc analysis. Chi-square test was used to compare two groups (dependent samples) expressed as a percentage.

A significant difference was considered for p-value < 0.05. Several computational models (Neural Network Bayesian Classifiers, *Discriminant analysis*) were built in order to find the best combination of markers able to discriminate benign from malignant thyroid samples.

The Neural Network is used to classify cases into malignant and benign categories and to classify BRAF mutational status, based on 4 input variables (KIT, miRNA 222, miRNA 146b, TC-1 expressions) by implementing a nonparametric method for classifying observations into one of benign and malignant groups, and into one of malignant BRAFV600E and malignant BRAFWT groups, based on the observed expression variables. The Discriminant analysis is used to determine which variables discriminate between two or more groups, given several quantitative (independent) variables (KIT, miRNA 222, miRNA 146b, TC-1) and a categorical (dependent) variable (malignant and benign; BRAF WT and BRAFV600E). These analyses were all performed by using MedCalc for Windows, version 12 (MedCalc Software, Mariakerke, Belgium) and Statgraphics, version 15.

Principal Component Analysis (PCA) and k-means clustering were conducted as descriptive tools by using a R software (code "princomp"), and was used a logarithmic transformation of the data to stabilize the variances of the variables, since the PCA is sensitive to the relative scaling of the data.

To determine the diagnostic accuracy of the molecular computational model, we calculated the area under the curve (AUC) of the receiver operating characteristic (ROC) curve for each gene individually by using logistic regression analysis (Medcalc 11, Medcalc Software, Stata Software).

In this analysis the true positive rate (Sensitivity) is plotted in function of the false positive rate (100-Specificity) for different cut-off points. Each point on the ROC plot represents a sensitivity/specificity pair corresponding to a particular decision threshold. A test with perfect discrimination (no overlap in the two distributions) has a ROC plot that passes through the upper left corner (100% sensitivity, 100% specificity). Therefore the closer the ROC plot is to the upper left corner, the higher the overall accuracy of the test [103].

In order to evaluate the biological importance of the markers analyzed, a multiple variable analysis was performed to analyze the correlation between the markers. These analyses were all performed by using Statgraphics Centurion (V. 15, StatPoint, Inc.).

4 RESULTS

4.1 BRAF status characterization

All 169 FNA samples analyzed in this study were molecularly characterized for the presence of the V600E BRAF mutation in exon 15: 64/103 malignant samples carried the V600E mutation (62%) while all 66 benign samples were wild type for BRAF exon15 as shown in figure 1.

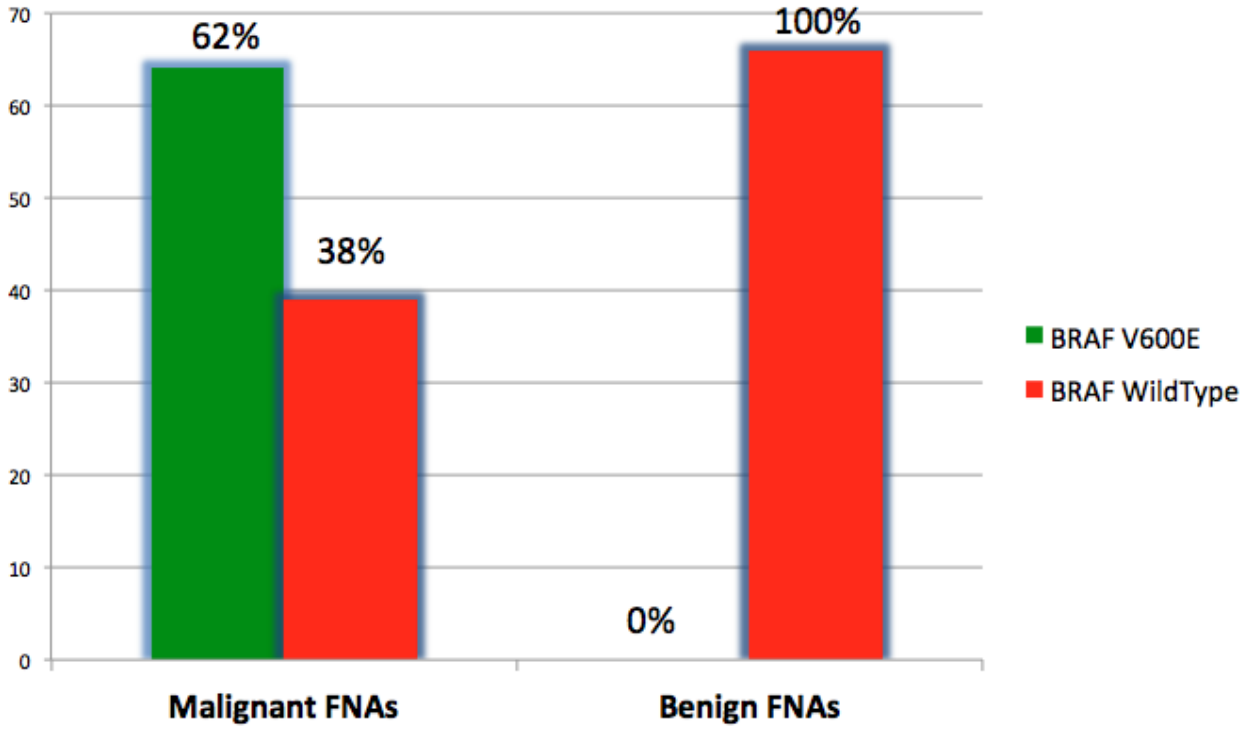

Figure 4.1: BRAF V600E distribution in our FNA sample dataset

4.2 c-KIT gene in thyroid transformation

Previous studies have been conducted in our laboratory to evaluate the expression levels of the c-KIT gene from 82 FNA smears, 46 malignant and 36 benign at the histology. The value of KIT expression resulted to range between 0 and 9.34. To evaluate a possible relationship with the

biological behaviour of lesions, KIT expression values (ev) were arbitrarily organized in four classes. Class I and IV contain 100% of the samples malignant or benign respectively. In class II the percentage of malignant cases resulted higher than benign (65% vs 35%) and the class III had a higher percentage of benign cases than malignant ones (86% vs 14%) (Table 4.1)

Class	KIT ev	PTC		BN		p value
		n	%	n	%	
I	0	19	100	0	0	< 0.0001
II	> 0 - ≤ 0.5	24	65	13	35	= 0.1400
III	> 0.5 - ≤ 3.0	3	14	18	86	< 0.0001
IV	> 3	0	0	5	100	= 0.0091
		46		36		

Table 4.1: Classes of KIT expression value. KIT ev: KIT expression value. PTC: papillary thyroid carcinoma. BN: benign nodule.

4.2.1 Methylation status of c-KIT promoter:

Investigation of the methylation status of c-KIT promoter was conducted on 68 FNA smears histologically diagnosed as 26 benign and 42 malignant thyroid nodules. We conducted an association analysis between promoter methylation and benign/malignant status, c-kit classes of expression and presence/absence of c-kit gene expression. The results showed no significative association between promoter methylation and benign/malignant status (results not shown). However the presence of methylation decreased as the c-kit gene expression increased (χ^2 test, p-value = 0.06). In fact, in c-kit class-1 the methylation was present in 4/14 (28.57%), in c-kit class-2 it was present in 13/20 (65%), and in c-kit class-3 it was present in 5/7 (71.42%) samples (Figure 4.2A). Moreover the group of samples with no c-kit expression had a significantly higher frequency of methylated cases (10 out of 14, i.e. 71.43%) than samples with c-kit expression (9 out 27, i.e. 33.34% methylated) (χ^2 test p-value = 0.02) (Figure 4.2B)

A

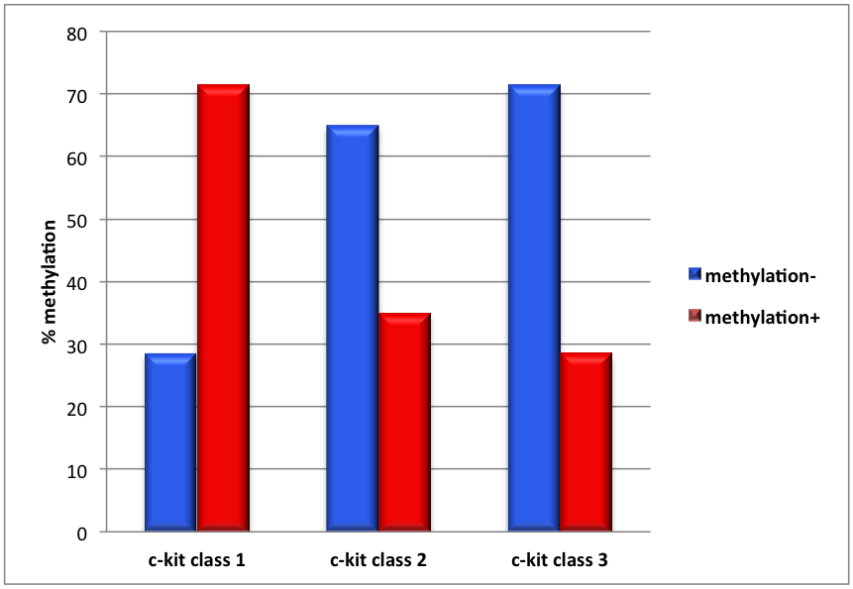

B

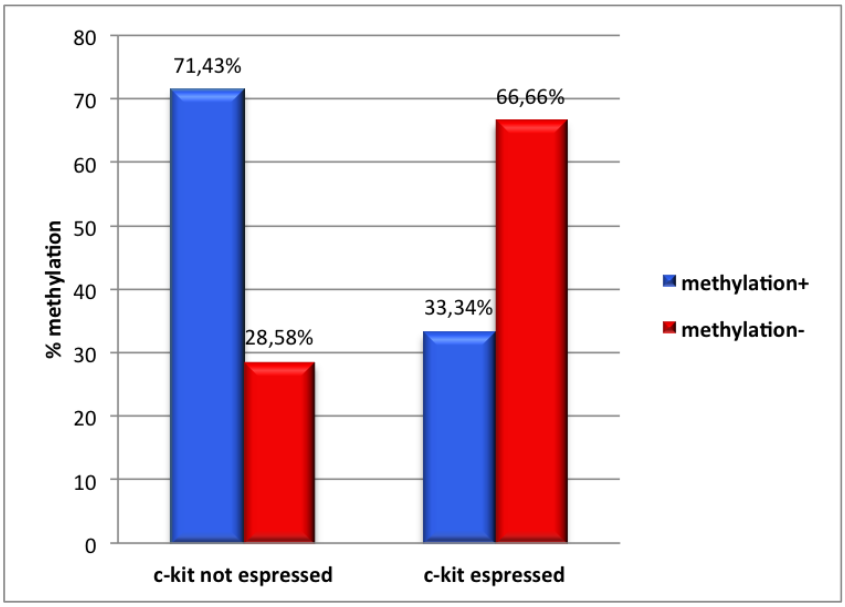

Figure 4.2: (A) correlation between methylation and c-kit classes of expression; (B) association between methylation status and presence or absence of c-kit gene expression

4.2.2 c-KIT SNP rs3733542 analysis:

The analysis of L862L [G/C] in c-KIT exon 18 from 125 FNA smears: 32 benign and 86 malignant samples. The digestion occurs between the thymine and cytosine nucleotide. We obtained after enzymatic digestion with SAC I that DNA/CDNA samples with polymorphism showed 3 fragments of different lengths:

	Fragment I	Fragment II	Fragment III
DNA	229 bp	195 bp	34 bp
CDNA	131 bp	108	23 bp

(Figure 4.3A)

The SNP rs3733542 was present in 10/86 (11.6%) and in 6/32 (18.7%) malignant and benign thyroid lesions respectively. The distribution difference between groups was not statistically significant. The level of c-KIT expression was slightly lower in the samples carrying the polymorphism as expected but did not reach any statistical significance (Figure 4.3B).

A

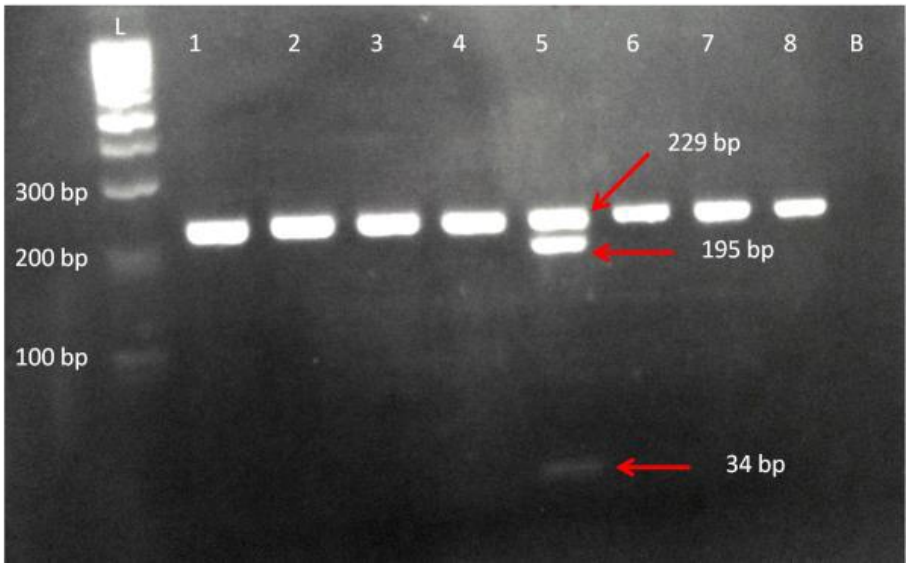

B

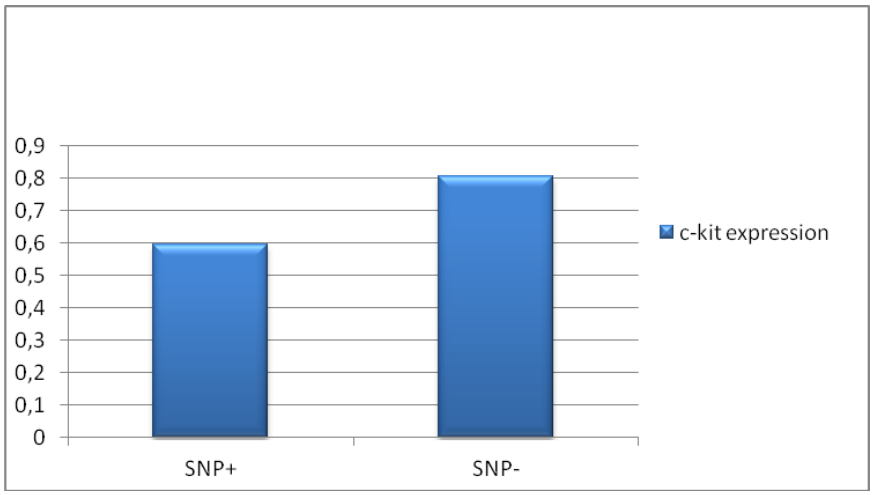

Figure 4.3: (A) SAC1 Digestion is represented in sample No. 5:intact DNA 229 bp, digested DNA 195 bp fragment and 34 bp fragment. Samples 1-4 and 6-8 are not digested by SAC1. L: Ladder. B: Blank; (B) c-KIT expression level and presence of c-KIT ex18 SNP rs3733542

4.2.3 Correlation among miRNA 146b, miRNA 222 and c-KIT expression:

The miRNA 146b and 222 expression was analyzed by qPCR in 57 FNA samples and correlated to the expression of c-KIT.

The group of samples with no c-kit expression (n= 16, 28%) showed a significant up-regulation of both miRNAs compared with the group of samples with c-kit expression (n= 41, 72%) (miRNA146b: mean 250.99 vs 103.74 ; miRNA222: mean 38.50 vs 6.62 respectively) (Figure 4.4 A, B). In order to assess the sign of the relationship of miRNA146b and miRNA222 with c-kit, we looked at the correlation coefficient: both miRNA146b and miRNA222 are negatively correlated with c-kit ($r = -0.29$, $r = -0.12$, respectively).

Moreover, based on c-kit classes distribution (Class I: KIT ev = 0; Class II: KIT ev > 0 and ≤ 0.5; Class III: KIT ev > 0.5 and ≤ 3; Class IV: KIT ev > 3) we obtained, by ANOVA and Tukey test, that in class I the expression level of miRNA 146b was significantly higher compared to class 4 (p-value <0.05) (Figure 4. 5).

A

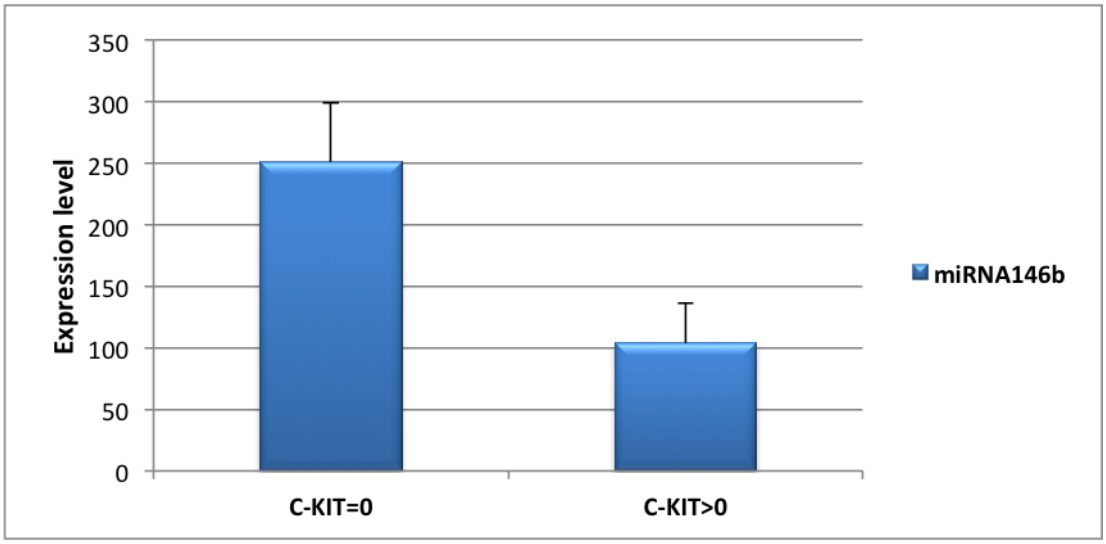

B

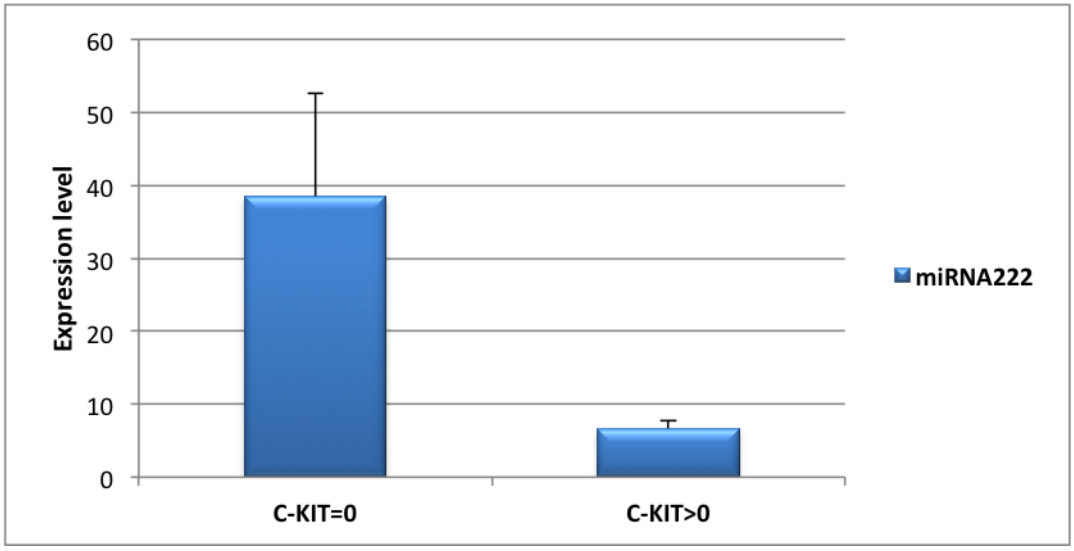

Figure 4.4: Expression levels of (A) miRNA146b and (B) miRNA222 compared with c-KIT expression: c-KIT =0 and c-KIT>0 (p-value = 0.01693; p-value = 0.0008 respectively)

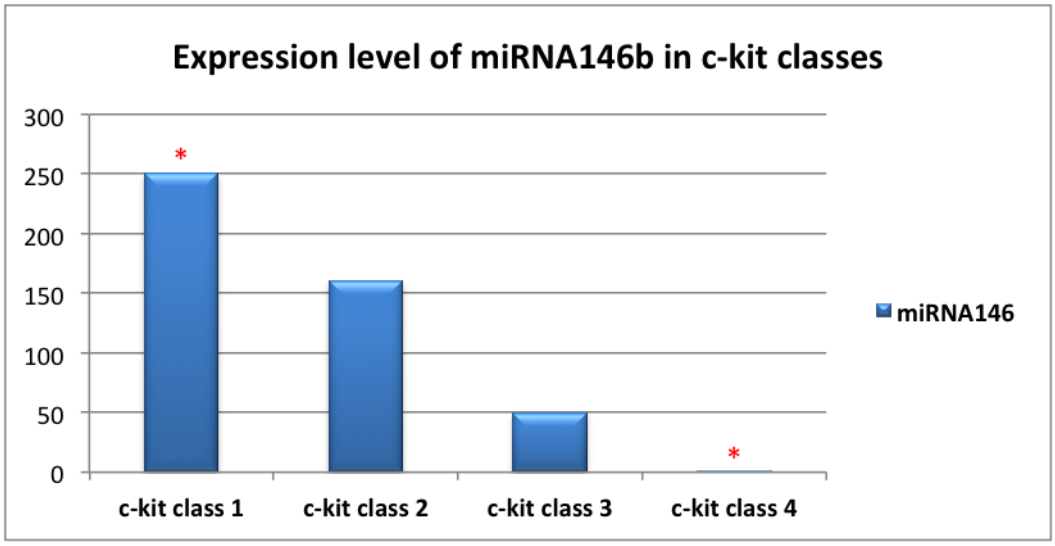

Figure 4.5: Expression levels of miRNA146b in c-kit classes.

4.2.4 PAX8 and TTF1 expression levels:

We analysed the expression levels of PAX8 (69 FNA smears) and TTF1 (54 FNA smears) genes to study the relationships of the expression of these genes in malignant and benign samples and we evaluated the possible correlation to c-KIT expression.

Studies conducted on PAX8 gene showed that expression level was significantly higher in the benign group (n=39, mean=61,58) compared to the malignant group (n=30, mean=25) (p=0.03) (Figure 4.6A).

Based on c-kit classes distribution, PAX8 gene expression values were significantly higher in class 2 and 3 compared to class 1 ($p<0.05$) (the comparison analysis with c-kit class 4 was not conducted due the lack of samples) (Figure 4.6B). C-kit gene expression resulted to be significantly correlated to pax8 gene expression (r^2 =0.1319) (p=0.003) (Figure 4.6C).

As regards TTF1 gene we found a lower expression in the benign group (n=33, mean=27.29) compared to the malignant group (n=21,mean=74.15) (p=0.06) (Figure 4.7A). There was neither significant difference between TTF1 gene expression values based on c-kit classes distribution nor correlation between c-KIT and TTF1 gene expression (r^2 =0.017) (the comparison analysis with c-kit class 4 was not conducted due the lack of samples) (Figure 4.7B,C).

A

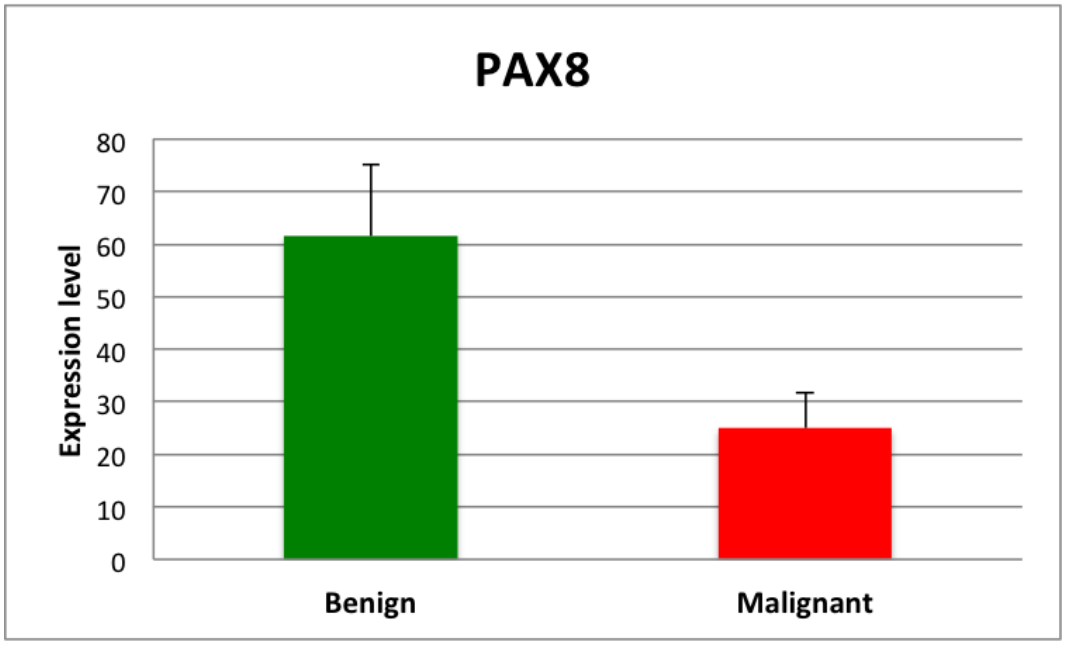

B

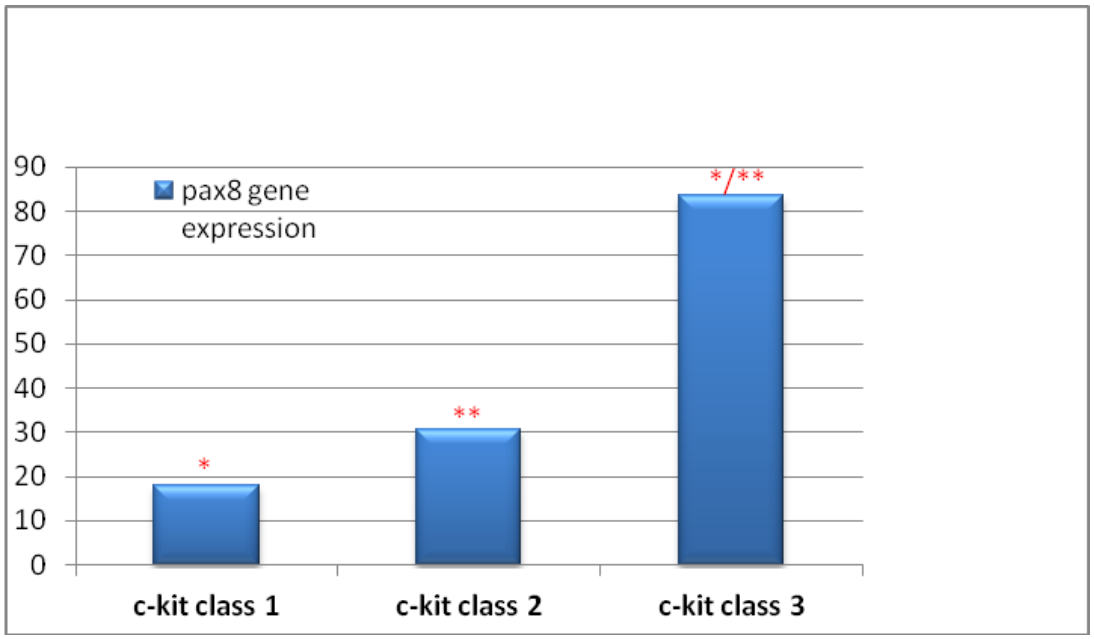

C

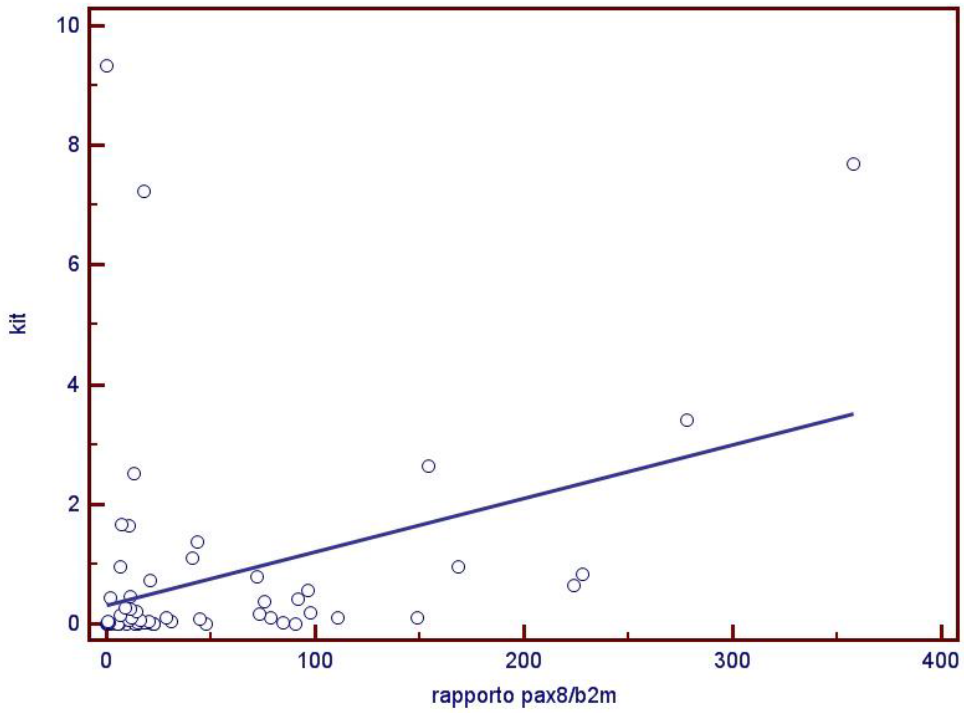

Figure 4.6: A) expression levels of pax8 in benign and malignant thyroid lesions; B) expression levels of PAX 8 in c-kit classes. C) linear regression analysis.

A

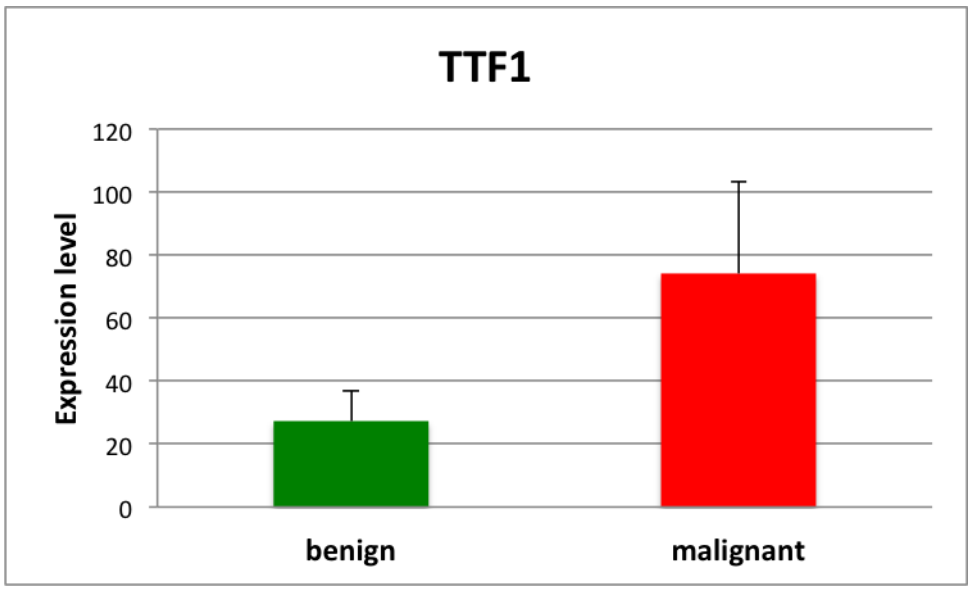

B

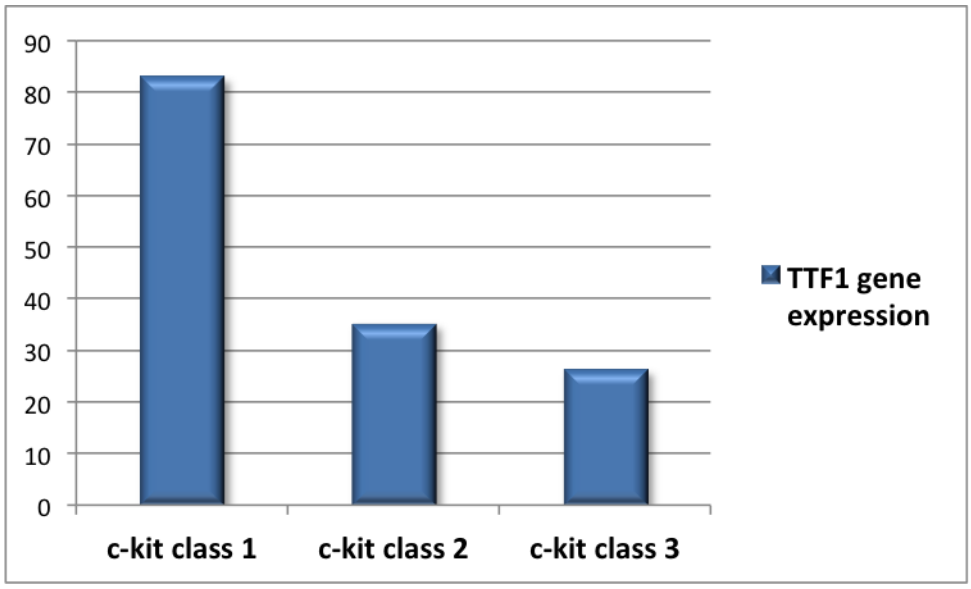

Figure 4.7: A) expression levels of TTF1 gene in benign and malignant thyroid lesions; B) correlation between expression of TTF1 gene and c-kit classes.

4.2.5 C-KIT functional studies:

We have grown K1 and SKMEL 3 cell lines and, by Real-Time PCR, we have obtained K1 cell line with no c-KIT gene expression and SKMEL cell line that expressed c-KIT mRNA.

By means of immunocytochemistry, we confirmed the absence of c-KIT in K1 cells and the presence of c-KIT in SKMEL cells, also at the protein level (Figure 4.8A,B). SKMEL cells were used as positive controls for c-KIT expression. We successfully subcloned the c-kit gene into the pTarget Vector apt to transfect eukaryotic cells. The sequence of the whole transcript was checked correctly by cycle sequencing. The transfection in K1 cells is ongoing and no results of functional studies have been obtained yet. These experiments belong to our future perspectives.

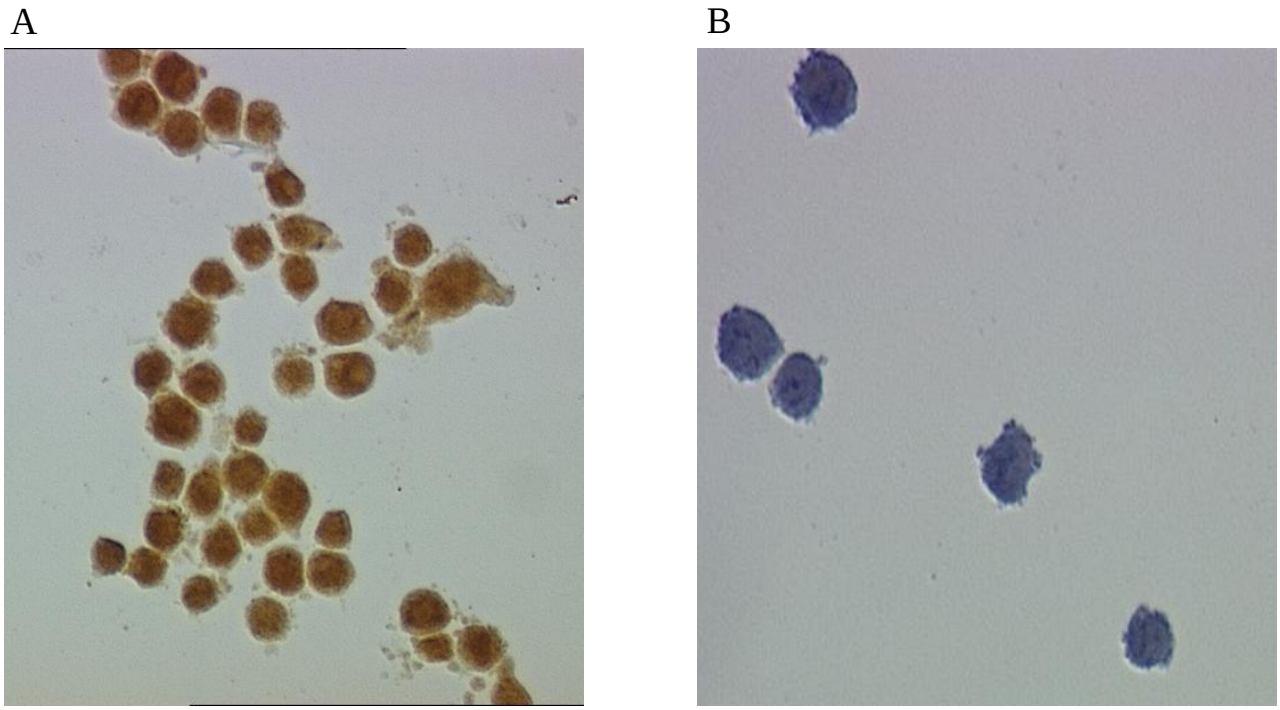

Figure 4.8: Immunocytochemistry analysis. (A) SKMEL cells positive for c-KIT protein, (B) K1 thyroid carcinoma cells negative for c-KIT protein.

4.3 Other molecular markers to improve cytological diagnostic accuracy

4.3.1 NIS gene expression level:

Analyzing 50 (24 benign and 26 malignant) of the 82 FNA smears, previously analyzed for c-kit expression, we found that NIS mRNA expression level was higher in benign (mean=0.27) thyroid tumours in comparison to the malignant ones (mean=0.026), even though it didn't reach statistical significance (p=0.06) (Figure 4.9)

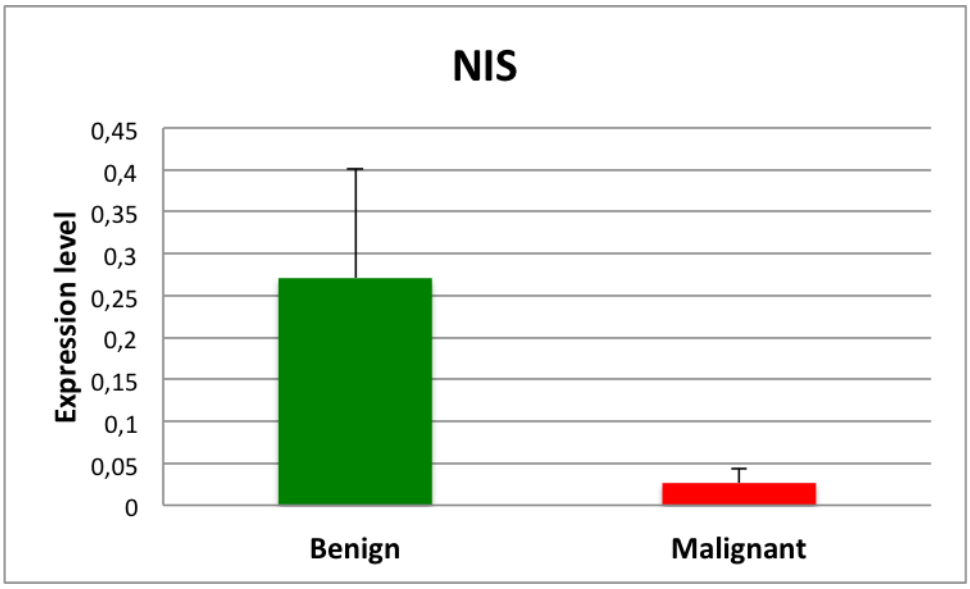

Figure 4.9: Expression levels of Nis gene in benign and malignant thyroid lesions

4.3.2 TC1 gene expression level:

We tested TC1 gene expression in a total of 109 patients (65 malignant, 44 benign). We found that TC1 was significantly over-expressed in malignant lesions (mean= 0.28) compared to the benign ones (mean= 0.08) (p-value 0.04) (Figure 4.10).

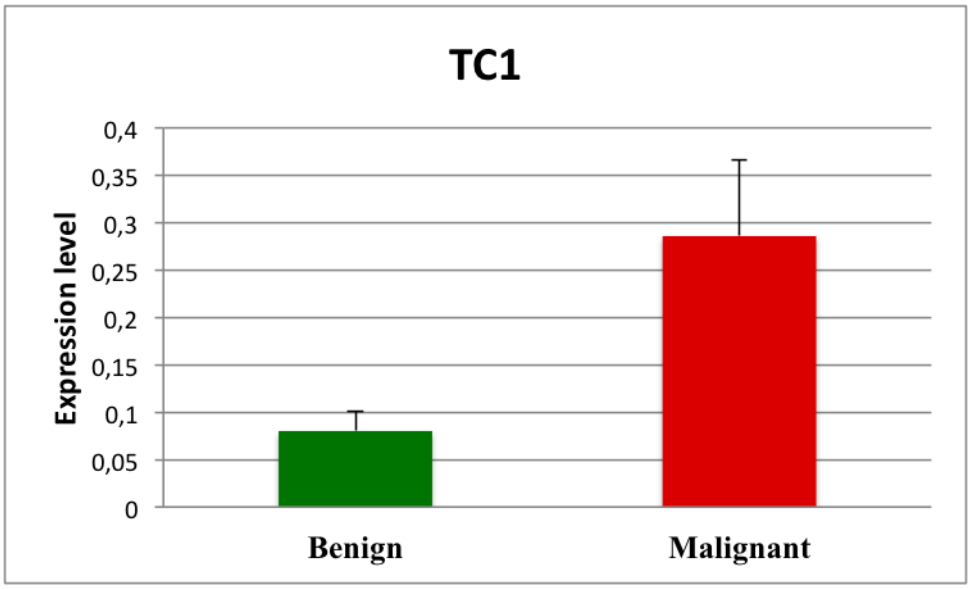

Figure 4.10: TC1 expression in benign and malignant thyroid samples

4.3.3 miRNA 146b and miRNA222 expression levels:

We have evaluated miRNA146b and miRNA222 expression 58 FNA smears (41 malignant and 17 benign) to better understand the relationships of their expression between malignant and benign FNA samples.

Comparing the expression values for each miRNA relative to SNORD61 in malignant and benign samples, we found that miRNA146b was significantly higher in the malignant group (mean=205.839) than in the benign group (mean=2.09) (p-value = 0.0005) (Figure 4.11A). Specificity and sensitivity of the diagnostic performance of miR-146b were evaluated by ROC analysis, which showed 100% of specificity and 87.8% of sensitivity, the AUC was 0.9 with C.I 95% 0,8 -0,9 and p <0.0001. (Figure 4.11B)

As regards the miRNA222, we saw a higher expression in the malignant group compared to the benign group, but there was no significance (results not shown).

A

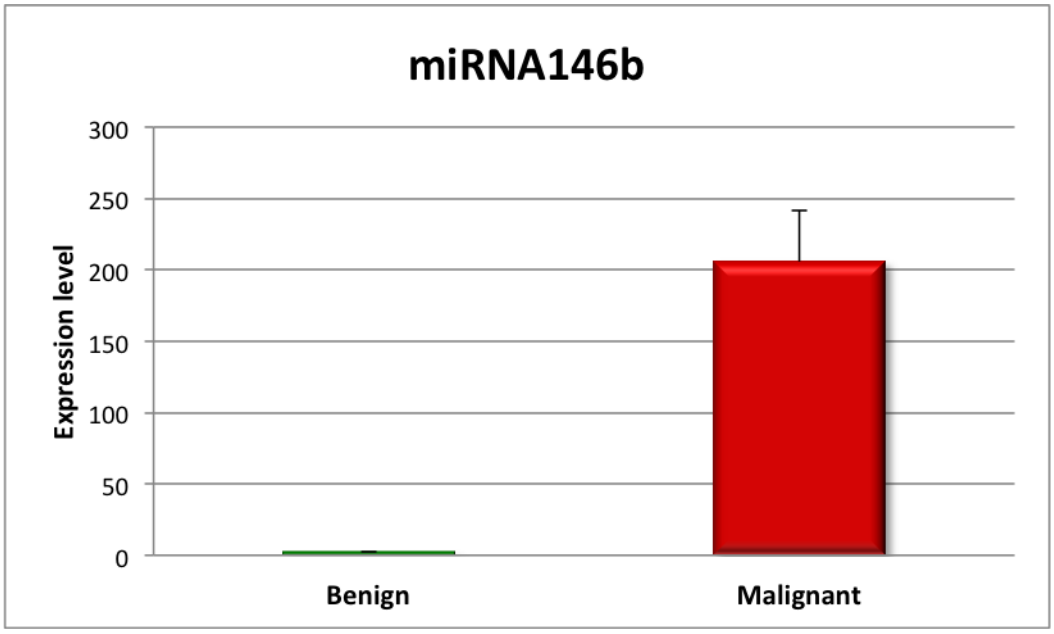

B

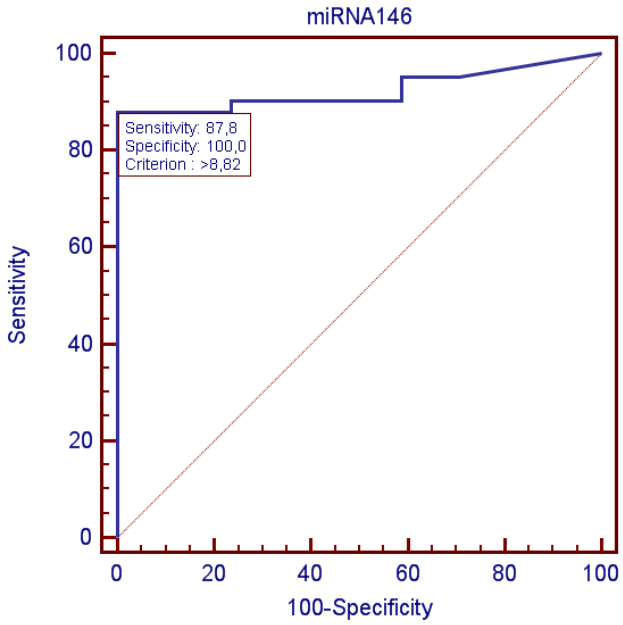

Figure 4.11: (A) miRNA146b expression in benign and malignant thyroid samples. (B) ROC analysis for miRNA146b expression. The true positive rate (Sensitivity) is plotted in function of the false positive rate (100-Specificity) for different cut-off points. Each point on the ROC plot represents a sensitivity/specificity pair corresponding to a particular decision threshold. (AUC = 0.9, C.I 95% 0.8 -0.9; p <0.0001)

4.4 Building Molecular computational models

4.4.1 Classification of malignant and benign samples

Different gene expression data was used to build Bayesian Neural Networks (BNN) and to perform Discriminant Analysis in order to estimate the probability of thyroid malignancy.

We built several BNNs in order to find the most predictive one. This procedure uses a Probabilistic Neural Network (PNN) to classify cases into malignant and benign categories, based on 7 input variables (KIT, TC1, miRNA222, miRNA146b, NIS, PAX8, TTF1) by implementing a nonparametric method for classifying observations into one of benign and malignant groups based on the observed expression variables. After different tests we obtained that the Neural Network Bayesian Classifier made up of KIT, TC1, miRNA222, miRNA146b on 51 FNA (38 malignant and 13 benign) (Table 4.2), resulted to have the highest predictive power of 94.12%, it is interesting to notice that this model correctly classifies 95% of the samples in the malignant group and 92.31% of the samples in the benign group (Figure 4.12).

CASE	HD	CD	BRAF
1	PTC	MCP	WT
2	PTC	CP	V600E
3	PTC	CA	WT
4	PTC	CP	V600E
5	PTC	SCP	V600E
6	PTC	SCP	V600E
7	PTC	CP	WT
8	PTC	CP	WT
9	PTC	CP	WT
10	PTC	SCP	WT
11	PTC	MCP	V600E
12	PTC	SCP	V600E
13	PTC	SCP	V600E
14	PTC	CP	V600E
15	PTC	SCP	V600E
16	PTC	CP	V600E
17	PTC	CP	V600E
18	PTC	MCP	WT
19	PTC	MI	WT
20	PTC	SCP	V600E
21	PTC	CP	V600E
22	PTC	CP	V600E
23	PTC	CP	V600E
24	PTC	CP	V600E
25	PTC	MCP	WT
26	PTC	CP	V600E
27	PTC	CP	WT
28	PTC	CP	V600E
29	PTC	MCP	WT
30	BN	BN	WT
31	BN	BN	WT

32	BN	MI	WT
33	BN	BN	WT
34	BN	BN	WT
35	BN	BN	WT
36	BN	MIO	WT
37	BN	MI	WT
38	BN	MI	WT
39	BN	MI	WT
40	PTC	MIB	WT
41	BN	MI	WT
42	PTC	CP	WT
43	PTC	SCP	WT
44	PTC	SCP	WT
45	PTC	MCP	WT
46	PTC	SCP	V600E
47	PTC	SCP	WT
48	PTC	MI	WT
49	PTC	MIO	WT
50	BN	BN	WT
51	BN	BN	WT

Table 4.2: Morphological and molecular diagnosis in 51 thyroid nodules

HD: histological diagnosis. CD: cytological diagnosis. PTC: papillary thyroid carcinoma. SPTC: suspicious for PTC. CP = papillary carcinoma. CA = anaplastic carcinoma. MIO = microfollicolare with cells ossifile. MCP = metastatic papillary carcinoma. MI =microfollicolare. BN: benign nodule. WT: wild type.

A

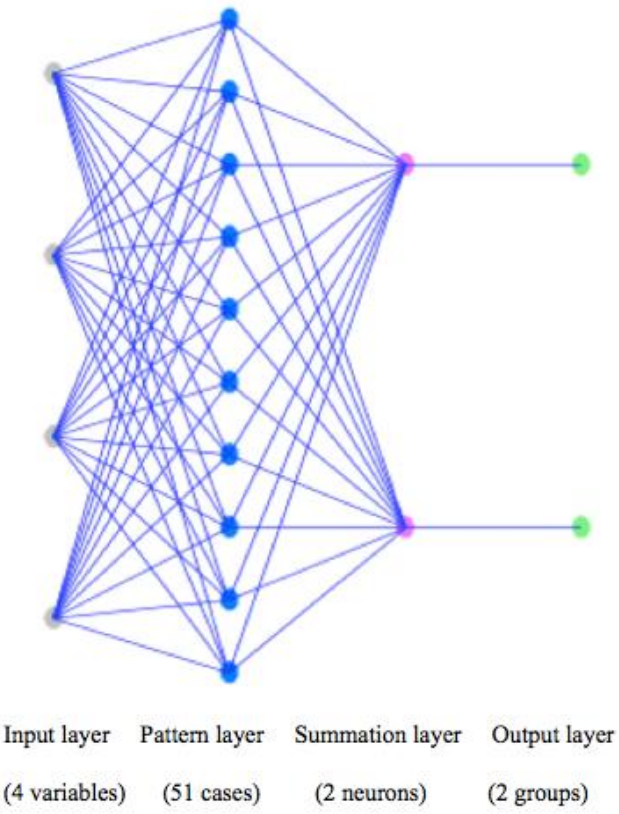

B

Classification Table

Actual	*Group*	*Predicted*	
mal_ben	*Size*	*0*	*1*
0	13	12	1
		(92.31%)	(7.69%)
1	38	2	36
		(5.26%)	(94.74%)

Percent of training cases correctly classified: 94.12%

	Actual	*Highest*	*Highest*	*2nd Highest*	*2nd Highest*
Row	*Group*	*Group*	*Score*	*Group*	*Score*
3	1	0*	0.824696	1	0.175304
20	1	0*	0.660876	1	0.339124
43	0	1*	0.751332	0	0.248668

* = incorrectly classified.

Figure 4.12: Predictive power of KIT, TC1, miRNA222, miRNA146b in discriminating malignant from benign by ANN.
(A) ANN uses a probabilistic neural network (PNN) to classify cases into different Malignant vs Benign, based on 4 input variables. (B) Classification table shows the results of using the trained neural network to classify observations. Amongst the 51 cases used to train the model, 94.12% were correctly classified.

The predictive power of KIT, TC1, miRNA222, miRNA146b expression to discern malignant from benign patients was confirmed also by means of the Discriminant Analysis analysis that showed a predictive power 92.16%, so slightly less than Neural Network Bayesian and, more important, it correctly classifies 100,00% of the samples in the malignant group and 69.23% of the samples in the benign group (Figure 4.13).

Classification variable: **Malignant** vs **Benign**
Independent variables:
c_kit
tc1
miRNA222
miRNA146

Number of complete cases: 51
Number of groups: 2

Discriminant	*Eigenvalue*	*Relative*	*Canonical*
Function		*Percentage*	*Correlation*
1	1.04361	100.00	0.71461

Functions	*Wilks*			
Derived	*Lambda*	*Chi-Square*	*DF*	*P-Value*
1	0.489331	33.5917	4	0.0000

Classification Table

Actual	*Group*	*Predicted*	*mal_ben*
mal_ben	*Size*	*0*	*1*
0	13	9	4
		(69.23%)	(30.77%)
1	38	0	38
		(0.00%)	(100.00%)

Percent of cases correctly classified: 92.16%

	Prior
Group	*Probability*
1	0,5000
2	0,5000

	Actual	*Highest*	*Highest*	*Squared*		*2nd Highest*	*2nd Highest*	*Squared*	
Row	*Group*	*Group*	*Value*	*Distance*	*Prob.*	*Group*	*Value*	*Distance*	*Prob.*
1	1	1	-0.996281	0.0704307	0.8839	0	-3.02616	4.13018	0.1161
2	1	1	-1.24553	0.126248	0.8610	0	-3.06878	3.77276	0.1390
3	1	1	-1.13294	0.995233	0.5860	0	-1.4804	1.69015	0.4140
4	1	1	-0.146934	0.0000101817	0.9329	0	-2.77925	5.26464	0.0671
5	1	1	0.444883	0.0586689	0.9607	0	-2.7513	6.45104	0.0393
6	1	1	0.959299	0.116463	0.9684	0	-2.46447	6.964	0.0316
7	1	1	-0.0437119	0.0456246	0.8956	0	-2.19258	4.34336	0.1044
8	1	1	-0.35565	0.0060648	0.9213	0	-2.81636	4.92749	0.0787
9	1	1	-0.772161	0.236599	0.8208	0	-2.29419	3.28065	0.1792
10	1	1	-0.909852	0.173664	0.8432	0	-2.59199	3.53794	0.1568
11	1	1	-0.978737	0.0830749	0.8784	0	-2.95613	4.03787	0.1216
12	1	1	-0.0884061	0.000111853	0.9318	0	-2.70375	5.23081	0.0682
13	1	1	2.95808	0.500472	0.9861	0	-1.30703	9.0307	0.0139

14	1	1	4.42059	3.26349	0.9989	0	-2.36984	16.8443	0.0011
15	1	1	-1.18884	0.124011	0.8618	0	-3.01936	3.78505	0.1382
16	1	1	0.893555	0.0104766	0.9466	0	-1.98127	5.76013	0.0534
17	1	1	-0.768977	0.0310464	0.9033	0	-3.00378	4.50064	0.0967
19	1	1	1.50373	0.117109	0.9685	0	-1.92221	6.96899	0.0315
20	1	1	-1.33819	0.566862	0.7129	0	-2.24791	2.38631	0.2871
21	1	1	-0.644114	0.0165925	0.9124	0	-2.98779	4.70395	0.0876
22	1	1	-1.00743	0.0899351	0.8755	0	-2.95803	3.99113	0.1245
23	1	1	-0.614894	0.0297171	0.9041	0	-2.85845	4.51684	0.0959
25	1	1	-0.83946	0.0455392	0.8956	0	-2.98879	4.34419	0.1044
26	1	1	1.28208	0.247275	0.9777	0	-2.50012	7.81169	0.0223
28	1	1	-0.355491	0.000281892	0.9309	0	-2.95656	5.20242	0.0691
29	1	1	-1.23095	0.141747	0.8550	0	-3.00554	3.69093	0.1450
30	1	1	-0.809608	0.0373955	0.8998	0	-3.00494	4.42805	0.1002
31	1	1	1.39246	0.073457	0.9631	0	-1.86993	6.59823	0.0369
32	1	1	2.73132	1.06855	0.9934	0	-2.28344	11.0981	0.0066
33	0	0	10.64	14.3598	1.0000	1	-0.706503	37.0528	0.0000
34	0	0	-0.462702	1.20031	0.5306	1	-0.585055	1.44501	0.4694
36	0	0	0.644535	0.145789	0.8535	1	-1.11781	3.67048	0.1465
38	0	0	7.67354	5.9752	0.9997	1	-0.582584	22.4875	0.0003
40	0	*1	-1.19548	1.03641	0.5746	0	-1.496	1.63745	0.4254
41	0	0	8.1872	7.8541	0.9999	1	-0.891717	26.0119	0.0001
42	0	0	0.546552	0.166674	0.8457	1	-1.15506	3.56989	0.1543
43	0	*1	-1.33338	0.177548	0.8418	0	-3.00488	3.52053	0.1582
45	0	*1	-1.31058	0.713334	0.6680	0	-2.00964	2.11145	0.3320
46	1	1	-0.965599	0.0847317	0.8777	0	-2.93642	4.02638	0.1223
47	0	0	2.60575	0.00221143	0.9263	1	0.0741535	5.06541	0.0737
48	1	1	0.0980452	0.0137514	0.9483	0	-2.81104	5.83193	0.0517
49	1	1	0.122645	0.00124895	0.9382	0	-2.5982	5.44295	0.0618
50	1	1	-0.62535	0.0207164	0.9096	0	-2.93429	4.6386	0.0904
51	1	1	2.17636	0.60257	0.9881	0	-2.24687	9.44902	0.0119
52	1	1	-0.715366	0.0282095	0.9050	0	-2.9691	4.53569	0.0950
53	1	1	1.13048	0.33086	0.9813	0	-2.8308	8.25342	0.0187
54	1	1	-1.31618	0.161647	0.8476	0	-3.03204	3.59337	0.1524
55	1	1	-0.200962	0.00208922	0.9265	0	-2.73559	5.07134	0.0735
56	0	0	-0.517045	0.922166	0.6066	1	-0.950252	1.78858	0.3934
57	0	0	0.835918	0.100527	0.8711	1	-1.07523	3.92283	0.1289
58	0	*1	-1.31641	1.16719	0.5393	0	-1.47373	1.48184	0.4607

* = incorrectly classified.

Figure 4.13: Predictive power of KIT, TC1, miRNA222, miRNA146b in discriminating malignant from benign by Discriminant Analysis.

This procedure is designed to develop a set of discriminating functions which can help predict Malignant vs Benign based on the values of other quantitative variables. 51 cases were used to develop a model to discriminate among the 2 levels of Malignant vs Benign. 4 predictor variables were entered. The one discriminating function with P-value less than 0,05 is statistically significant at the 95.0% confidence level. To plot the discriminating functions, select Discriminant Functions from the list of Graphical Options. Classification table shows the results of using the derived discriminant functions to classify observations. It lists the two highest scores amongst the classification functions for each of the 51 observations used to fit the model, as well as for any new observations. Amongst the 51 observations used to fit the model, 47 or 92.16% were correctly classified.

Then the analysis was conducted on 11 unknown samples, with both discrimination analysis and neural network analysis (Table 4.3, 4.4), in order to confirm the accuracy of the model. The pathological diagnosis for each sample was kept blinded until the analysis was completed. When the blind was broken, we found that all 11 unknown samples were diagnosed by the model as malignant in concordance with the diagnosis determined by standard pathological criteria. The samples correctly classified were diagnosed as indeterminate samples (SPTC) at the cytological

level and were moved to the diagnostic group of malignant after pathological diagnosis. 7 out of the 11 SPTC samples used in this analysis were BRAF mutated. Therefore 4 BRAF wild-type patients remained SPTC. Our model assigned these 4 patients to the malignant group with a probability of 0.9065, 0.8631, 0,7890, 0.9585 by Discriminant analysis and 0.999, 0.824, 0,799, 1 by Neural network.

Unknown samples	Benign probability	Malignant probability	Predicted diagnosis	Cytological diagnosis	Pathological diagnosis
A	0.0700	0.9300	Malignant	SPTC	Malignant
B	0.0530	0.9470	Malignant	SPTC	Malignant
C	0.1075	0.8925	Malignant	SPTC	Malignant
D	0.0177	0.9823	Malignant	SPTC	Malignant
E	0.1964	0.8036	Malignant	SPTC	Malignant
F	0.1380	0.8620	Malignant	SPTC	Malignant
G	0.0935	0.9065	Malignant	SPTC	Malignant
H	0.1369	0.8631	Malignant	SPTC	Malignant
I	0.1458	0.8542	Malignant	SPTC	Malignant
L	0.2110	0.7890	Malignant	SPTC	Malignant
M	0.0415	0.9585	Malignant	SPTC	Malignant

Table 4.3: Probability values of the prediction model for the unknown samples by Discriminant Analysis

Unknown samples	Benign probability	Malignant probability	Predicted diagnosis	Cytological diagnosis	Pathological diagnosis
A	3.01989E-7	1.0	Malignant	SPTC	Malignant
B	1.08387E-8	1.0	Malignant	SPTC	Malignant
C	0.000446425	0.999554	Malignant	SPTC	Malignant
D	4.73155E-98	1.0	Malignant	SPTC	Malignant
E	0.32423	0.67577	Malignant	SPTC	Malignant
F	0.0223083	0.977692	Malignant	SPTC	Malignant
G	0.000936203	0.999064	Malignant	SPTC	Malignant
H	0.175866	0.824134	Malignant	SPTC	Malignant
I	0.0846736	0.915326	Malignant	SPTC	Malignant
L	0.200675	0.799325	Malignant	SPTC	Malignant
M	6.97178E-14	1.0	Malignant	SPTC	Malignant

Table 4.4: Probability values of the prediction model for the unknown samples by Neural Network

4.4.2 Principal Component Analysis

We then performed Principal Component Analysis[1] in order to visualize in a 3-dimensional space the discriminative power of all the four markers according to malignant and benign status (Figure 4.14). A separation between malignant and benign samples can be visually identified (Figure 4.14, left plot). A similar grouped structure is identified by an unsupervised analysis performed via "k-means" clustering (Figure 4.14, right plot).

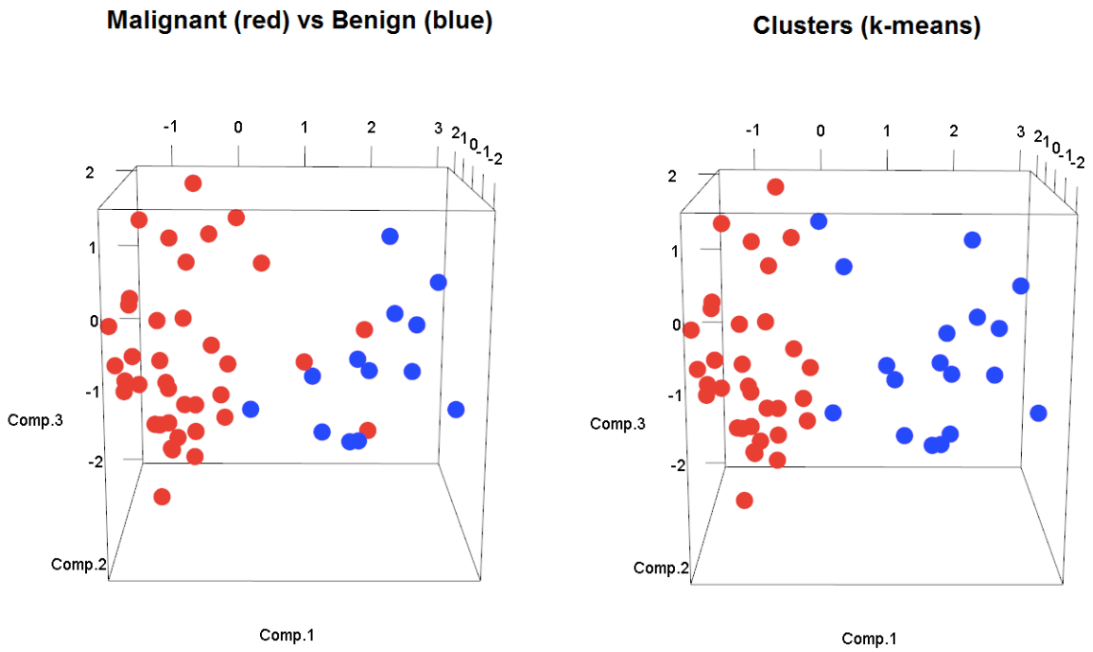

Figure 4.14: Principal Component analysis and k-means clustering. We plot the first 3 principal components of the space of the four log transformed[2] features TC1, c-KIT, miRNA146, miRNA222 in the context of classifying Malignant Vs Benign. The data points in the plots on the left are labelled according to their condition ("Malignant vs Benign"). The plots on the right show instead the clusters identified by the unsupervised analysis performed via k-means clustering. We can see that the separation induced by the conditions "Malignant vs Benign" approximately reproduces/reflects the intrinsic grouped structure of the data. This suggests that classifications based on the four discussed features should have a good discriminant power in classifying "Malignant vs Benign".

The comparison of the expression values between malignant and benign groups of each single gene (KIT, TC-1, miRNA222, and miRNA146b), taken singularly from the dataset used for the computational model and the PCA analysis (Table 4.2), is showed by box-plots in Figure 4.15. We obtained that c-KIT mRNA expression levels were significantly higher in benign thyroid tumours

[1] *Principal component analysis (PCA) is a classic tool for data analysis, visualization or compression that, starting from a multivariate data set, finds linear combinations of the variables called "principal components", corresponding to orthogonal directions maximizing variance in the data [d'Aspremont, Alexandre, Francis Bach, and Laurent El Ghaoui. "Optimal solutions for sparse principal component analysis." The Journal of Machine Learning Research 9 (2008): 1269-1294.]*

[2] *Here, for "log transformed" we mean "log(a+x)", where a>0 and x is the nonnegative variable that we want to transform. We need to introduce the constant a since in our case x can be equal to zero. In particular we chose a=0.05.*

compared to the malignant ones (p(KIT) = 0.00092). Instead the miRNA 146b and TC1 were significantly over-expressed in malignant lesions compared to the benign ones (p(miRNA146b) < 0.00001, p(TC1) = 0.015) and we found the same difference but not significant in miRNA222. These results confirm previous ones

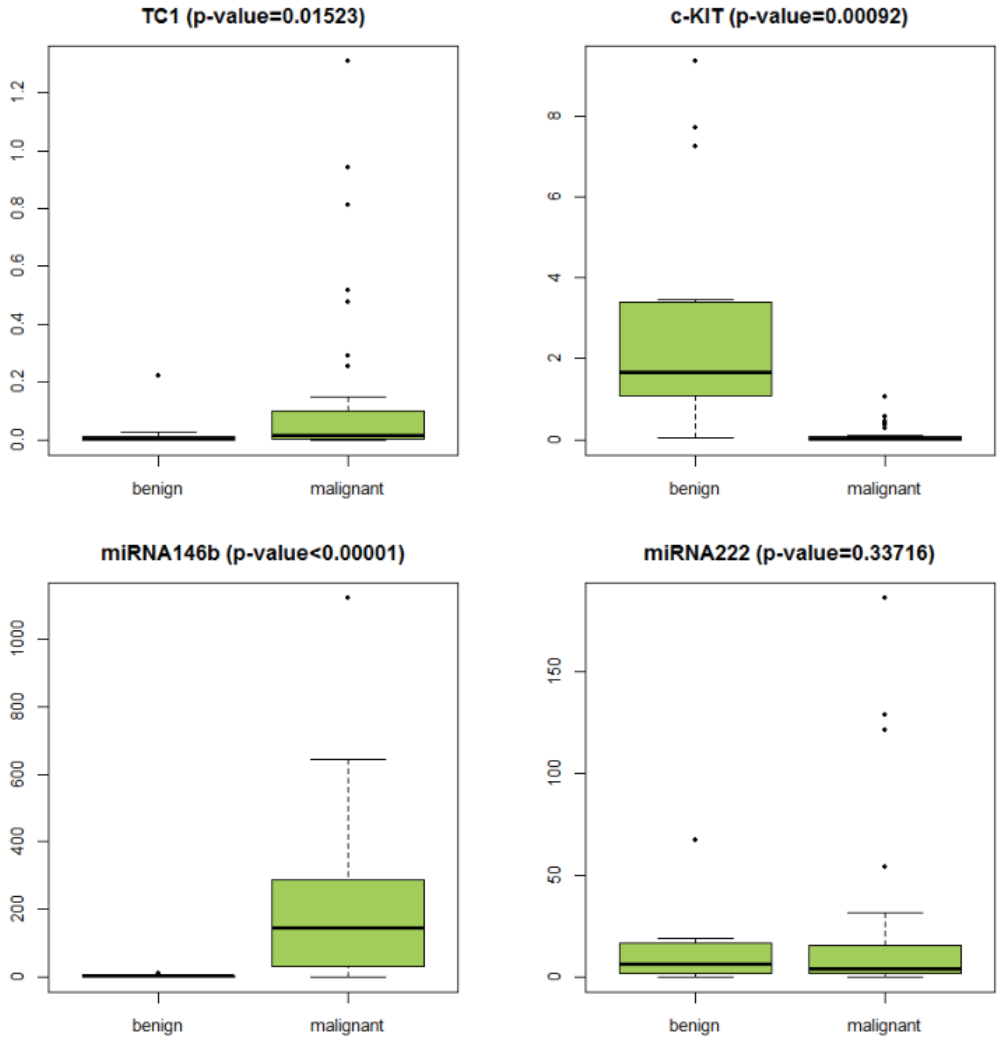

Figure 4.15. Differential expression of each single marker between malignant/benign group in the dataset used for the building of the computational model (Table 4.2).

4.4.3 ROC curve analysis

We finally employed receiver-operated characteristics (ROC) curve analyses using the expression of each marker individually (TC1, c-KIT, miRNA 146b, miRNA222), in order to determine model robustness for predicting malignancy in thyroid samples. (Figure 4.16, Table 4.5). Among the markers, KIT and miRNA146b showed the highest AUC (0.9) for malignant versus benign.

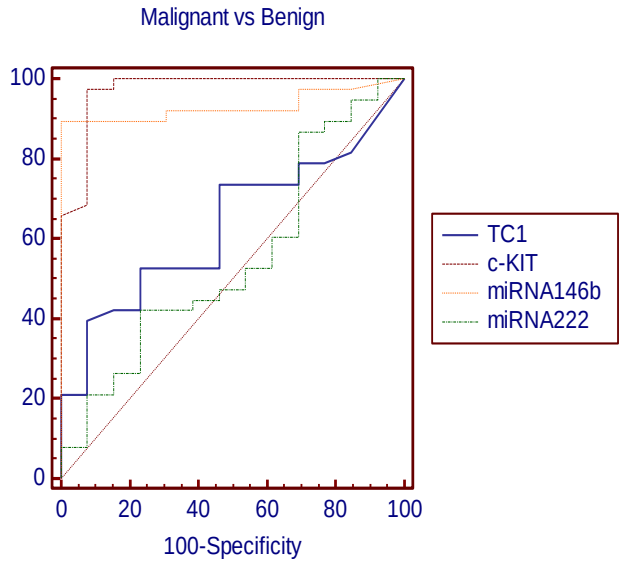

Figure 4.16: Singular ROC analysis for KIT, TC1, miRNA146b, miRNA222 in Malignant vs Benign

	Sensitivity	**Specificity**	**AUC[a]**	**SE[b]**	**95% CI[c]**	**p-value**
TC1	38.5	92.9	0.634	0.0816	0.487 to 0.764	0.0953
c-KIT*	95.7	88.2	0.973	0.0261	0.883 to 0.998	<0.0001
miRNA146b*	87.8	100.00	0.931	0.0364	0.824 to 0.983	<0.0001
miRNA222	48.8	68.7	0.551	0.0955	0.405 to 0.690	0.9171

Table 4.5: Individual ROC analysis for each marker in Malignant vs Benign. The asterisks indicate the genes with significant p-value: c-KIT p<0.0001; miRNA p<0.0001.

4.4.4 Correlation analysis

A multiple variable analysis was performed to analyze the correlation between the markers; the statistical correlation may reflect biologically correlation between markers.

We observed a significant correlation of c-KIT with miRNA146b (p<0.0001) (Figure 4.17)

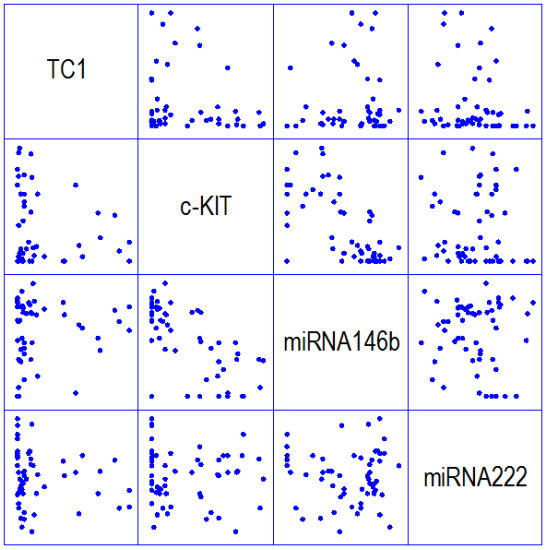

	TC1	c-KIT	miRNA146b	miRNA222
TC1		-0.1026	0.0979	-0.1577
		(52)	(53)	(52)
		0.4691	0.4854	0.2640
c-KIT	-0.1026		-0.7142	-0.0607
	(52)		(57)	(56)
	0.4691		0.0000	0.6565
miRNA146b	0.0979	-0.7142		-0.0622
	(53)	(57)		(57)
	0.4854	0.0000		0.6456
miRNA222	-0.1577	-0.0607	-0.0622	
	(52)	(56)	(57)	
	0.2640	0.6565	0.6456	

Figure 4.17: Correlation graph: the indicated variables (TC1, c-KIT, miRNA146b, miRNA222) are displayed on the vertical axis of every plot in that row and on the horizontal axis of every plot in that column. Each pair of variables is thus shown twice, once above the diagonal and once below it. This table shows Pearson product moment correlations between each pair of variables. Correlation coefficients range between -1 and +1 and measure the strength of the linear relationship between the variables. In parentheses is the number of pairs of data values used to compute each coefficient.
P-values < 0.05 indicate statistically significant non-zero correlations at the 95.0% confidence level. The following pairs of variables have P-values below 0.05: miRNA146b and c-KIT

4.5 Molecular stratification of the malignant population according to BRAF molecular status: multi-approach analysis of the genetic background related to BRAF V600E presence

4.5.1 Differential gene expression analysis approach:

In order to better characterize and stratify the group of malignant samples we analyzed the differential expression of different markers singularly according to V600E BRAF mutational status:

- We found a lower expression of NIS in BRAF V600E malignant samples (n= 14) (mean= 0,002) than BRAF wild type malignant samples (n= 11) (mean= 0,056), but the difference was not statistically significant (Figure 4.18).

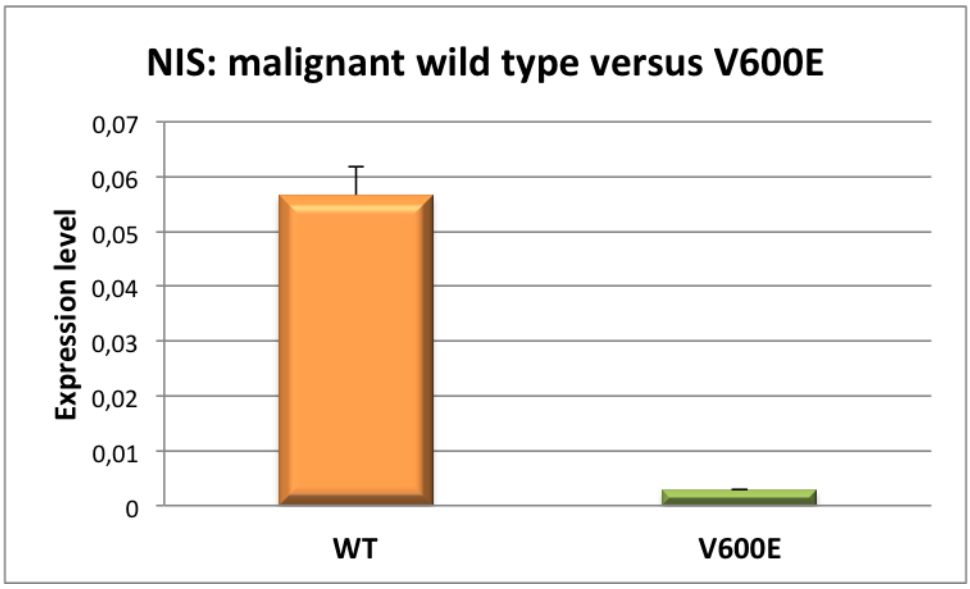

Figure 4.18. NIS expression in BRAF wild type versus V600E malignant lesions

- TC1 expression resulted significantly (p= 0.01) higher in BRAF wild type malignant samples (n=31) (mean= 0.46) as compared to the V600E ones (n= 34) (mean= 0.10) (Figure 4.19).

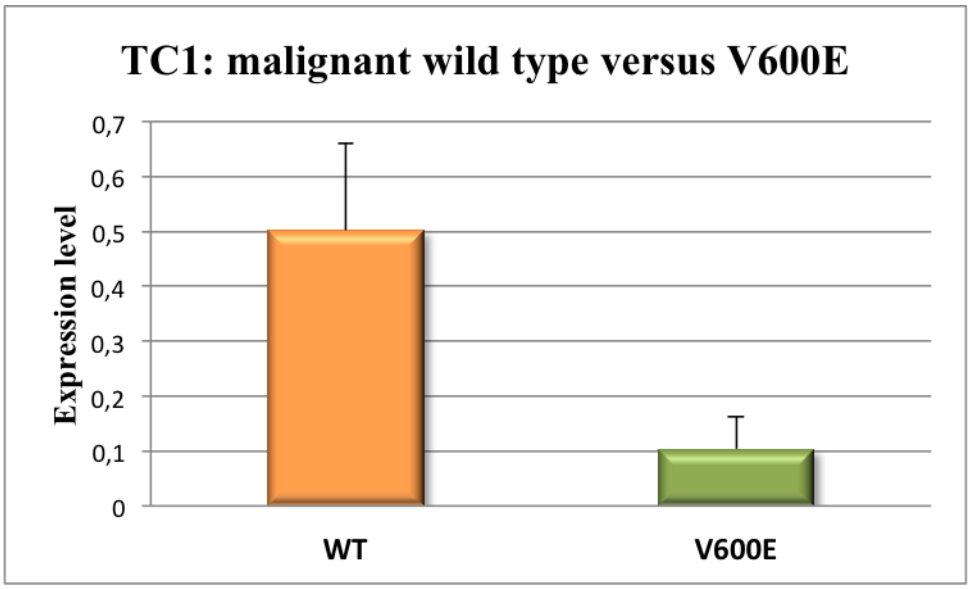

Figure 4.19: TC1 expression in BRAF wild type versus V600E malignant lesions

- We have also correlated the expression of miRNAs 146b e 222 in 41 malignant FNAs: 20/41 carried the V600E mutation on BRAF exon 15. We found that miRNA146b and miRNA222 were significantly down-regulated (p-value = 0.036; p-value = 0.037, respectively) in the malignant

samples with BRAF WT (mean= 146.56; mean= 7.62 respectively) compared to the malignant group with BRAF V600E (mean= 381.73; mean= 29.07 respectively) (Figure 4.20A,B)

A

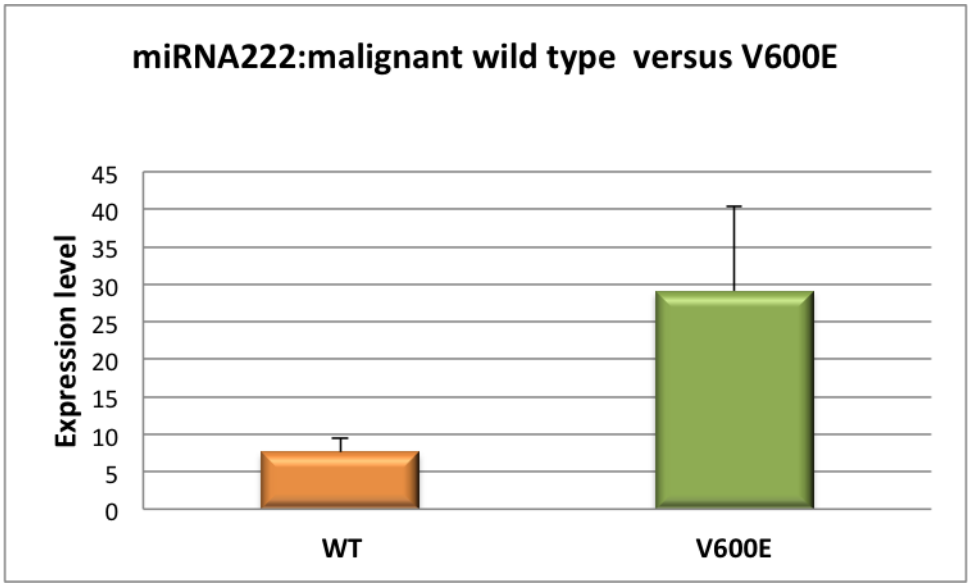

B

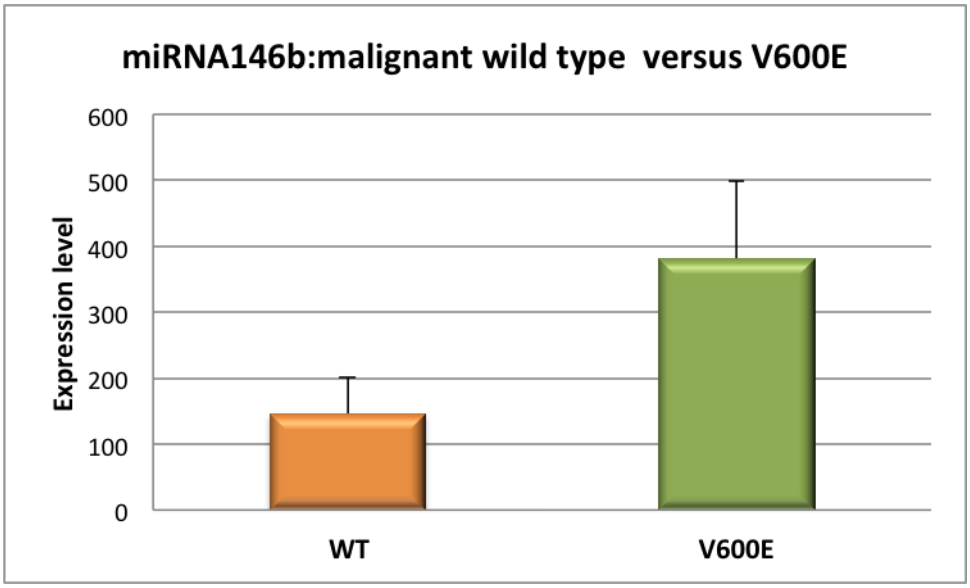

Figure 4.20. (A) miRNA222 and (B) miRNA146b expression in BRAF wild type versus V600E malignant lesions.

4.5.2 Computational model approach:

To better characterize and stratify the group of malignant samples, we also performed a Bayesian Neural Networks (BNN) and Discriminant Analysis built on the most predictive markers-

based model showed above (KIT, TC1, miRNA222, miRNA146b) in order to classify BRAF mutational status. We conducted this analysis only on malignant samples (n=38: 19WT and 19 BRAF V600e): the best results were provided by Discriminant Analysis showing a predictive power of 76.32%. In the BRAF V600E group, 94.74% of the samples were correctly classified while only 57.89% of the samples were correctly assigned to the BRAF WT group (Figure 4.21).

Classification variable: v600e_wt
Independent variables:
tc1
c_kit
miRNA146
miRNA222

Number of complete cases: 38
Number of groups: 2

Discriminant	*Eigenvalue*	*Relative*	*Canonical*
Function		*Percentage*	*Correlation*
1	0.553878	100.00	0.59703

Functions	*Wilks*			
Derived	*Lambda*	*Chi-Square*	*DF*	*P-Value*
1	0.643551	14.9856	4	0.0047

Classification Table

Actual	*Group*	*Predicted*	*v600e_wt*
v600e_wt	*Size*	*0*	*1*
0	19	11	8
		(57.89%)	(42.11%)
1	19	1	18
		(5.26%)	(94.74%)

Percent of cases correctly classified: 76.32%

	Actual	*Highest*	*Highest*	*Squared*		*2nd Highest*	*2nd Highest*	*Squared*	
Row	*Group*	*Group*	*Value*	*Distance*	*Prob.*	*Group*	*Value*	*Distance*	*Prob.*
1	0	*1	-1.09056	0.104515	0.6413	0	-1.67165	1.26669	0.3587
2	1	1	-1.34502	0.148666	0.6203	0	-1.83587	1.13037	0.3797
3	0	0	4.18975	4.6182	0.9847	1	0.0269081	12.9439	0.0153
4	1	1	-0.149836	0.000552366	0.7341	0	-1.16524	2.03136	0.2659
5	1	1	0.494869	0.0360129	0.7899	0	-0.829516	2.68478	0.2101
6	1	1	1.1574	0.230769	0.8514	0	-0.588018	3.7216	0.1486
7	0	0	2.25427	1.44518	0.9422	1	-0.536817	7.02735	0.0578
8	0	*1	-0.328426	0.000791609	0.7328	0	-1.33712	2.01817	0.2672
9	0	0	0.99444	0.0289092	0.7851	1	-0.301341	2.62047	0.2149
10	0	0	-0.0829684	0.113083	0.6370	1	-0.645236	1.23762	0.3630
11	1	1	-1.03037	0.203303	0.5978	0	-1.42659	0.995741	0.4022
12	1	1	-0.0150955	0.053638	0.6713	0	-0.729017	1.48148	0.3287
13	1	1	3.75507	2.6764	0.9683	0	0.33549	9.51556	0.0317
14	1	1	4.56902	1.10138	0.9289	0	1.99914	6.24113	0.0711
15	1	1	-1.25624	0.192205	0.6021	0	-1.67054	1.0208	0.3979
16	1	1	1.35593	0.581776	0.8961	0	-0.798551	4.89074	0.1039
17	1	1	-0.856647	0.0685026	0.6616	0	-1.52692	1.40904	0.3384

19	0	0	3.61227	2.29101	0.9624	1	0.369955	8.77564	0.0376
20	0	0	1.32014	0.494877	0.8878	1	-0.74848	4.63212	0.1122
21	1	1	-0.72044	0.0474461	0.6757	0	-1.45432	1.51521	0.3243
22	1	1	-1.10632	0.317259	0.5581	0	-1.33975	0.784115	0.4419
23	1	*0	-0.620426	0.135428	0.6263	1	-1.13673	1.16803	0.3737
25	1	1	-0.908063	0.12557	0.6309	0	-1.44413	1.19771	0.3691
26	0	0	1.87213	0.962312	0.9221	1	-0.598519	5.90361	0.0779
28	1	1	-0.464895	0.0654439	0.6635	0	-1.14373	1.42311	0.3365
29	0	*1	-1.29292	0.114881	0.6361	0	-1.85133	1.2317	0.3639
30	1	1	-0.874915	0.0818357	0.6536	0	-1.50992	1.35185	0.3464
31	1	1	1.85044	0.745829	0.9089	0	-0.45018	5.34708	0.0911
32	0	0	3.3671	2.29504	0.9625	1	0.122867	8.78351	0.0375
33	0	*1	-0.99412	0.0563999	0.6694	0	-1.69951	1.46718	0.3306
34	0	*1	-0.186732	0.119995	0.6336	0	-0.734329	1.21519	0.3664
35	0	0	0.622404	0.0786225	0.8109	1	-0.833277	2.98998	0.1891
36	0	*1	-0.98779	0.375886	0.5402	0	-1.14901	0.698336	0.4598
37	0	0	3.4125	3.55706	0.9777	1	-0.369342	11.1207	0.0223
38	1	1	-0.891801	0.186759	0.6043	0	-1.31516	1.03348	0.3957
39	0	*1	1.11251	0.0656648	0.8054	0	-0.308193	2.90706	0.1946
40	0	*1	-1.39684	0.231807	0.5871	0	-1.74877	0.935664	0.4129
41	0	0	-0.56526	0.344331	0.5497	1	-0.764584	0.742979	0.4503

* = incorrectly classified.

Figure 4.21: Predictive power of KIT, TC1, miRNA222, miRNA146b in classifying BRAF mutational status by Discriminant Analysis (StatGraphics software).

Instead we obtained by BNN a predictive power of 73.68% with 68.42% of the samples in the BRAF V600E group and 78.95% of the samples with BRAF WT group were correctly classified (Figure 4.22A,B).

A

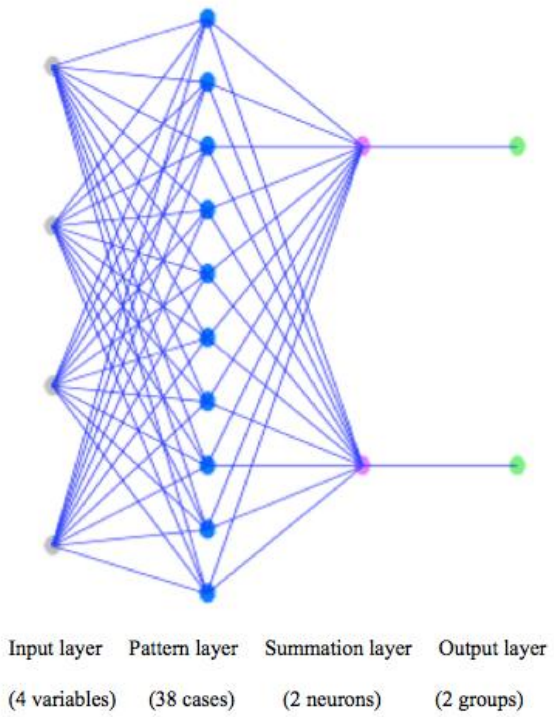

B

Classification Table

Actual	*Group*	*Predicted*	
v600e_wt	*Size*	*0*	*1*
0	*19*	*15*	*4*
		(78.95%)	*(21.05%)*
1	*19*	*6*	*13*
		(31.58%)	*(68.42%)*

Percent of training cases correctly classified: 73.68%

	Actual	*Highest*	*Highest*	*2nd Highest*	*2nd Highest*
Row	*Group*	*Group*	*Score*	*Group*	*Score*
1	0	1*	1.0	0	1.64536E-130
4	1	0*	1.0	1	5.4036E-213
5	1	0*	-1.#IND	1	-1.#IND
6	1	0*	-1.#IND	1	-1.#IND
8	0	1*	1.0	0	0.0
13	1	0*	-1.#IND	1	-1.#IND
14	1	0*	-1.#IND	1	-1.#IND
23	1	0*	-1.#IND	1	-1.#IND
36	0	1*	1.0	0	2.86169E-97
40	0	1*	1.0	0	1.00686E-43

* = incorrectly classified.

Figure 4.22: (A). Predictive power of KIT, TC1, miRNA222, miRNA146b in discriminating malignant BRAF V600E from malignant BRAF WT by ANN. ANN uses a probabilistic neural network (PNN) to classify cases into different malignant BRAF V600E vs BRAF WT, based on 4 input variables. (B) Classification table shows the results of using the trained neural network to classify observations. Amongst the 38 cases used to train the model, 73.68% were correctly classified.

4.5.3 Principal Component Analysis (PCA) approach:

We then performed Principal Component Analysis in order to visualize in a 3-dimensional space the discriminative power of all the four markers according to BRAF mutational status (Figure 4.23). A separation between BRAF V600E and wild type samples can be visually identified (Figure 4.23, left plot). A similar grouped structure is identified by an unsupervised analysis performed via "k-means" clustering (Figure 4.23, right plot).

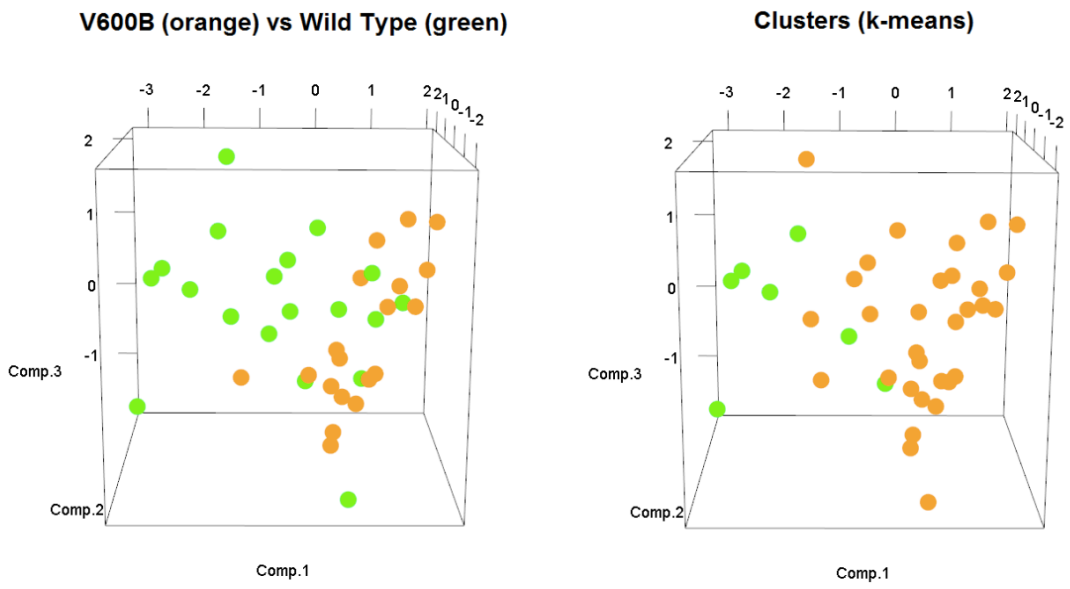

Figure 4.23. Principal Component analysis and k-means clustering: We plot the first 3 principal components of the space of the four log transformed features TC1, c-KIT, miRNA146, miRNA222 in the context of classifying BRAF mutational status. The data points in the plots on the left are labeled according to their condition ("V600B malignant vs WT malignant"). The plots on the right show instead the clusters identified by the unsupervised analysis performed via k-means clustering. We can see that the separation induced by the condition "V600B malignant vs WT malignant" approximately reproduces/reflects the intrinsic grouped structure of the data. This suggests that classifications based on the four discussed features should have a good discriminant power in classifying "V600B malignant vs WT malignant".

The comparison of the expression values between BRAF V600E and WT malignant group of each single gene (KIT, TC-1, miRNA222, and miRNA146b), taken singularly from the dataset used for the building of the computational model and the PCA analysis (Table 4.2), is showed by box-plots in Figure 4.24.

TC1 and c-KIT expression resulted significantly over-regulated in BRAF wild type malignant than BRAF V600E malignant samples ($p(TC1) = 0.00334$, $p(c\text{-}KIT) = 0.00341$), the opposite was found for miRNA222 and miRNA146b ($p(miRNA146b) = 0.036$, $p(miRNA222) = 0.037$); this confirm what we found in the previous section.

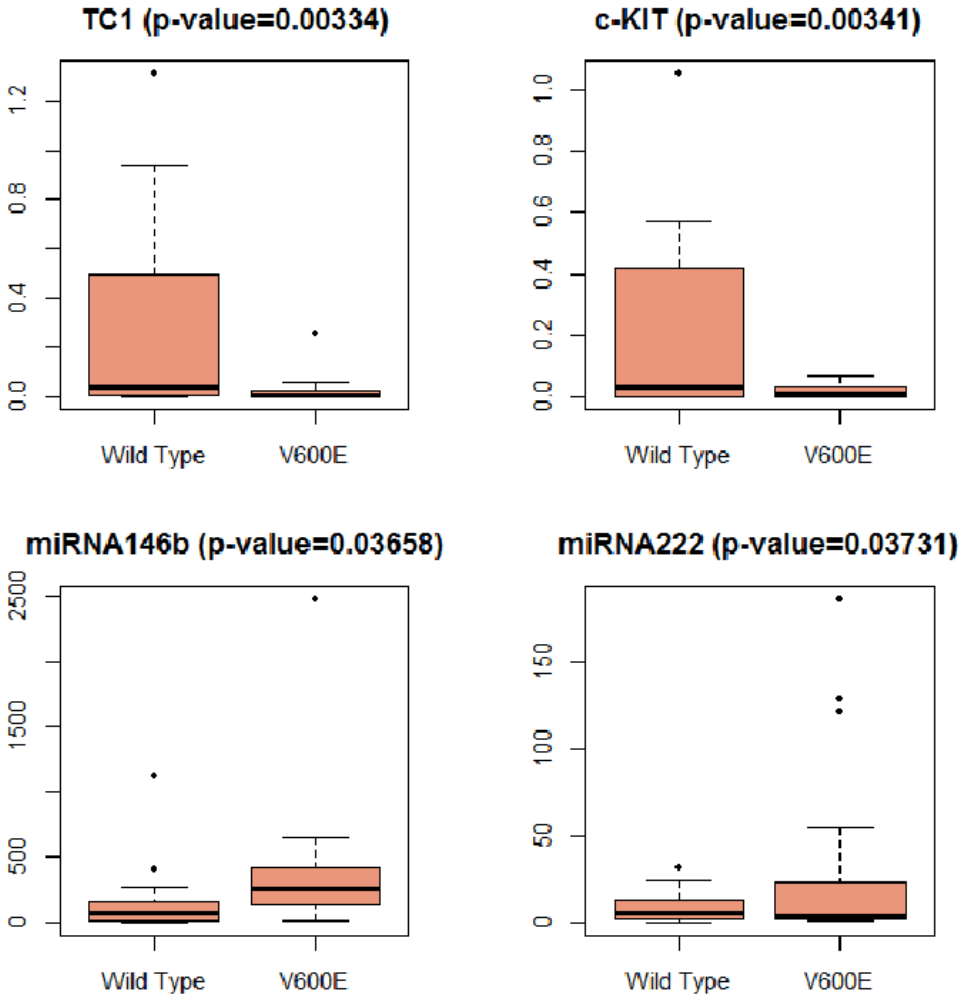

Figure 4.24. Differential expression of each single marker according to BRAF mutational status in the malignant samples analyzed on the dataset used for the building of the computational model (Tab3)

4.5.4 ROC curve analysis approach

We finally employed receiver-operated characteristics (ROC) curve analyses using the expression of each marker individually (TC1, c-KIT, miRNA 146b, miRNA222), in order to determine model robustness for predicting BRAF status. (Figure 4.25, Table 4.6). Among the markers, miRNA146b showed the highest AUC (0.7) for V600E versus WT malignant.

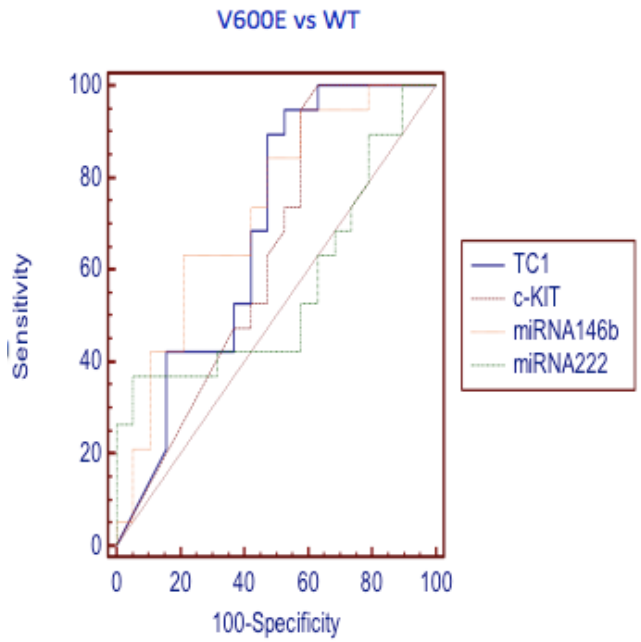

Figure 4.25: ROC analysis for KIT, TC1, miRNA146b, miRNA222 separately in V600E vs WT malignant.

	Sensitivity	Specificity	AUC[a]	SE[b]	95% CI[c]	p-value
TC1*	90	52.6	0.684	0.0904	0.513 to 0.825	0.0260
c-KIT*	100	42.9	0.633	0.0907	0.461 to 0.783	0.0491
miRNA146b*	65	81	0.729	0.0836	0.560 to 0.860	0.0005
miRNA222	35	90.05	0.558	0.0989	0.388 to 0.719	0.6798

Table 4.6. ROC analysis for each marker individually in WT malignant vs V600E. The asterisks indicate the genes with significant p-value: TC1 p=0.0260; c-KIT p=0.0491; miRNA 146b p =0.0005.

4.6 Gene expression analysis of a panel of 84 Human Tyrosine Kinases gene array

Quantitative PCR array technology was exploited to examine the transcript levels of 84 Tyrosine genes, on 8 benign samples and 12 malignant samples, and the processing of the data was obtained by means of several kinds of comparisons between samples. In order to expose the results, we have used the Fold-Regulation, which represents fold-change results in a biologically meaningful way, and the Fold-Change (2^(- Delta Delta Ct)) is the normalized gene expression (2^(- Delta Ct)) in the Test Sample divided the normalized gene expression (2^(- Delta Ct)) in the Control Sample.

Initially we compared all benign samples as a single group with all malignant samples as a single group. Transcript quantification by the $2^{-\Delta\Delta CT}$ method showed that, with the exception of KIT and EPHA5 that were down regulated with p>0.05, 53 tyrosine kinase genes were up regulated at least two fold times in malignant group than in the benign group, and particularly 14 of these with a significant p-value: ALK, AXLC, CSK, EPHA2, EPHA4, ERBB3, FGFR3, FGR, HCK, IGF1R, JAK3, LYN, MERTK, MST1R (Table 4.7, Figure 4.26A,B).

Malignant samples vs Benign samples		
Tyrosine Kinases name	p-value	fold up or down
ABL1	0,078733	3,5095
ABL2	0,090759	5,0078
ALK	0,02089	4,5683
AXL	0,023475	3,2052
BLK	0,364858	1,8093
BTK	0,142424	1,4069
CSF1R	0,337199	2,6906
CSK	0,015	6,3975
DDR1	0,335951	3,4802
DDR2	0,342303	1,4053
EGFR	0,927169	2,1911
EPHA1	0,079751	2,8081
EPHA2	0,026185	11,2258
EPHA3	0,503131	1,0145
EPHA4	0,044067	4,9674
EPHA5	0,247184	-2,269
EPHA7	0,050713	-1,96
EPHA8	0,72647	-1,1557
EPHB1	0,283071	2,2352
EPHB2	0,210557	2,5359
EPHB3	0,184338	2,2928
EPHB4	0,091108	3,1113
EPHB6	0,602841	1,5489
ERBB2	0,224554	4,8302
ERBB3	0,042713	25,0994
ERBB4	0,053654	7,021
FER	0,090949	2,2828
FES	0,248551	2,488
FGFR1	0,170782	5,2613
FGFR2	0,434054	2,0485
FGFR3	0,034528	4,2945
FGFR4	0,325155	2,2032
FGR	0,0471	3,5936
FLT1	0,461141	1,694
FLT3	0,892472	-1,2864
FLT4	0,311998	2,4333
FRK	0,441031	1,1319
FYN	0,065814	12,6224

HCK	0,028615	2,1791
IGF1R	0,027255	3,866
IGF2R	0,072264	11,8899
INSR	0,202495	9,3152
INSRR	0,224744	1,488
ITK	0,864426	-1,0911
JAK1	0,14329	2,9223
JAK2	0,38949	1,6803
JAK3	0,040946	2,6674
KDR	0,432088	1,1006
KIT	0,192859	-5,461
LCK	0,832743	1,2927
LTK	0,915645	1,3325
LYN	0,029164	8,1681
MATK	0,062273	5,5645
MERTK	0,037934	6,9023
MET	0,073381	16,0416
MST1R	0,027979	6,7136
MUSK	0,537506	1,617
NTRK1	0,434666	1,1032
NTRK2	0,800117	1,4948
NTRK3	0,134752	2,4418
PDGFRA	0,921158	2,2967
PDGFRB	0,479187	1,0029
PTK2	0,786393	1,8774
PTK2B	0,555445	2,6042
PTK6	0,254569	1,2805
PTK7	0,309666	4,4038
RET	0,483323	1,3751
ROR1	0,5567	2,8879
ROR2	0,253785	-1,3368
ROS1	0,84381	-1,0392
RYK	0,536358	2,4305
SRC	0,793006	5,5774
SRMS	0,168092	-1,8618
SYK	0,227986	1,2842
TEC	0,245954	-1,0003
TEK	0,421818	-1,1647
TIE1	0,222614	-1,5355
TNK1	0,109385	1,3539
TNK2	0,91698	2,6231
TXK	0,076006	3,0791
TYK2	0,273992	3,5216
TYRO3	0,537825	1,8698
YES1	0,253332	1,5833
ZAP70	0,238128	-1,0184

Table 4.7. Up-Down Regulation in Malignant samples vs Benign samples: Fold-regulation values < 0 indicate a negative or down-regulation and the fold-regulation values > 0 indicate a positive- or an up-regulation; Fold-regulation values greater than 2 are indicated in red; fold-regulation values less than -2 are indicated in blue; p values less than 0.05 are indicated in red.

A

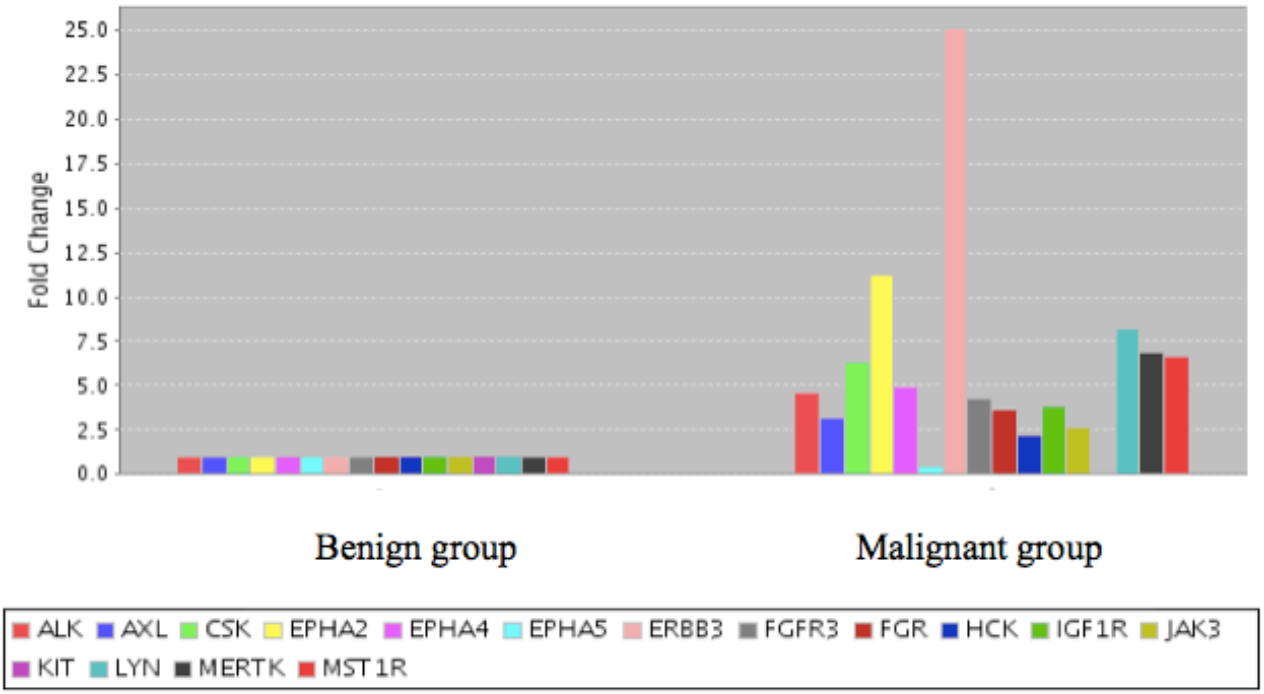

B

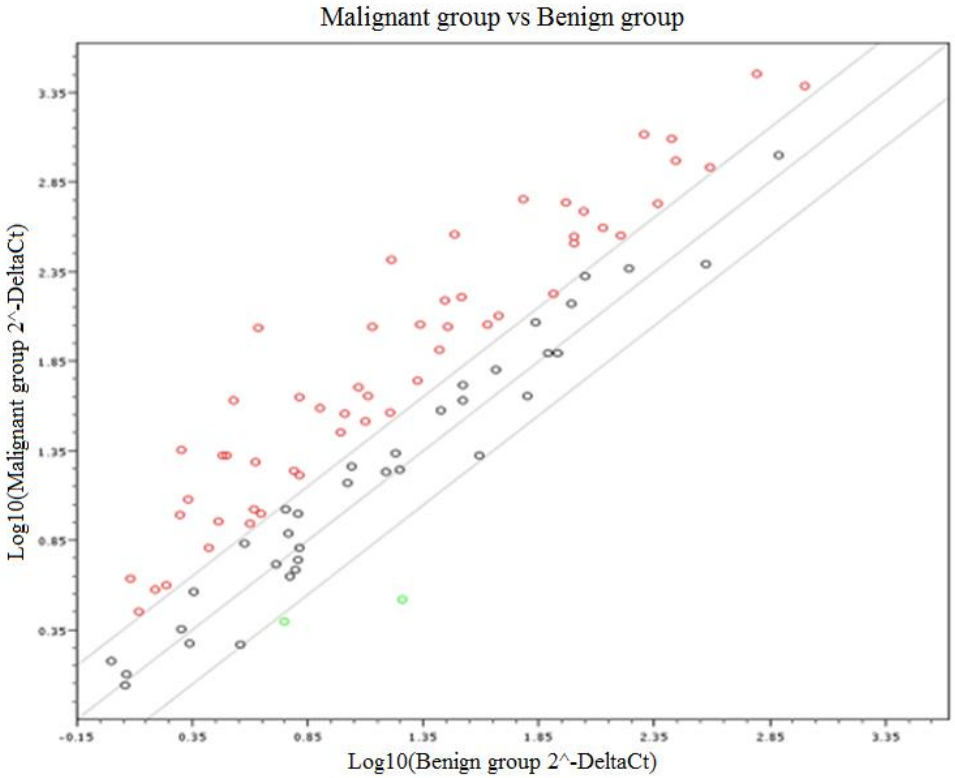

Figure 4.26: Comparison between malignant group and benign group: (A) The Histogram shows the genes that are significantly up-expressed and down-expressed ($p<0.05$) in malignant group than benign group, with the exception of KIT and EPHA5 $p>0.05$. (B) In the scatter plot the red dots indicate in malignant group the over-expressed genes with fold ≥ 2 and the green dots indicate the down-expressed genes with fold ≤ -2 (KIT, EPHA5) respect to benign group.

Afterwards we compared the benign group versus two groups: the group of malignant samples with BRAF WT (n=6) and the group of malignant samples with BRAF V600E (n=6). Lastly we compared the malignant group with BRAF WT versus the malignant group with BRAF V600E.

The comparison of the Tyrosine Kinases expression profile among the benign group versus group of malignant samples with BRAF WT and the group of malignant samples with BRAF V600E demonstrated a 2 fold up-regulation of 50 genes in BRAF V600E group and 48 genes in BRAF WT compared to the benign group. Particularly we obtained 22 genes significantly ($p<0.05$) over-expressed in BRAF V600E and 7 significantly overexpressed in BRAF WT compared to the benign group. The genes significantly overexpressed that are in common in these two groups respect to the benign group were: ALK, CSK, HCK, MST1R. On the other hand, only 5 genes (EPHA5/7, KIT, SRMS, TIE1) in the BRAF V600E group and 3 genes (EPHA5/7, KIT) in BRAF WT were 2 fold down-regulated in respect to the benign group with no statistical significance (Table 4.8, Figure 4.27)

Finally the comparison of the Tyrosine Kinases expression profile between the BRAF V600E malignant group and the BRAF WT malignant group, showed in malignant group BRAF V600E
36 genes with at least 2 fold down-regulation and 12 genes with at least 2 fold up-regulation compare to the malignant BRAF WT group. Four genes were significantly down-expressed ($p<0,05$): INSR, KIT, PTK2, TNK1 (Table 4.9, Figure 4.28).

By means of Venn diagram, we found the genes with significantly altered expression in common to all conducted comparisons: in particular, in the comparison among V600E vs benign and V600E vs WT malignant there was one gene in common (INSR); the comparison among V600E vs benign and all malignant vs benign had twelve genes in common (ALK, ERBB3, FGR3, FGR, IGF1, JAK3, LYN, MERTK, ALK, CSK, HCK, MST1R); instead the comparison among WT malignant vs benign and V600E vs benign had four genes in common (ALK, CSK, HCK, MSTIR); finally the comparison among WT malignant vs benign and all malignant vs benign had five genes in common (EPHA2, ALK, CSK, HCK, MST1R). We didn't find genes in common among V600E vs WT malignant and WT malignant vs benign, and between V600E vs WT malignant and all malignant vs benign.

Moreover in three (all malignant vs benign; V600E vs benign; WT malignant vs benign) of the four conducted comparisons, we found four genes (ALK, CSK, HCK e MSTR1) in common that had a significantly altered expression (Figure 4.29).

Malignant samples BRAF V600E and BRAF WT vs benign group				
	BRAF V600E		**BRAF WT**	
Tyrosine Kinases name	fold up or down	p-value	fold up or down	p-value
ABL1	4,3232	0,023592	2,8489	0,072369
ABL2	4,6214	0,011912	5,4264	0,068446
ALK	6,3386	0,02176	3,2925	0,034481
AXL	6,2495	0,002608	1,6439	0,279645
BLK	1,3476	0,779615	2,4291	0,225088
BTK	1,5819	0,101747	1,2512	0,29074
CSF1R	2,0533	0,276445	3,5257	0,241102
CSK	5,6863	0,019216	7,1975	0,017377
DDR1	4,0723	0,112888	2,9742	0,24157
DDR2	1,3503	0,478986	1,4624	0,279587
EGFR	2,662	0,638007	1,8035	0,795498
EPHA1	4,3057	0,061891	1,8314	0,234122
EPHA2	10,8184	0,055475	11,6486	0,021246
EPHA3	-1,1968	0,369534	1,2319	0,871874
EPHA4	11,801	0,001316	2,091	0,162923
EPHA5	-3,3048	0,066703	-1,5579	0,798417
EPHA7	-2,9332	0,104683	-1,3096	0,253086
EPHA8	-1,0864	0,873932	-1,2294	0,704124
EPHB1	1,843	0,384627	2,7109	0,244456
EPHB2	2,6882	0,30459	2,3922	0,177012
EPHB3	2,2769	0,255582	2,3087	0,174216
EPHB4	2,3227	0,201964	4,1675	0,031282
EPHB6	2,1779	0,661374	1,1016	0,642793
ERBB2	4,4704	0,058554	5,2189	0,129126
ERBB3	52,6338	0,000138	11,9692	0,088103
ERBB4	6,8093	0,097668	7,2392	0,025826
FER	4,5683	0,020287	1,1408	0,228267
FES	2,7352	0,399167	2,2632	0,206907
FGFR1	4,5961	0,063994	6,0227	0,13303
FGFR2	2,3984	0,702566	1,7497	0,313353
FGFR3	7,3615	0,030316	2,5053	0,10728
FGFR4	1,8229	0,141493	2,6627	0,197683
FGR	6,1706	0,013232	2,0928	0,189061
FLT1	1,1793	0,320611	2,4333	0,25265
FLT3	-1,8446	0,15719	1,1147	0,494982
FLT4	1,5897	0,608539	3,7246	0,169118
FRK	-1,3728	0,688182	1,7588	0,272829
FYN	15,9585	0,034164	9,9838	0,105085
HCK	2,0855	0,015677	2,2769	0,046454
IGF1R	8,2249	0,001222	1,8171	0,117181
IGF2R	22,4322	0,007332	6,3021	0,089558
INSR	9,1604	0,000789	9,4725	0,12004
INSRR	1,521	0,239213	1,4557	0,242195
ITK	-1,0383	0,680427	-1,1467	0,971951

JAK1	3,5894	0,023342	2,3791	0,130989
JAK2	1,491	0,784548	1,8938	0,285669
JAK3	5,6226	0,005677	1,2654	0,265372
KDR	-1,127	0,869769	1,3653	0,255384
KIT	-10,2556	0,310593	-2,9079	0,424885
LCK	1,3237	0,712179	1,2625	0,931707
LTK	1,8372	0,899905	-1,0347	0,75667
LYN	16,8246	0,013714	3,9655	0,104384
MATK	4,525	0,038403	6,8428	0,06481
MERTK	12,3841	0,04082	3,847	0,069857
MET	38,1978	0,056689	6,7369	0,057
MST1R	8,8945	0,037007	5,0674	0,036017
MUSK	1,7932	0,698999	1,4582	0,484047
NTRK1	1,1454	0,362805	1,0625	0,630251
NTRK2	1,571	0,874373	1,4224	0,818104
NTRK3	5,9158	0,026135	1,0078	0,717821
PDGFRA	2,5264	0,979606	2,0879	0,909712
PDGFRB	-1,5404	0,387412	1,5494	0,856608
PTK2	1,6334	0,453283	2,1578	0,856535
PTK2B	2,7559	0,614571	2,4609	0,750886
PTK6	1,0601	0,415616	1,5467	0,449108
PTK7	3,757	0,463564	5,162	0,504321
RET	1,1958	0,465537	1,5815	0,781164
ROR1	4,5132	0,693012	1,8478	0,67132
ROR2	-1,5435	0,413321	-1,1577	0,449601
ROS1	-1,1457	0,408158	1,061	0,775109
RYK	1,6794	0,598422	3,5176	0,256186
SRC	4,2933	0,566533	7,2455	0,896966
SRMS	-3,9222	0,325696	1,1316	0,356901
SYK	-1,1681	0,404186	1,9263	0,407752
TEC	-1,0777	0,415131	1,077	0,432811
TEK	-1,2731	0,399503	-1,0656	0,731902
TIE1	-2,3929	0,399969	1,0148	0,40095
TNK1	-1,1424	0,246089	2,094	0,28954
TNK2	1,9459	0,421707	3,5359	0,575643
TXK	2,7007	0,189869	3,5105	0,072921
TYK2	3,4037	0,445766	3,6437	0,456509
TYRO3	1,6649	0,607475	2,1	0,728531
YES1	2,4291	0,422076	1,032	0,440036
ZAP70	1,8505	0,421395	-1,9191	0,411084

Table 4.8. Up-Down Regulation in Malignant samples BRAF V600E and BRAF WT vs benign group: Fold-regulation values < 0 indicate a negative or down-regulation and the fold-regulation values > 0 indicate a positive- or an up-regulation; Fold-regulation values greater than 2 are indicated in red; fold-regulation values less than -2 are indicated in blue; p values less than 0.05 are indicated in red.

Malignant samples BRAF V600E vs BRAFWT		
Tyrosine Kinases name	p-value	fold up or down
ABL1	0,364223	-1,1054
ABL2	0,103815	-1,9696
ALK	0,526697	1,1477
AXL	0,375407	2,2664
BLK	0,31046	-3,0236
BTK	0,443858	-1,3268
CSF1R	0,555035	-2,8804
CSK	0,137852	-2,1232
DDR1	0,253266	-1,2251
DDR2	0,645331	-1,8166
EGFR	0,384843	-1,1365
EPHA1	0,864424	1,4016
EPHA2	0,230345	-1,8061
EPHA3	0,36368	-2,473
EPHA4	0,73816	3,3646
EPHA5	0,299458	-3,5585
EPHA7	0,143035	-3,757
EPHA8	0,191771	-1,4824
EPHB1	0,311231	-2,4673
EPHB2	0,154073	-1,4927
EPHB3	0,177157	-1,7008
EPHB4	0,110635	-3,0096
EPHB6	0,741172	1,1786
ERBB2	0,092467	-1,9583
ERBB3	0,941266	2,6215
ERBB4	0,376938	-1,7833
FER	0,227588	2,3874
FES	0,212904	-1,3879
FGFR1	0,302402	-2,1981
FGFR2	0,52584	-1,2237
FGFR3	0,801802	1,7517
FGFR4	0,278838	-2,4502
FGR	0,43829	1,7578
FLT1	0,051706	-3,4611
FLT3	0,208707	-3,4492
FLT4	0,05047	-3,9301
FRK	0,193248	-4,05
FYN	0,340007	-1,0494
HCK	0,256826	-1,8314
IGF1R	0,243558	2,6984
IGF2R	0,741609	2,122
INSR	0,030354	-1,7346
INSRR	0,396327	-1,6054
ITK	0,379769	-1,5188
JAK1	0,404274	-1,1118
JAK2	0,213766	-2,1306
JAK3	0,527017	2,6489
KDR	0,333918	-2,581

KIT	0,031272	-5,9158
LCK	0,443672	-1,5998
LTK	0,52867	1,1332
LYN	0,420109	2,5293
MATK	0,093166	-2,5366
MERTK	0,738393	1,9191
MET	0,926933	3,3801
MST1R	0,460688	1,0464
MUSK	0,419616	-1,3641
NTRK1	0,349541	-1,5561
NTRK2	0,464462	-1,5188
NTRK3	0,827937	3,4993
PDGFRA	0,813023	-1,3863
PDGFRB	0,147041	-4,0035
PTK2	0,017917	-2,2159
PTK2B	0,086696	-1,4979
PTK6	0,263465	-2,4474
PTK7	0,1499	-2,3047
RET	0,172113	-2,2185
ROR1	0,172252	1,4561
ROR2	0,30149	-2,2365
ROS1	0,262511	-2,0391
RYK	0,074706	-3,5135
SRC	0,229916	-2,8309
SRMS	0,265488	-7,4449
SYK	0,318883	-3,7744
TEC	0,334845	-1,947
TEK	0,096757	-2,004
TIE1	0,149684	-4,0734
TNK1	0,017853	-4,0127
TNK2	0,333986	-3,0481
TXK	0,275567	-2,1804
TYK2	0,285261	-1,7957
TYRO3	0,159373	-2,1159
YES1	0,985257	1,4032
ZAP70	0,248808	2,1171

Table 4.9: Up-Down Regulation in Malignant samples BRAF V600E vs BRAFWT: Fold-regulation values < 0 indicate a negative or down-regulation and the fold-regulation values > 0 indicate a positive- or an up-regulation; Fold-regulation values greater than 2 are indicated in red; fold-regulation values less than -2 are indicated in blue; p values less than 0.05 are indicated in red.

A

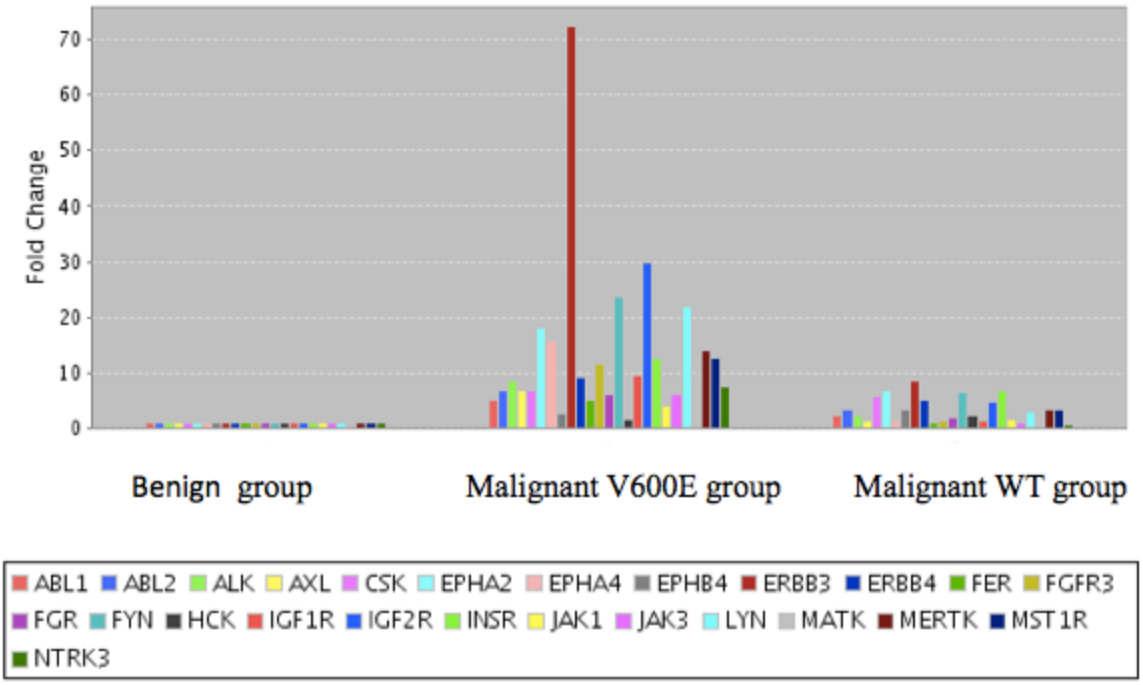

B

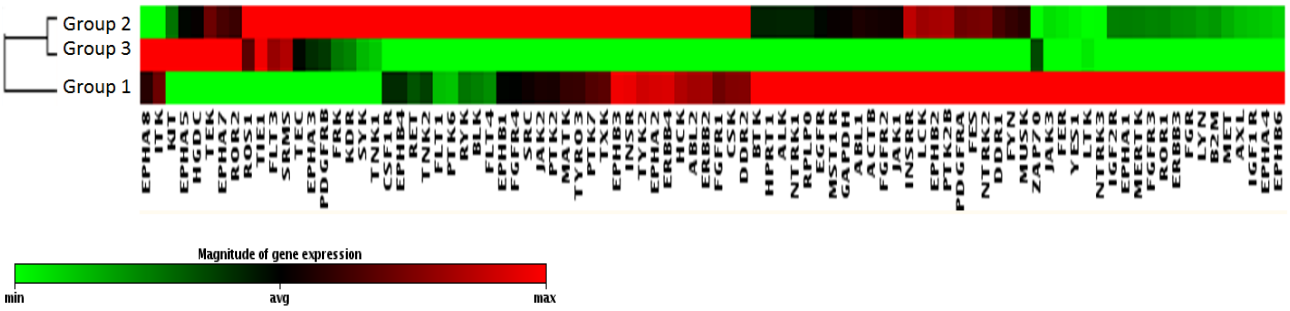

Figure 4.27 A-B: Tyrosine Kinases genes in malignant samples,V600E and WT, vs Benign samples. (A) The Histogram shows the genes that are significantly different expressed in malignant V600E group and malignant WT group than benign group; in malignant WT group the are shown also the genes that are different expressed in malignant V600E group than benign group, in order to compare the difference of this genes in both groups, malignant V600E group and malignant WT group. (B) Expression matrix of Tyrosine Kinases genes in malignant samples, V600E (Group 1) and WT (Group 2), vs Benign samples (Group 3): 2 fold up-regulated genes are in red, 2 fold down-regulated genes are in green, according to the bar shown below the matrix. Each row represents the colour coded expression of a specific gene; the column represents the colour coded Tyrosine Kinases profiles, obtained for each type of comparison between groups: Group 1= V600E malignant vs Group 3=benign; Group 2 = WT malignant vs Group 3=benign; V600E malignant vs WT malignant.

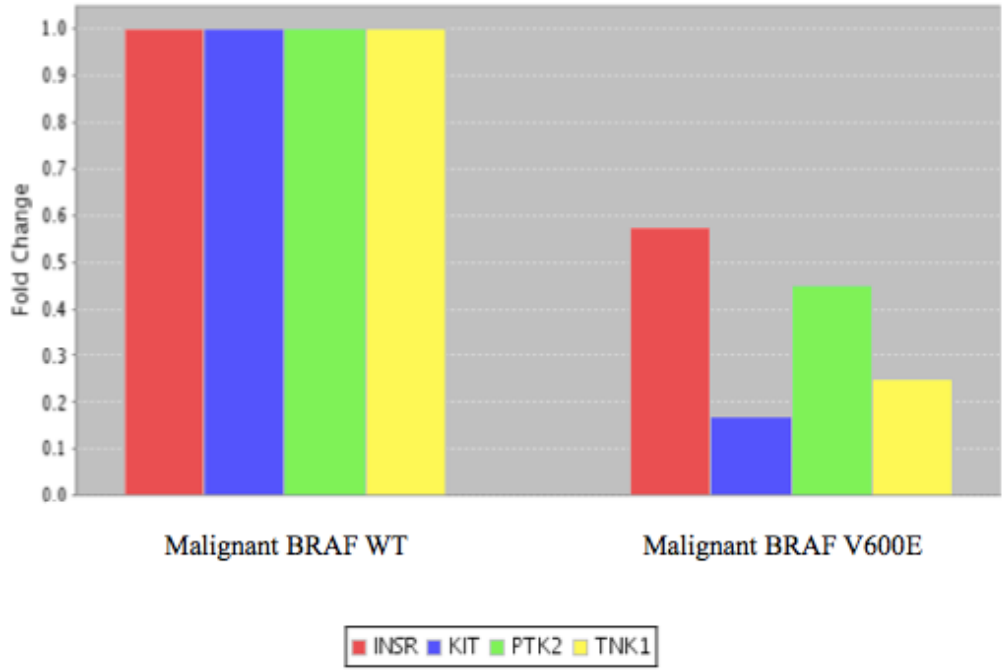

Figure 4.28: Comparison between malignant samples BRAF V600E and malignant samples BRAF WT: The Histogram shows the genes that are significantly differentially expressed in malignant BRAF V600E group than malignant BRAF WT group.

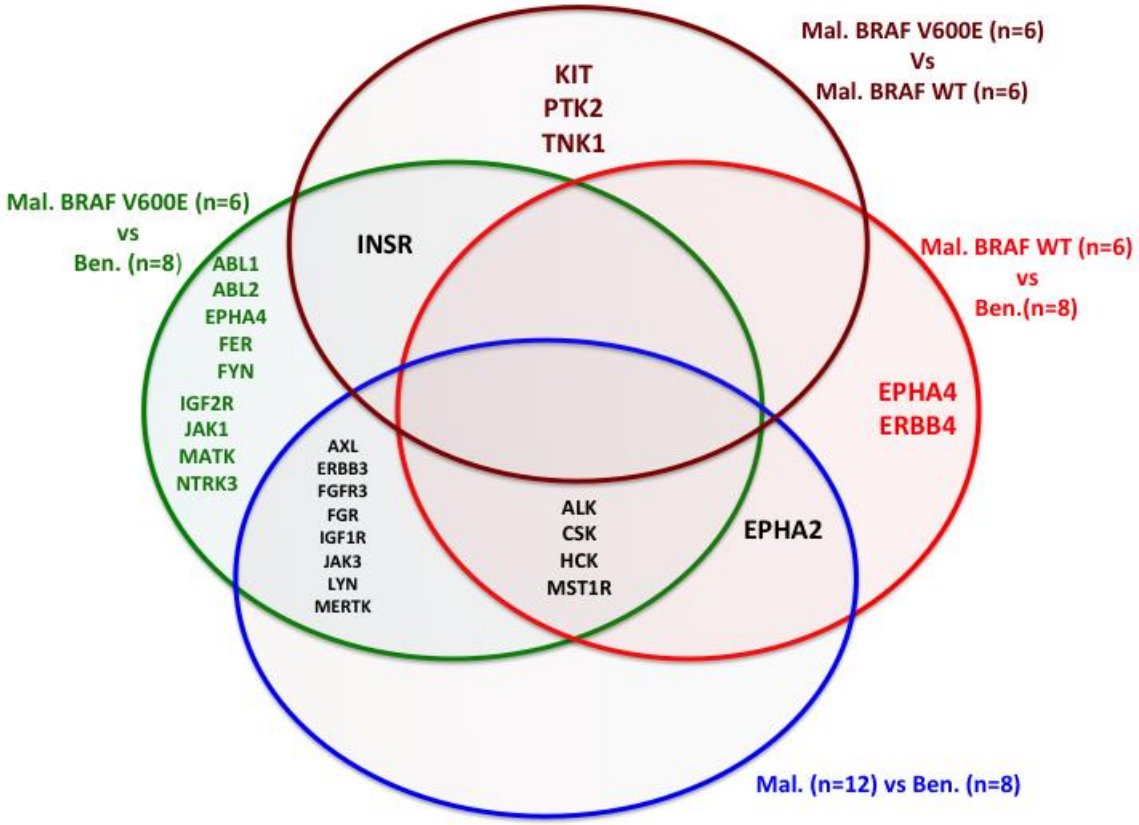

Figure 4.29. Venn diagram: the venn diagram was build on 4 comparisons: malignant vs benign (blue), V600E vs benign (green), WT malignant vs benign (red), V600E vs WT malignant (brown). The diagram shows the genes with significantly altered expression that are in common to various combinations of the conducted comparisons (black).

5. DISCUSSION

Papillary thyroid carcinoma (PTC) is the most common malignancy in thyroid tissue; about 80% of incident thyroid cancers are PTC. Although PTC is usually associated with alterations in the RET/PTC-RAS-BRAF signalling pathway [9, 46], the detailed molecular mechanism is unclear. A few papers mentioning a role for c-KIT in thyroid malignancies suggested to perform an analysis of c-KIT expression on thyroid cells obtained by FNAC from benign and malignant thyroid nodules, with the double aim to study a human model of thyroid cancer and, at the same time, to verify if c-KIT expression analysis could be of any clinical interest.

To date, the biological significance of loss of c-KIT in thyroid tumors is not elucidated. Surprisingly, the depletion of c-KIT expression in thyroid tumors in contrast with the gain of function of other tyrosine kinase receptors such as c-RET and c-MET or of oncogenes such as c-RAS, suggesting that different tyrosine kinase receptor signaling pathways may exert opposite biological effects in a given cell type, alternatively controlling mitogenesis or cell differentiation. SCF, the c-KIT ligand, is not mitogenic in primary cultures of thyrocytes even in conjunction with thyroid-stimulating hormone [103], a result which would indicate that SCF/c-KIT pathway may control some aspects of the thyrocyte differentiated phenotype rather than cell division.

In the present study the aim was to investigate thoroughly the role of the c-KIT gene in thyroid cancerogenesis, to characterize in details the c-KIT signaling pathway and the cause of its down-regulation in thyroid cancer; because of this down-regulation, we wanted to demonstrate that c-KIT is involved in the differentiation rather than in the proliferation during thyroid malignant transformation.

To understand the cause of the down expression of c-KIT gene in malignant than benign thyroid lesions, we have investigated the presence of the SNP in exon 18 of c-KIT and c-KIT promoter methylation status. As shown in our results, the c-KIT SNP located in exon 18 was not associated neither to the biological behavior of thyroid lesions nor the c-KIT expression levels, while the c-KIT promoter methylation could account for part of the c-KIT down-expression in malignant lesions. In fact, we found that the group of samples with no c-KIT expression had a significantly higher frequency of methylated cases than samples with c-KIT expression (p-value = 0.02) (Figure 4.2 B). Moreover if we correlate the frequency of methylation with the c-kit expression level, which was

previously divided in 4 classes, there is a trend of correlation between c-kit expression and methylation status, showing a decrease of methylation with an increase of c-KIT gene express (Figure 4.2 A). This correlation could become significant if we increment the number of samples for each class and if we have approximately the same number of observations, in particular in class 3 where there were only seven samples.

The results of methylation analysis could be a really important cause of the knockdown of c-KIT gene in thyroid carcinogenesis since it is known in literature that the silencing of thyroid-specific genes often occurs with progression and dedifferentiation of thyroid cancer [104]

In this sense, methylation, and hence silencing, of these genes might be a driving force for thyroid cancer pathogenesis and progression, albeit through an undefined mechanism [105]. Regardless of its biological mechanism and relevance in thyroid tumorigenesis, methylation-mediated silencing of thyroid-specific genes is clearly clinically relevant because it is a cause of the loss of radioiodine avidity and hence radioiodine treatment failure and consequent progression of thyroid cancer [106]. An important question remains unanswered as to whether silencing of these thyroid specific genes, which are not classical tumor suppressor genes, plays some primary role in driving thyroid tumorigenesis or is simply a secondary event of aberrant activation of other signaling pathways, such as the BRAF/ MEK/MAPK pathway in PTC [68].

Several miRNAs have been predicted to target KIT, including those over-expressed in PTC, in fact it was demonstrated that in PTC tissues, in which miR-146b, miR-221, and miR-222 were strongly over-expressed, there was a down-regulation of KIT transcript and protein [91]; therefore, in order to investigate the possible cause of the c-KIT down-expression, we have also conducted expression study of miRNA (146b and 222) in our FNA samples.

This study showed that the expressions of miRNA146b, miRNA222 by qPCR were significantly up-regulated in the group of samples with no c-kit expression compared with the group of samples with c-kit expression (p-value = 0.01693; p-value = 0.0008 respectively) (Figure 4.4 A, B).

C-KIT and miRNAs expressions were inversely correlated, as demonstrated by the higher expression of the miRNA 146b in c-kit class I with no expression of the gene than class IV with the highest expression of the gene (p-value <0.05) (Figure 4.5). This observation indicates that these miRNAs, and mostly miRNA146b, could be involved in

the regulation of c-KIT in thyroid cancer and that a novel therapeutic target for the treatment of thyroid cancer could be the regulation of this miRNAs for c-KIT negative in thyroid cancer

In order to demonstrate the hypothetical role of c-KIT in differentiation during thyroid malignant transformation, we wanted to investigate if there are genetic markers, usually expressed in the differentiated thyrocyte, which could be involved as downstream targets of the signal transduction pathways of c-KIT. In order to do this, we correlated the expression level of c-KIT with some known differentiation markers of the thyroid [107]. By expression analysis for PAX8 gene, we found that c-KIT gene expression resulted to be directly correlated to PAX8 gene expression significantly (r^2 =0.1319) (p=0.003) (Figure 4.6 C). Moreover we correlated the PAX8 gene expression with c-KIT classes' distribution, and we obtained that PAX8 gene expression values were significantly higher in class 2 and 3 compared to class 1 ($p<0.05$) (Figure 4.6 B). The significant correlation of c-KIT expression with PAX8 expression supports the hypothesis of c-kit involvement in the differentiation pathway during thyroid cancerogenesis, nevertheless their reciprocal placement in the pathway architecture is not clearly known.

PAX8 is expressed in various thyroid cancers but the pattern of expression is somewhat controversial [108]; one study showed that the nuclear PAX8 staining is correlated with the thyroid differentiation phenotype, while others demonstrated that PAX8 is a useful marker for the diagnosis of anaplastic carcinomas. More studies are required to determine the expression pattern and the role of PAX8 in thyroid cancers [107]. In light of what, we also valuated the relationship of PAX8 expression with our malignant and benign FNA samples, and we found that the expression level was significantly higher in the benign group compared to the malignant group (p=0.03) (Figure 4.5 A), so the same difference that we found previously for c-KIT expression. Those results indicate as c-KIT and PAX8 genes seem to follow the same direction during the epithelium thyroid transformation, and once again c-KIT could be involved in the differentiation pathway, but further functional studies are needed to understand the underlying mechanisms.

We also conducted the same analysis described above with another differentiation thyrocyte marker: TTF1 [109]. The correlation between TTF1 and c-KIT seems to be inverse and it wasn't statistically significant. Moreover we found (not statistically significant) an over-expression of TTF1 in malignant samples than benign, this is

agreement with it is known in literature [93]. TTF-1 is one of the most commonly used markers in diagnostic pathology [110]. It has shown a very high sensitivity and specificity in the diagnosis of tumors of pulmonary and thyroid lineage.
Diffuse and strong TTF-1 nuclear staining was seen in all papillary carcinomas, follicular adenomas, follicular carcinoma, and poorly differentiated carcinomas, whereas its expression in medullary carcinomas was variable and TTF-1 was generally negative in anaplastic carcinomas [108].
Many candidate markers of thyroid cancer have been identified in microarray studies that require analytic and clinical validation in a cohort large enough to permit evaluation of the clinical utility of these markers. Another aim of my study is to identify new molecular markers to improve cytological diagnostics accuracy. By RT-PCR of NIS mRNA we found that the expression level was higher in benign thyroid tumors in comparison to the malignant ones, even though it didn't show any statistical significance; it is difficult to compare our data to the literature because studies addressing NIS gene expression are sparse. Some studies have demonstrated a decrease or loss on NIS expression in thyroid cancer cells suggesting a possible role of this gene in the pathway of thyroid cell transformation [94], while either increased or decreased NIS expression in benign lesions has been reported [95]. Based on our results, the NIS expression is associated to the biological behavior of thyroid nodules because the gene is more expressed in benign lesions, this confirms what we expected since the NIS gene codes for a functional symporter in normal thyrocytes.

Regarding TC1, several studies reported a higher expression of this protein in thyroid malignancies compared to benign nodules [96, 111]. Concordant to the literature, we observed that TC1 was significantly over-expressed in malignant lesions compared to the benign ones (p-value 0.04) (Figure 4.10). The exact function of the protein coded by this gene is still unknown.

miRNA expression profiles resulted in being different not only between tumors and healthy tissues but also between different histopathological lesions of the same tissue, between tumors at different stages of malignancy, and between primary tumors and metastases. Different studies were conducted to compare global miRNA expression in human PTCs versus unaffected thyroid tissue [65].
Therefore, we investigated in our study the diagnostic ability of a two miRNAs

(miRNA222 and miRNA146b) in the discrimination of malignancy and benignity in our FNA samples.

We found that miRNA146b was significantly over-expressed in malignant group compared to the benign group according to the literature (p-value = 0.0005) (Figure 4.11 A). Moreover, a ROC analysis was performed to measure the specificity and sensitivity of the diagnostic performance of miR-146b showing its good efficacy in predicting the malignant and benign events with 100% of specificity and 87.8% of sensitivity (AUC = 0.9 C.I 95% 0.8 -0.9; $p < 0.0001$), respectively (Figure 4.11 B).

Regarding miRNA222, its expression was higher in the malignant group compared to the benign group, but there was no significance, while miRNA 146b is more accurate at differentiating malignant from benign thyroid lesions on FNA, and it suggests that FNA miRNA 146b analysis could be a useful adjunct in the management of patients with thyroid nodules.

Among the purposes of the present study there is the search for a diagnostically accurate preoperative assay able to help the discrimination of the benign from malignant thyroid neoplasms. Currently, the diagnosis of thyroid nodules relies primarily on cytology. For the majority of patients with PTC, FNA-based cytology can make a diagnosis with high accuracy. However, there is a significant proportion of neoplasm in which the FNA-based preoperative cytological diagnosis fails.

Computation model like Discriminant Analysis and Bayesian Neural Networks (BNN) have been used as a supplement or alternative to standard statistical techniques [112]. Bayesian classification has been applied across the spectrum of medicine, from optimization of pharmacotherapy dosing [113,114], predicting cancer screening [115] and diagnostic test results [116,117], to determining injury severity [118], assessing operative risk [119] and predicting surgical outcomes [120-123].

The Bayesian Artificial Neural Network and Discriminant Analysis, made up of KIT, TC1, miRNA222, miRNA146b on data collected from FNA samples, showed a very strong predictive value (94.12 % and 92.16 % respectively) in discriminating malignant from benign patients. It is interesting to notice that Discriminant Analysis showed a correct classification of 100.00 % of the samples in the malignant group, and 95.00 % by BNN (Figure 4.12, 4.13). Based on the Discriminant Analysis results, the probability

of the prediction of diagnosis for almost all the samples resulted to range between 85% and 100%, thus, although the general prediction value is 88.23%, the predictive power to assess each sample individually can reach a value of 100%. Moreover no classification errors came out when the probability of diagnosis was higher than 85%; thus allowing us to use this model as a correct predictor of samples with a probability score >85% ($p < 0.0001$), and these data strengthen the importance of the 4-markers model as an adjunctive tool for the preoperative diagnosis of thyroid nodules.

It's important to notice that we have put in the models also miRNA222 that was not a significant marker in discrimination of malignant from benign samples, while its contribution in the discriminative power seems to be relevant. In fact, even though a variable is not significant, its combination with other variables may be significant

The neural network and discriminant analysis was then validated on 11 unknown samples. The models determined the accurate diagnosis of 11 unknown samples tested, based on a comparison to the gold standard pathological diagnosis as determined by clinical pathologists (Table 4.3, 4.4).

The samples correctly classified were diagnosed as indeterminate samples (SPTC) at the cytological level; 7 out of the 11 SPTC samples used in this analysis were BRAF mutated. Therefore there were four patients left out that even after BRAF mutational analysis remained SPTC. The use of our model could have assigned also these 4 patients to the malignant group making the diagnosis of malignancy more certain for the surgeon with a probability of 0.9065, 0.8631, 0,7890, 0.9585 by Discriminant analysis and 0.999, 0.824, 0.8, 1 by Neural network. We had a 36.36% improvement of the diagnostic accuracy. It is important to point out that SPTC lesions are often very difficult to diagnose and in this study we developed a molecular approach that is able to correctly classify as certain malignant 100% (11/11) of SPTC lesions, so this model could be very useful to help the diagnosis in the preoperative setting of indeterminate lesions such as SPTC. Because our markers panel is 100% sensitive for malignant pathology of indeterminate FNA lesions, it would be reasonable to recommend a total thyroidectomy if malignancy is predicted.

In order to visualize in a 3-dimensional space the discriminative power of all the four markers, we applied the Principal Component Analysis to the benign and malignant samples. We obtained an overall separation among them according to the expression of the 4 markers in the study, this suggests that the four markers can together discriminate

between benign and malignant status (Figure 4.14).

Using the dataset of the computational model and the PCA analysis, we took singularly the expression values of each single gene (KIT, TC-1, miRNA222, and miRNA146b), in comparison between malignant and benign group, and we showed the results into boxplots (Figure 4.15). We obtained the same results reported in the previous sections, namely the marker significantly over-expressed in benign samples was c-kit, while malignant samples were characterized by an over-expression of both miRNAs ($p > 0.05$ as for miRNA 222) and TC1.

We also performed the receiver operating characteristic (ROC) curves analysis in order to optimize the model for negative and positive predictive value in our thyroid cohort. The ROC curve of c-KIT and miRNA146b had a high diagnostic accuracy FNAsamples, therefore they alone and in combination, can be used to distinguish between malignants and benigns. On the other hand the ROC curve of TC1 had a high specificity (92.9), this means that when tc1 is over-expressed in our samples it has a high probability to identify correctly the samples as malignant, so a low risk of false positive, but it had a low sensitivity (38.5) so when the value of TC1 is low there is a high probability to have a false benign (Table 4.5).
We have also performed a multiple variable analysis among all the markers analyzed, independently on the diagnostic classification, in order to evaluate a possible functional correlation among the markers. We observed a significant correlation of c-KIT with miRNA146b ($p<0.0001$), this is in accord with the previously section.

In conclusion, in this study we were able to develop a statistical model that accurately differentiates malignant from benign indeterminate lesions on thyroid FNAs using a panel of 2 miRNAs and 2 genes (miRNA146b, miRNA222, c-KIT, TC1); We want to propose in this study the using of BRAF molecular analysis (after uncertain cytological diagnosis) to assess the malignancy of thyroid nodules in the first place, followed by the use of the 4-markers model (miRNA222, miRNA146b, TC1 and c-KIT) to help the diagnosis of the nodules that otherwise would remain suspicious.

Finally we have conducted molecular stratification of the malignant population according to BRAF status through different approaches.

As reported in literature [23, 25], we find a dysregulation of NIS in the samples carrying the mutation V600E. This dysregulation is showed as a down-regulation of NIS expression in the BRAFV600E samples compared with the BRAF WT ones; even if it was not significant, maybe due to a small number of the samples analyzed.

By gene expression analysis we found that the expression of TC1 was significantly higher in the malignant BRAF WT as compared to thyroid cancers bearing BRAF V600E mutation (p-value= 0.01). This result suggests a potential influence of BRAF status in modulating TC1 expression. Otherwise we can suggest two kinds of malignant transformations driven by the two genes: when the malignant transformation is driven by mutated BRAF, TC1 expression seems to not influence the transformation; when BRAF is WT instead, TC1 has a major role in the neoplastic transformation and its expression becomes significative.

Moreover, as shown in the results of the comparison between miRNAs expression and BRAF status in malignant samples, miRNA146b and miRNA222 were over-expressed when BRAF was mutated (V600E) (p-value = 0.036; p-value = 0.037, respectively): this let us to better characterized and stratify the group of malignant samples and confirms, as for TC1, that miRNA 146b and miRNA 222 expressions may be involved in the collateral molecular alterations due to the expression of the mutated oncogene BRAF.

This is an important finding; in fact since BRAF V600E has been shown to be associated with higher tumor aggressiveness [124-126], the high expression of this miRNAs markers emerges as sign of more malignant tumor behaviour and should be prospectively evaluated.

The mechanisms underlying TC1 down expression and miRNA 146b-222 over expressions in BRAF V600E malignant samples are currently unknown and further studies are warranted to exploit this phenomenon. Discriminant analysis and artificial neural network were performed using the 4 gene model to show how it exists a clear differential genetic background related to presence or absence of the BRAF V600E mutation. As a matter of fact the model was able to classify BRAF mutational with a predictive power of about 75%. In particular 94.74% of the samples in the BRAF V600E group were correctly classified by Discriminant Analysis and 68.42% by BNN. Instead 57.89% of the samples in BRAF WT group were correctly classified by

Discriminant Analysis and 78.95% by BNN. Therefore we can classified correctly more samples in the BRAF V600E group by Discriminant analysis, and more samples in the BRAF WT group by BNN.

Moreover also the Principal Component Analysis showed an overall separation among the two groups, confirming that the markers have a good discriminant power in classifying V600B malignants versus WT malignants (Figure 4.23)

ROC curves analysis discriminated the malignant BRAF V600E from malignant WT samples in our dataset of FNA samples. The AUC for each significant marker was for TC1 0.684, c-KIT 0.633, miRNA146b 0.729 all with significant p-value (p= 0.0260; 0.0491; 0.0005, respectively) and for miRNA222 0.558 (table 4.6). Observing the sensitivity and specificity of the curve for each gene, TC1 and c-KIT have an excellent capacity to correctly identify the sample as WT with a low risk of false negative. On the other hand miRNA 146b and miRNA 222 have a high capacity to correctly identify the sample as BRAF mutated with a low risk of false positives.

Finally, we have investigated possible news biomarkers in thyroid cancer by Human Tyrosine Kinases RT² Profiler PCR Array.
Quantitative PCR array technology was conduced to examine the transcript levels of 84 Tyrosine genes, on 8 benign samples and 12 malignant samples, and the processing of the data was obtained by means of several kinds of comparisons between sample: malignant vs benign, V600E malignant vs benign, malignant WT vs benign, V600E malignant vs malignant WT.
Based on the conducted comparisons, it was shown that most of the differences in the expressions profile were driven by the group of malignant BRAF V600E, in fact BRAF V600E had 22 significantly alterated genes in comparison with benigns, while the malignant WT group had only 7 compared to benigns, and 4 of them are in common with V600E group suggesting a driving influence on the thyroid malignant transformation process (Table 4.8, Figure 4.27)
As shown in the Venn diagram analysis, the 4 genes (ALK, CSK, HCK and MSTR1) in common to all comparisons except for BRAF V600E vs BRAF WT, can be defined as the thyroid specific malignant genes (Figure 4.29). These genes seemed to be correlated

to thyroid neoplastic processes. We found that many of the analyzed gene, that were differentially expressed in the conducted comparisons, have or may have a role in thyroid cancer giving additional value to our study. One of the genes that is always differentially expressed in our study is ***ALK*** (Anaplastic Lymphoma Receptor Tyrosin) that encodes a insulin receptor tyrosine kinase. It was recently reported the discovery of ALK activation, via point mutation, in thyroid cancer with high level of expression of endogenous ALK [127]. Furthermore, in one study conducted by Nikiforov was reported STRN-ALK rearrangement in dedifferentiated types of thyroid cancer [128]. ***HCK*** (Hemopoietic cell kinase) encodes for a protein a protein-tyrosine kinase hat is predominantly expressed in hemopoietic cell types, and belongs to the Src family of tyrosine. The aberrant activation of Src family kinases (SFK) plays a critical role in tumorigenesis by driving a number of cellular events including proliferation, adhesion, survival, and invasion. Given its prevalent role in tumorigenesis, Src offers an attractive therapeutic target for the treatment of a wide variety of cancer. Recently studied characterized a tyrosine kinome profile in tumors relative to matched normal thyroid tissue, showing that tyrosine kinome profiling of thyroid tumors identified upregulation of Src activity in the majority of invasive thyroid cancers and functional experiments confirm that Src inhibition is effective in decreasing proliferation and invasion in human PTC cell lines [123]. Tyrosine-protein kinase ***CSK*** also known as C-Src kinase or C-terminal Src kinase is an enzyme that in humans is encoded by the CSK gene.

This enzyme phosphorylates tyrosine residues located in the C-terminal en of Src-family kinases (SFKs) including SRC, HCK, FYN, LCK, LYN and YES1, resulting in the suppression of their activities. ***MSTR1*** Macrophage Stimulating 1 Receptor encodes a cell surface receptor for macrophage-stimulating protein (MSP) with tyrosine kinase activity. This receptor has been identified as an important mediator of KRAS oncogene addiction and is overexpressed in the majority of pancreatic cancers, Moreover the overexpression and/or activation of MSTR1 has been implicated in the progression and metastasis of diverse epithelial cancers, where it plays a causal role in tumor development by promoting growth, survival, and motility of tumor cells. Studied conducted of thyroid tissues by immunohistochemistry showed that MSTR1 was hardly detected in normal thyroid cells, moderately expressed in adenoma samples, but overexpressed in about half of papillary and follicular cancer specimens. Moreover, in cultured thyroid cancer cells, MSTR1 was highly expressed, with constitutive phosphorylation. Activation of MSTR1 increased cell growth and migration via the

MAP kinase and AKT pathways. Silencing MSTR1expression significantly prevented cell growth and increased cell apoptotic death [124].

Amog genes that are significant different expressed in our study we can mention ***Eph-A2 and Eph-A4.*** The Ephrin receptors (Ephs) are frequently overexpressed in a wide variety of human malignant tumors, being associated with tumor growth, invasion, metastasis and angiogenesis [131]. Recent studies showed Eph-A2 to be widely expressed in highly proliferating human tissues and overexpressed in several types of malignancy, such as melanoma, prostate, breast, ovarian, esophageal, liver, lung and gastrointestinal cancer [133-136]. Moreover was showed that Eph-A2 but not Eph-A4 expression was enhanced in cases with malignant compared to those with benign thyroid lesions, and especially in papillary carcinomas compared to hyperplastic nodules [137]. Expression of mutant inactive Eph-A2 variants resulted in tumor mass reduction, whereas Eph-A2 upregulation was correlated with tumor stage and progression in several cancers [131].

IGFR1 *r*eceptor binds insulin-like growth factor with a high affinity and it plays a critical role in transformation events. IGFR1 is highly overexpressed in most malignant tissues where it functions as an anti-apoptotic agent by enhancing cell survival. In this study, showed that a blocking anti-insulin-like growth factor 1 receptor (IGF1R) monoclonal antibody (mAb) inhibited colony formation in correlation with IGF1R expression and decreased P-AKT, and a blocking anti-stem cell factor (SCF) mAb also inhibited colony formation of two cell lines expressing C-KIT and SCF, and decreased P-AKT. Moreover was showed that primary cells frequently co-expressed IGF1R/IGF1 but not C-KIT/SCF, suggesting that in vivo autonomous growth could be possible via IGF1R. Despite their similar role in clonogenic growth and shared signaling pathway, IGF1R and C-KIT had opposite prognostic values, suggesting that they were surrogate markers. This study could suggest as the proliferation cells is conduct by insulin receptor in papillary thyroid and instead the c-KIT follows the path of differentiation [138].

.

6. CONCLUSIONS

The results of this research support the idea that c-KIT is driving a thyroid cell differentiation pathway which results altered in thyroid neoplasm transformation. However specific functional studies are still needed to clarify the molecular mechanisms underlying c-KIT differentiation. Different molecular events have been investigated and methylation and miRNA transcriptional activity have been identified as some of the possible causes of c-KIT down-regulation in thyroid cancer.

In the same study a 4 gene model was build able to discriminate with high probability between benign and malignant FNAs. The model is proposed to be added to the routinely BRAF diagnostic test in order to improve FNA diagnostic accuracy solving the problems of the nodules that otherwise would remain suspicious.

To identify other possible genes involved in thyroid cancer 84 gene expression array were analysed. The results showed statistically significant differential expression of several tyrosine kinase genes, related and not related to c-KIT, between malignant and benign thyroid nodules. Many of the genes have been already involved in cancer and all need to be investigated further. Moreover the present study shows clearly how the presence of the BRAF V600E mutation is accompanied by a specific genetic scenario in which sets of genes specifically discriminate the mutational and wild-type status, supporting the hypothesis of a higher tumor aggressivity associated to the BRAFV600E mutation.

7. FUTURE PERSPECTIVES:

The transfection of pTarget-c-kit in K1 cells is ongoing and our future goal will be to perform functional studies such as proliferation, migration, and survival assays to better understand the involvement of c-KIT in thyroid malignant transformation.

Furthermore, we also intend to perform functional studies on thyroid tumor cell lines, with the genes that we found dysregulated by gene expression analysis, such as TC1 and PAX8. In addiction we will further characterize, through functional studies, the genes (e.g. ALK, CSK, HCK, MSTR1) that seemed more interesting in the array analysis, validate their role in the malignant transformation pathway of the thyroid and evaluate the possibility to exploit them as a potential therapeutic target for thyroid cancer.

REFERENCES

1. Cummings CW, et al. Thyroid anatomy. In: Cummings CW, ed. Otolaryngology - Head and Neck Surgery. 3rd ed. St. Louis, Mo: Mosby; 1998:2445-49.
2. Thyroid gland. In: Williams PL, Bannister LH, et al. Gray's Anatomy. 38th ed. New York, NY: Churchill Livingstone; 1995:1891-6.
3. Robbins. Basic pathology. Edi. Saunders. 8th. 758 -775
4. DaviesL, Welch HG. Increasing incidence of thyroid cancer in the United States, 1973–2002. JAMA 295, 2164– 2167 (2006).
5. LeenhardtL, Grosclaude P, Cherie-Challine L. Increased incidence of thyroid carcinoma in france: a true epidemic or thyroid nodule management effects? Report from the French Thyroid Cancer Committee. Thyroid 14, 1056–1060 (2004).
6. CooperDS, Doherty GM, Haugen BR et al. Management guidelines for patients with thyroid nodules and differentiated thyroid cancer. Thyroid 16, 109–142 (2006).
7. DeLellisRA, Lloyd RV, Heitz PU et al. (Eds). World Health Organization Classification of Tumours. Pathology and Genetics of Tumours of Endocrine Organs. IARC Press, Lyon, France (2004).
8. RobinsonMJ, Cobb MH. Mitogenactivated protein kinase pathways. Curr. Opin. Cell Biol. 9, 180–186 (1997).
9. KimuraET, Nikiforova MN, Zhu Z et al. High prevalence of BRAF mutations in thyroid cancer: genetic evidence for constitutive activation of the RET/PTC-RAS-BRAF signaling pathway in papillary thyroid carcinoma. Cancer Res. 63, 1454–1457 (2003).
10. SoaresP, Trovisco V, Rocha AS et al. BRAF mutations and RET/PTC rearrangements are alternative events in the etiopathogenesis of PTC. Oncogene 22, 4578–4580 (2003).
11. FrattiniM, Ferrario C, Bressan P et al. Alternative mutations of BRAF, RET and NTRK1 are associated with similar but distinct gene expression patterns in papillary

thyroid cancer. Oncogene 23, 7436–7440 (2004).

12. GiordanoTJ, Kuick R, Thomas DG et al. Molecular classification of papillary thyroid carcinoma: distinct BRAF, RAS, and RET/PTC mutation-specific gene expression profiles discovered by DNA microarray analysis. Oncogene 24, 6646–6656 (2005).

13. AdeniranAJ, Zhu Z, Gandhi M et al. Correlation between genetic alterations and microscopic features, clinical manifestations, and prognostic characteristics of thyroid papillary carcinomas. Am. J. Surg. Pathol. 30, 216–222 (2006).

14. GarciaRostanG, Costa AM, PereiraCastro I et al. Mutation of the PIK3CA gene in anaplastic thyroid cancer. Cancer Res. 65, 10199–10207 (2005).

15. HouP, Liu D, Shan Y et al. Genetic alterations and their relationship in the phosphatidylinositol 3kinase/Akt pathway in thyroid cancer. Clin. Cancer Res. 13, 1161–1170 (2007).

16. WangY, Hou P, Yu H et al. High prevalence and mutual exclusivity of genetic alterations in thephosphatidylinositol3kinase/ akt pathway in thyroid tumors. J. Clin. Endocrinol. Metab. 92, 2387–2390 (2007).

17. Cohen Y, Xing M, Mambo E, Guo Z, Wu G, Trink B, Beller U, Westra WH, Ladenson PW, Sidransky D. BRAF mutation in papillary thyroid carcinoma. J Natl Cancer Inst 95:625-627 (2003).

18. Xing M . BRAF mutation in thyroid cancer. Endocr Relat Cancer 12:245-262 (2005)

19. Ciampi R, Nikiforov YE (2005) Alterations of the BRAF gene in thyroid tumors. Endocr Pathol 16:163-172

20. Adeniran AJ, Zhu Z, Gandhi M, Steward DL, Fidler JP, Giordano TJ, Biddinger PW, Nikiforov YE (2006) Correlation between genetic alterations and microscopic features, clinical manifestations, and prognostic characteristics of thyroid papillary carcinomas. Am J Surg Pathol 30:216-222

21. Wan PT, Garnett MJ, Roe SM, Lee S, Niculescu-Duvaz D, Good VM, Jones CM, Marshall CJ, Springer CJ, Barford D, Marais R (2004) Mechanism of activation of the RAF-ERK signaling pathway by oncogenic mutations of B-RAF. Cell 116:855-

867

22. Namba H, Nakashima M, Hayashi T, Hayashida N, Maeda S, Rogounovitch TI, Ohtsuru A, Saenko VA, Kanematsu T, Yamashita S (2003) Clinical implication of hot spot BRAF mutation, V599E, in papillary thyroid cancers. J Clin Endocrinol Metab 88:4393-4397

23. Xing M, Westra WH, Tufano RP, Cohen Y, Rosenbaum E, Rhoden KJ, Carson KA, Vasko V, Larin A, Tallini G, Tolaney S, Holt EH, Hui P, Umbricht CB, Basaria S, Ewertz M, Tufaro AP, Califano JA, Ringel MD, Zeiger MA, Sidransky D, Ladenson PW (2005). BRAF mutation predicts a poorer clinical prognosis for papillary thyroid cancer. J Clin Endocrinol Metab 90:6373-6379

24. Kim TY, Kim WB, Rhee YS, Song JY, Kim JM, Gong G, Lee S, Kim SY, Kim SC, Hong SJ, Shong YK (2006) The BRAF mutation is useful for prediction of clinical recurrence in 67 low---risk patients with conventional papillary thyroid carcinoma. Clin Endocrinol (Oxf) 65:364-368

25. Riesco-Eizaguirre G, Gutierrez-Martinez P, Garcia-Cabezas MA, Nistal M, Santisteban P (2006) The oncogene BRAF V600E is associated with a high risk of recurrence and less differentiated papillary thyroid carcinoma due to the impairment of Na+/I. targeting to the membrane. Endocr Relat Cancer 13:257-269

26. Trovisco V, Vieira de Castro I, Soares P, Maximo V, Silva P, Magalhaes J, Abrosimov A, Guiu XM, Sobrinho---Simoes M (2004) BRAF mutations are associated with some histological types of papillary thyroid carcinoma. J Pathol 202:247-251

27. Carta C, Moretti S, Passeri L, Barbi F, Avenia N, Cavaliere A, Monacelli M, Macchiarulo A, Santeusanio F, Tartaglia M, Puxeddu E (2006) Genotyping of an Italian papillary thyroid carcinoma cohort revealed high prevalence of BRAF mutations, absence of RAS mutations and allowed the detection of a new mutation of BRAF oncoprotein (BRAF(V599lns)). Clin Endocrinol (Oxf) 64:105-109

28. Hou P, Liu D, Xing M (2007) Functional characterization of the T1799-1801del and A1799-1816ins BRAF mutations in papillary thyroid cancer. Cell Cycle 6:377-379

29. Begum S, Rosenbaum E, Henrique R, Cohen Y, Sidransky D, Westra WH (2004) BRAF mutations in anaplastic thyroid carcinoma: implications for tumor origin, diagnosis and treatment. Mod Pathol 17:1359-1363

30. Nikiforova MN, Kimura ET, Gandhi M, Biddinger PW, Knauf JA, Basolo F, Zhu Z, Giannini R, Salvatore G, Fusco A, Santoro M, Fagin JA, Nikiforov YE (2003) BRAF mutations in thyroid tumors are restricted to papillary carcinomas and anaplastic or poorly differentiated carcinomas arising from papillary carcinomas. J Clin Endocrinol Metab 88:5399-5404

31. Unger K, Zitzelsberger H, Salvatore G, Santoro M, Bogdanova T, Braselmann H, Kastner P, Zurnadzhy L, Tronko N, Hutzler P, Thomas G (2004) Heterogeneity in the distribution of RET/PTC rearrangements within individual post-Chernobyl papillary thyroid carcinomas. J Clin Endocrinol Metab 89:4272-4279

32. Namba H, Rubin SA, Fagin JA (1990) Point mutations of ras oncogenes are an early event in thyroid tumorigenesis. Mol Endocrinol 4:1474-1479

33. Zhu Z, Gandhi M, Nikiforova MN, Fischer AH, Nikiforov YE (2003) Molecular profile and clinical-pathologic features of the follicular variant of papillary thyroid carcinoma. An unusually high prevalence of ras mutations. Am J Clin Pathol 120:71-77

34. Hara H, Fulton N, Yashiro T, Ito K, DeGroot LJ, Kaplan EL (1994) N-ras mutation: an independent prognostic factor for aggressiveness of papillary thyroid carcinoma. Surgery 116:1010-1016

35. Suarez HG, du Villard JA, Severino M, Caillou B, Schlumberger M, Tubiana M, Parmentier C, Monier R (1990) Presence of mutations in all three ras genes in human thyroid tumors. Oncogene 5:565-570

36. Motoi N, Sakamoto A, Yamochi T, Horiuchi H, Motoi T, Machinami R (2000) Role of ras mutation in the progression of thyroid carcinoma of follicular epithelial origin. Pathol Res Pract 196:1-7

37. Basolo F, Pisaturo F, Pollina LE, Fontanini G, Elisei R, Molinaro E, Iacconi P, Miccoli P, Pacini F (2000) N-ras mutation in poorly differentiated thyroid

carcinomas: correlation with bone metastases and inverse correlation to thyroglobulin expression. Thyroid 10:19-23

38. Garcia-Rostan G, Zhao H, Camp RL, Pollan M, Herrero A, Pardo J, Wu R, Carcangiu ML, Costa J, Tallini G (2003) ras mutations are associated with aggressive tumor phenotypes and poor prognosis in thyroid cancer. J Clin Oncol 21:3226-3235

39. Nikiforov YE (2008) Thyroid carcinoma: molecular pathways and therapeutic targets. Mod Pathol 21 Suppl 2:S37-43

40. Reddi HV, McIver B, Grebe SK, Eberhardt NL (2007) The paired box---8/peroxisome proliferator-activated receptor-gamma oncogene in thyroid tumorigenesis. Endocrinology 148:932-935

41. Fusco A, Grieco M, Santoro M, Berlingieri MT, Pilotti S, Pierotti MA, Della Porta G, Vecchio G (1987) A new oncogene in human thyroid papillary carcinomas and their lymph-nodal metastases. Nature 328:170-172

42. Grieco M, Santoro M, Berlingieri MT, Melillo RM, Donghi R, Bongarzone I, Pierotti MA, Della Porta G, Fusco A, Vecchio G (1990) PTC is a novel rearranged form of the ret proto-oncogene and is frequently detected in vivo in human thyroid papillary carcinomas.

43. Nikiforov YE (2002) RET/PTC rearrangement in thyroid tumors. Endocr Pathol 13:3-16

44. Tallini G, Asa SL (2001) RET oncogene activation in papillary thyroid carcinoma. Adv Anat Pathol 8:345-354

45. Knauf JA, Kuroda H, Basu S, Fagin JA (2003) RET/PTC-induced dedifferentiation of thyroid cells is mediated through Y1062 signaling through SHC-RAS-MAP kinase. Oncogene 22:4406-4412

46. Melillo RM, Castellone MD, Guarino V, De Falco V, Cirafici AM, Salvatore G, Caiazzo F, Basolo F, Giannini R, Kruhoffer M, Orntoft T, Fusco A, Santoro M (2005) The RET/PTC-RAS-BRAF linear signaling cascade mediates the motile and mitogenic phenotype of thyroid cancer cells. J Clin Invest 115:1068-1081

47. Mitsutake N, Knauf JA, Mitsutake S, Mesa C, Jr., Zhang L, Fagin JA (2005) Conditional BRAFV600E expression induces DNA synthesis, apoptosis, dedifferentiation, and chromosomal instability in thyroid PCCL3 cells. Cancer Res 65:2465-2473
48. Zhu Z, Ciampi R, Nikiforova MN, Gandhi M, Nikiforov YE (2006) Prevalence of RET/PTC rearrangements in thyroid papillary carcinomas: effects of the detection methods and genetic heterogeneity. J Clin Endocrinol Metab 91:3603-3610
49. Kroll TG, Sarraf P, Pecciarini L, Chen CJ, Mueller E, Spiegelman BM, Fletcher JA (2000) PAX8---PPARgamma1 fusion oncogene in human thyroid carcinoma [corrected]. Science 289:1357-1360
50. French CA, Alexander EK, Cibas ES, Nose V, Laguette J, Faquin W, Garber J, Moore F, Jr., Fletcher JA, Larsen PR, Kroll TG (2003) Genetic and biological subgroups of low- stage follicular thyroid cancer. Am J Pathol 162:1053-1060
51. Nikiforova MN, Lynch RA, Biddinger PW, Alexander EK, Dorn GW, 2nd, Tallini G, Kroll TG, Nikiforov YE (2003) RAS point mutations and PAX8-PPAR gamma rearrangement in thyroid tumors: evidence for distinct molecular pathways in thyroid follicular carcinoma. J Clin Endocrinol Metab 88:2318-2326
52. Dwight T, Thoppe SR, Foukakis T, Lui WO, Wallin G, Hoog A, Frisk T, Larsson C, Zedenius J (2003) Involvement of the PAX8/peroxisome proliferator-activated receptor gamma rearrangement in follicular thyroid tumors. J Clin Endocrinol Metab 88:4440-4445
53. Nikiforova MN, Biddinger PW, Caudill CM, Kroll TG, Nikiforov YE (2002) PAX8-PPARgamma rearrangement in thyroid tumors: RT-PCR and immunohistochemical analyses. Am J Surg Pathol 26:1016-1023
54. Gregory Powell J, Wang X, Allard BL, Sahin M, Wang XL, Hay ID, Hiddinga HJ, Deshpande SS, Kroll TG, Grebe SK, Eberhardt NL, McIver B (2004) The PAX8/PPARgamma fusion oncoprotein transforms immortalized human thyrocytes
55. Giordano TJ, Au AY, Kuick R, Thomas DG, Rhodes DR, Wilhelm KG, Jr., Vinco M, Misek DE, Sanders D, Zhu Z, Ciampi R, Hanash S, Chinnaiyan A, Clifton-Bligh RJ, Robinson BG, Nikiforov YE, Koenig RJ (2006) Delineation, functional validation, and bioinformatic evaluation of gene expression in thyroid follicular carcinomas with the PAX8-PPARG translocation. Clin Cancer Res 12:1983-1993

56. Reddi HV, McIver B, Grebe SK, Eberhardt NL (2007) The paired box-8/peroxisome proliferator-activated receptor-gamma oncogene in thyroid tumorigenesis. Endocrinology 148:932-935
57. Chevillard S, Ugolin N, Vielh P, Ory K, Levalois C, Elliott D, Clayman GL, El-Naggar AK (2004) Gene expression profiling of differentiated thyroid neoplasms: diagnostic and clinical implications. Clin Cancer Res 10:6586-6597
58. Huang Y, Prasad M, Lemon WJ, Hampel H, Wright FA, Kornacker K, LiVolsi V, Frankel W, Kloos RT, Eng C, Pellegata NS, de la Chapelle A (2001) Gene expression in papillary thyroid carcinoma reveals highly consistent profiles. Proc Natl Acad Sci U S A 98:15044-15049
59. Lubitz CC, Fahey TJ, 3rd (2005) The differentiation of benign and malignant thyroid nodules. Adv Surg 39:355-377
60. Prasad NB, Somervell H, Tufano RP, Dackiw AP, Marohn MR, Califano JA, Wang Y, Westra WH, Clark DP, Umbricht CB, Libutti SK, Zeiger MA (2008) Identification of genes differentially expressed in benign versus malignant thyroid tumors. Clin Cancer Res 14:3327-3337
61. Knauf JA, Sartor MA, Medvedovic M, Lundsmith E, Ryder M, Salzano M, Nikiforov YE, Giordano TJ, Ghossein RA, Fagin JA (2011) Progression of BRAF-induced thyroid cancer is associated with epithelial-mesenchymal transition requiring concomitant MAP kinase and TGFbeta signaling. Oncogene 30:3153-3162
62. Vasko V, Espinosa AV, Scouten W, He H, Auer H, Liyanarachchi S, Larin A, Savchenko V, Francis GL, de la Chapelle A, Saji M, Ringel MD (2007) Gene expression and functional evidence of epithelial-to-mesenchymal transition in papillary thyroid carcinoma invasion. Proc Natl Acad Sci U S A 104:2803-2808
63. Chen YT, Kitabayashi N, Zhou XK, Fahey TJ, 3rd, Scognamiglio T (2008) MicroRNA analysis as a potential diagnostic tool for papillary thyroid carcinoma. Mod Pathol 21:1139-1146
64. He H, Jazdzewski K, Li W, Liyanarachchi S, Nagy R, Volinia S, Calin GA, Liu CG, Franssila K, Suster S, Kloos RT, Croce CM, de la Chapelle A (2005) The role of microRNA genes in papillary thyroid carcinoma. Proc Natl Acad Sci U S A 102:19075-19080
65. Nikiforova MN, Chiosea SI, Nikiforov YE (2009) MicroRNA expression profiles in thyroid tumors. Endocr Pathol 20:85-91

66. Pallante P, Visone R, Ferracin M, Ferraro A, Berlingieri MT, Troncone G, Chiappetta G, Liu CG, Santoro M, Negrini M, Croce CM, Fusco A (2006) MicroRNA deregulation in human thyroid papillary carcinomas. Endocr Relat Cancer 13:497-508
67. Nikiforova MN, Tseng GC, Steward D, Diorio D, Nikiforov YE (2008) MicroRNA expression profiling of thyroid tumors: biological significance and diagnostic utility. J Clin Endocrinol Metab 93:1600-1608
68. Xing M (2007) Gene methylation in thyroid tumorigenesis. Endocrinology 148:948-953
69. Zuo H, Gandhi M, Edreira MM, Hochbaum D, Nimgaonkar VL, Zhang P, Dipaola J, Evdokimova V, Altschuler DL, Nikiforov YE (2010) Downregulation of Rap1GAP through epigenetic silencing and loss of heterozygosity promotes invasion and progression of thyroid tumors. Cancer Res 70:1389-1397
70. Russo D, Damante G, Puxeddu E, Durante C, Filetti S (2011) Epigenetics of thyroid cancer and novel therapeutic targets. J Mol Endocrinol 46:R73-81
71. Hu S, Liu D, Tufano RP, Carson KA, Rosenbaum E, Cohen Y, Holt EH, Kiseljak---Vassiliades K, Rhoden KJ, Tolaney S, Condouris S, Tallini G, Westra WH, Umbricht 72 CB, Zeiger MA, Califano JA, Vasko V, Xing M (2006) Association of aberrant methylation of tumor suppressor genes with tumor aggressiveness and BRAF mutation in papillary thyroid cancer. Int J Cancer 119:2322-2329
72. Nikiforov YE1, Yip L, Nikiforova MN. New strategies in diagnosing cancer in thyroid nodules: impact of molecular markers (2013).
73. Mazzanti C., Zeiger M. A., Costouros N. G., Umbricht C., Westra W. H., Smith D., Somervell H., Bevilacqua G., Alexander H. R. and Libutti S. K. Using gene expression profiling to differentiate benign versus malignant thyroid tumors. Cancer Res. 64(8):2898-903 (2004)
74. Nikiforov YE, Steward DL, Robinson-Smith TM, Haugen BR, Klopper JP, Zhu Z, Fagin JA, Falciglia M, Weber K, Nikiforova MN (2009) Molecular testing for mutations in improving the fine-needle aspiration diagnosis of thyroid nodules. J Clin Endocrinol Metab 94:2092-2098
75. Cantara S, Capezzone M, Marchisotta S, Capuano S, Busonero G, Toti P, Di Santo A, Caruso G, Carli AF, Brilli L, Montanaro A, Pacini F (2010) Impact of proto-oncogene mutation detection in cytological specimens from thyroid nodules improves the diagnostic accuracy of cytology. J Clin Endocrinol Metab 95:1365-1369

76. Ohori NP, Nikiforova MN, Schoedel KE, LeBeau SO, Hodak SP, Seethala RR, Carty SE, Ogilvie JB, Yip L, Nikiforov YE (2010) Contribution of molecular testing to thyroid fine-needle aspiration cytology of "follicular lesion of undetermined significance/atypia of undetermined significance". Cancer Cytopathol 118:17-23
77. Moses W, Weng J, Sansano I, Peng M, Khanafshar E, Ljung BM, Duh QY, Clark OH, Kebebew E (2010) Molecular testing for somatic mutations improves the accuracy of thyroid fine---needle aspiration biopsy. World J Surg 34:2589-2594
78. Grogan RH, Mitmaker EJ, and Clark OH. The evolution of biomarkers in thyroid Cancer—from mass screening to a personalized biosignature. 2010 May 20;2(2):885-912.
79. Huang, S., et al., Enforced c-KIT expression renders highly metastatic human melanoma cells susceptible to stem cell factor-induced apoptosis and inhibits their tumorigenic and metastatic potential. Oncogene, 13(11): 2339-47 (1996)
80. De Silva CM, Reid R (2003) Gastrointestinal stromal tumors (GIST): C-kit mutations, CD117 expression, differential diagnosis and targeted cancer therapy with Imatinib. Pathol Oncol Res 9:13-19
81. D'Amato G, Steinert DM, McAuliffe JC, Trent JC (2005) Update on the biology and therapy of gastrointestinal stromal tumors. Cancer Control 12:44-56
82. McIntyre A, Summersgill B, Grygalewicz B, Gillis AJ, Stoop J, van Gurp RJ, Dennis N, Fisher C, Huddart R, Cooper C, Clark J, Oosterhuis JW, Looijenga LH, Shipley J (2005) Amplification and overexpression of the KIT gene is associated with progression in the seminoma subtype of testicular germ cell tumors of adolescents and adults. Cancer Res 65:8085-8089
83. All-Ericsson C, Girnita L, Muller-Brunotte A, Brodin B, Seregard S, Ostman A, Larsson O (2004) c-Kit dependent growth of uveal melanoma cells: a potential therapeutic target? Invest Ophthalmol Vis Sci 45:2075-2082
84. Ulivi P, Zoli W, Medri L, Amadori D, Saragoni L, Barbanti F, Calistri D, Silvestrini R (2004) c-kit and SCF expression in normal and tumor breast tissue. Breast Cancer Res Treat 83:33-42
85. Natali PG, Berlingieri MT, Nicotra MR, Fusco A, Santoro E, Bigotti A, Vecchio G (1995) Transformation of thyroid epithelium is associated with loss of c---kit receptor. Cancer Res 55:1787-1791
86. Rosen J, He M, Umbricht C, Alexander HR, Dackiw AP, Zeiger MA, Libutti SK (2005) A six-gene model for differentiating benign from malignant thyroid tumors on the basis of gene expression. Surgery 138:1050-1056; discussion 1056-1057

87. Mazeh H, Mizrahi I, Halle D, Ilyayev N, Stojadinovic A, Trink B, Mitrani Rosenbaum S, Roistacher M, Ariel I, Eid A, Freund HR, Nissan A (2011) Development of a microRNA based molecular assay for the detection of papillary thyroid carcinoma in aspiration biopsy samples. Thyroid 21:111-118
88. Mingzhao Xing. Minireview: Gene Methylation in Thyroid Tumorigenesis. (2007)
89. YamadaY, Enokida H, Kojima S, Kawakami K, Chiyomaru T, Tatarano S, Yoshino H, Kawahara K, Nishiyama K, Seki N, Nakagawa M. Cancer Sci. (2011 Mar);102(3):522-9. MiR-96 and miR-183 detection in urine serve as potential tumor markers of urothelialcarcinoma: correlation with stage and grade, and comparison with urinary cytology.
90. Huiling He, Krystian Jazdzewski, Wei Li, Sandya Liyanarachchi, Rebecca Nagy, Stefano Volinia, George A. Calin, Chang-gong Liu, Kaarle Franssila, Saul Suster, Richard T. Kloos, Carlo M. Croce, and Albert de la Chapelle. The role of microRNA genes in papillary thyroid carcinoma. (2005)
91. Muller Fabbri, Nicola Valeri and George A.Calin. REVIEW: MicroRNAs and genomic variations: from Proteus tricks to Prometheus gift. (2009)
92. Francesca Marini, Ettore Luzi, and Maria Luisa Brandi. Review:MicroRNA Role in Thyroid Cancer Development. (2011)
93. Marie Gilbert-Sirieix1, Joelle Makoukji, Shioko Kimura3, Monique Talbot, Bernard Caillou, Charbel Massaad, Liliane Massaad-Massade Wnt/b-Catenin Signaling Pathway Is a Direct Enhancer of Thyroid Transcription Factor-1 in Human Papillary Thyroid Carcinoma Cells. (2011)
94. Filetti et al., Sodium/Iodide symporter: a key transport system in thyroid cancer cell metabolism. European Journal of Endocrinology. 167(6), (2012)
95. Denise P. Carvalho; Andrea C.F. Ferreira. The importance of sodium/iodide symporter (NIS) for thyroid cancer management. (2007)
96. Sunde M, McGrath KC, Young L, Matthews JM, Chua EL, Mackay JP, Death AK (2004) TC-1 is a novel tumorigenic and natively disordered protein associated with thyroid cancer. Cancer Res 64:2766-2773
97. Marina N. Nikiforova & Simon I. Chiosea & Yuri E. Nikiforov. MicroRNA Expression Profiles in Thyroid Tumors. (2009)
98. H. He, K. Jazdzewski, W. Li et al., "The role of microRNA genes in papillary thyroid carcinoma,"Proceedings of the National Academy of Sciences of the United States of America, vol. 102, no. 52, pp. 19075–19080 (2005).

99. Chang HH, Ramoni MF (2009) Transcriptional network classifiers. BMC Bioinformatics 10 Suppl 9:S1 76

100. Stojadinovic A, Peoples GE, Libutti SK, Henry LR, Eberhardt J, Howard RS, Gur D, Elster EA, Nissan A (2009) Development of a clinical decision model for thyroid nodules. BMC Surg 9:12

101. Liu YI, Kamaya A, Desser TS, Rubin DL (2011) A bayesian network for differentiating benign from malignant thyroid nodules using sonographic and demographic features. AJR Am J Roentgenol 196:W598-605

102. Zweig MH, Campbell G (1993) Receiver-operating characteristic (ROC) plots: a fundamental evaluation tool in clinical medicine. Clin Chem 39:561-577

103. Zsebo KM, Williams DA, Geissler EN, Broudy VC, Martin FH, Atkins HL, Hsu RY, Birkett NC, Okino KH, Murdock DC, et al. (1990) Stem cell factor is encoded at the Sl locus of the mouse and is the ligand for the c---kit tyrosine kinase receptor.

104. Josena K. Stephen 1, Dhananjay Chitale 2, Vinod Narra 3, Kang Mei Chen, Raja Sawhney and Maria J. Worsham (2011) DNA Methylation in Thyroid. Cancers, 3, 1732-1743; doi:10.3390

105. Hou, P.; Bojdani, E.; Xing, M. (2010) Induction of thyroid gene expression and radioiodine uptake in thyroid cancer cells by targeting major signaling pathways. J. Clin. Endocrinol. Metab. 95, 820-828.

106. Venkataraman, G.M.; Yatin, M.; Marcinek, R.; Ain, K.B. (1999) Restoration of iodide uptake in dedifferentiated thyroid carcinoma: Relationship to human na+/i-symporter gene methylation status. J. Clin. Endocrinol. Metab, 84, 2449-2457.

107. Shioko Kimura (2011). Thyroid-Specific Transcription Factors and Their Roles in Thyroid Cancer. Thyroid Research Volume 2011, doi:10.4061

108. Nonaka D1, Tang Y, Chiriboga L, Rivera M, Ghossein R. (2007) Diagnostic utility of thyroid transcription factors Pax8 and TTF-2 (FoxE1) in thyroid epithelial neoplasms. Modern Pathology , 21, 192–200; doi:10.1038

109. Ordonez NG. (2000) Thyroid transcription factor-1 is a marker of lung and thyroid carcinomas. Adv Anat Pathol;7:123–127.

110. Srodon M1, Westra WH. (2002).Immunohistochemical staining for thyroid transcription factor-1: A helpful aid in discerning primary site of tumor origin in patients with brain metastases. Hum Pathol;33(6):642-5.

111. Chua EL, Young L, Wu WM, Turtle JR, Dong Q (2000) Cloning of TC-1 (C8orf4), a novel gene found to be overexpressed in thyroid cancer. Genomics 69:342-347

112. Sargent DJ (2001) Comparison of artificial neural networks with other statistical approaches: results from medical data sets. Cancer 91:1636-1642
113. Rodvold KA, Pryka RD, Kuehl PG, Blum RA, Donahue P (1990) Bayesian forecasting of serum gentamicin concentrations in intensive care patients. Clin Pharmacokinet 18:409-418
114. Wakefield J, Racine-Poon A (1995) An application of Bayesian population pharmacokinetic/pharmacodynamic models to dose recommendation. Stat Med 14:971-986
115. Burnside ES, Rubin DL, Fine JP, Shachter RD, Sisney GA, Leung WK (2006) Bayesian network to predict breast cancer risk of mammographic microcalcifications and reduce number of benign biopsy results: initial experience. Radiology 240:666-673
116. Christiansen CL, Wang F, Barton MB, Kreuter W, Elmore JG, Gelfand AE, Fletcher SW (2000) Predicting the cumulative risk of false-positive mammograms. J Natl Cancer Inst 92:1657-1666
117. Edwards FH, Schaefer PS, Cohen AJ, Bellamy RF, Thompson L, Graeber GM, Barry MJ (1989) Use of artificial intelligence for the preoperative diagnosis of pulmonary lesions. Ann Thorac Surg 48:556-559
118. Burd RS, Ouyang M, Madigan D (2008) Bayesian logistic injury severity score: a method for predicting mortality using international classification of disease-9 codes. Acad Emerg Med 15:466-475 78
119. Fazio VW, Tekkis PP, Remzi F, Lavery IC (2004) Assessment of operative risk in colorectal cancer surgery: the Cleveland Clinic Foundation colorectal cancer model. Dis Colon Rectum 47:2015-2024
120. Biagioli B, Scolletta S, Cevenini G, Barbini E, Giomarelli P, Barbini P (2006) A multivariate Bayesian model for assessing morbidity after coronary artery surgery. Crit Care 10:R94
121. Edwards FH, Peterson RF, Bridges C, Ceithaml EL 1995 (1988): use of a Bayesian statistical model for risk assessment in coronary artery surgery. Updated in 1995. Ann Thorac Surg 59:1611-1612
122. Hoot N, Aronsky D (2005) Using Bayesian networks to predict survival of liver transplant patients. AMIA Annu Symp Proc: 345-349
123. Lenihan CR, O'Kelly P, Mohan P, Little D, Walshe JJ, Kieran NE, Conlon PJ (2008) MDRD-estimated GFR at one year post-renal transplant is a predictor of long-term graft function. Ren Fail 30:345-352

124. Kim SJ, Lee KE, Myong JP, Park JH, Jeon YK, Min HS, Park SY, Jung KC, Koo do H, Youn YK (2012) BRAF V600E mutation is associated with tumor aggressiveness in papillary thyroid cancer. World J Surg 36:310-317.

125. Kebebew E, Weng J, Bauer J, Ranvier G, Clark OH, Duh QY, Shibru D, Bastian B, Griffin A (2007) The prevalence and prognostic value of BRAF mutation in thyroid cancer. Ann Surg 246:466-470; discussion 470-461

126. Lee X, Gao M, Ji Y, Yu Y, Feng Y, Li Y, Zhang Y, Cheng W, Zhao W (2009) Analysis of differential BRAF (V600E) mutational status in high aggressive papillary thyroid microcarcinoma. Ann Surg Oncol 16:240-245

127. Murugan AK1, Xing M. (2011) Anaplastic thyroid cancers harbor novel oncogenic mutations of the ALK gene. Cancer Res. ;71(13):4403-11. doi: 10.1158/0008-5472.

128. Lindsey M. Kelly, Guillermo Barila, Pengyuan Liu, Viktoria Evdokimova, Sumita Trivedi, Federica Panebianco, Manoj Gandhi1, Sally E. Carty, Steven P. Hodak, Jianhua Luo, Sanja Dacic, Yan Ping Yu, Marina N. Nikiforova, Robert L. Ferris, Daniel L. Altschuler, Yuri E. Nikiforov. (2013) Identification of the transforming STRN-ALK fusion as a potential therapeutic target in the aggressive forms of thyroid cancer

129. Cho NL1, Lin CI, Du J, Whang EE, Ito H, Moore FD Jr, Ruan DT (2012) Global tyrosine kinome profiling of human thyroid tumors identifies Src as a promising target for invasive cancers

130. Wang MH1, Lee W, Luo YL, Weis MT, Yao HP. (2007) Altered expression of the RON receptor tyrosine kinase in various epithelial cancers and its contribution to tumourigenic phenotypes in thyroid cancer cells. J Pathol. 213(4):402-11.

131. Nikolaos P. Karidis, Constantinos Giaginis, Gerasimos Tsourouflis, Paraskevi Alexandrou, Ioanna Delladetsima, Stamatios Theocharis. (2011) Eph-A2 and Eph-A4 expression in human benign and malignant thyroid lesions: An immunohistochemical study. Med Sci Monit, 17(9): BR257-265

132. Brannan JM, Sen B, Saigal B et al. (2009), EphA2 in the early pathogenesis and progression of non-small cell lung cancer. Cancer Prev Res (Phila Pa); 2(12): 1039–49

133. Feng YX, Zhao JS, Li JJ et al. (2010), Liver cancer: EphrinA2 promotes tumorigenicity through Rac1/Akt/NF-kappaB signaling pathway 120. Hepatology; 51(2): 535-44

134. Lu C, Shahzad MM, Wang H et al. (2008), EphA2 overexpression promotes ovarian cancer growth. Cancer Biol Ther; 7(7): 1098–103

135. Nakamura R, Kataoka H, Sato N et al. (2005), EPHA2/EFNA1 expression in human gastric cancer. Cancer Sci; 96(1): 42–47

136. Walker-Daniels J, Coffman K, Azimi M et al. (199), Overexpression of the EphA2 tyrosine kinase in prostate cancer. Prostate; 41(4): 275–80

137. Hafner C, Schmitz G, Meyer S et al. (2004), Differential gene expression of Eph receptors and ephrins in benign human tissues and cancers. Clin Chem; 50(3): 490–99

138. D Chiron, S Maiga, S Surget, G Descamps, P Gomez-Bougie, S Traore, N Robillard, P Moreau, S Le Gouill, R Bataille, M Amiot, and C Pellat-Deceunynck. (2013) Autocrine insulin-like growth factor 1 and stem cell factor but not interleukin 6 support self-renewal of human myeloma cells Blood Cancer Journal 3, e120; doi:10.1038;

ACKNOWLEDGMENTS

The years spent during the program of my PhD allowed me to grow at scientific and personal level. Through my stay in Pisa and during my time abroad, I met people and known places that I'll bring in my heart forever and that allowed me to became the person I am now.

There are some people that have contributed in different ways at the completion of this thesis and whom I would like to mention here.

I wish to thank prof. Generoso Bevilacqua to allow me to be part of this PhD program and to gave me the possibility to spend 4 months in London, at Research Cancer Institute, under the supervision of Prof. Peter Parker and 6 months in US, at Department of Pathology, University of Pittsburgh, under the supervision of Dr. Yuri Nikiforov, where I'm still here as researcher.

I would like to express my gratitude to my tutor Chiara whose motivation, encouragement, understanding, and kindness guided me day by day during my Phd experience. I thank her for everything that taught me, for helping me to shape my interest and ideas, for encouraged me during my permanents in USA, and to help me to growth as a researcher. I appreciate her vast knowledge and skill in many areas; Chiara is the tutor who truly made a difference in this part of my life, she became more a mentor and friend more than a tutor.

A very special thanks goes out to Katia, she was the first person in the laboratory that understood my personality and character. I thank her to listen and support me every time that I needed, I thank her for the good suggestions she gives me.

I would like to thanks Dr. Marchetti which, by his knowledge, contributed to realize this work, and thank him for his friendship.

Thank Paolo for his goodness to help me with the statistical part of the Thesis.

In addition, I would like to thanks the other PhD students and doctors that are part of the Molecular Pathology Team; among them, Dr. Sara Tomei, Dr. Sara Franceschi, Dr. Valerio Ortenzi, Dr. Ivana Amorgida, Dr. Al-Zoubi Mazhar, Dr. Francesca Lessi, Dr. Chiara Gugliemi, Dr. Alessando Apollo.

Each one of them helped me many times and in different ways during my PhD training.

I want to thank a special person, Alessandro Pirosa, for his love, never-ending support and all the laughter he gave me throughout those years, which were not always so easy.

Finally, I would like to thank my family, especially my mother and sister for always believing in me, for their continuous love and their support in my decisions. Without whom I could not have made it here.

Federica Panebianco